

## 2. Site Background and Physical Setting

10

## 2. SITE BACKGROUND AND PHYSICAL SETTING

### 2.1 Site Background

The INEL is a Government-owned test site managed by DOE. A large variety of laboratory activities and test facilities support DOE and other Government-sponsored research, development programs, and projects at the INEL.

Most INEL facilities are operated by one of five Government contractors: Argonne National Laboratory-West; EG&G Idaho; Babcock and Wilcox Idaho, Inc.; Westinghouse Electric Corporation; and Westinghouse Idaho Nuclear Company. These contractors conduct various programs at the INEL under the administration of three DOE offices: Idaho Field Office (DOE-ID), Pittsburgh Naval Reactors Office, and Chicago Operations Office. DOE-ID has responsibility for the INEL and designates to the Government contractors the authority to operate the Site.

EG&G Idaho, a prime operating contractor and the Site services contractor for the INEL, provides a variety of programmatic and support services related to nuclear reactor design and development, nonnuclear energy development, materials testing and evaluation, operational safety, and radioactive waste management. EG&G Idaho has current responsibility for operation of RWMC.

#### 2.1.1 INEL Location and Description

The INEL Site occupies approximately 890 mi<sup>2</sup> of the northwestern portion of the eastern Snake River Plain in southeast Idaho. The Site is nearly 39 mi long from north to south (extreme latitudes are 43° 26' and 44° 01' N) and about 36 mi in its broadest southern portion (extreme longitudes are 112° 28' and 113° 9' W). The INEL includes portions of five Idaho counties (Bingham, Bonneville, Butte, Clark, and Jefferson) and lies within Townships 2 to 8 N and Ranges 28 to 34 E, Boise baseline and meridian. Figure 2-1 shows the configuration for the INEL and identifies some of its major facilities.

The surface of the INEL is a relatively flat, semiarid, sagebrush desert, with predominant relief being manifested either as volcanic buttes jutting up out of the desert floor or as unevenly surfaced basalt flows or flow vents and fissures. Elevations on the INEL range from 5,200 ft in the northeast to 4,750 ft in the central lowlands, with the average being 4,975 ft. The elevations of the SDA are between 5,010 and 5,020 ft.

**2.1.1.1 History of the INEL** The INEL Site was established in 1949 as the National Reactor Testing Station by the U.S. Atomic Energy Commission as a site for building, testing, and operating various nuclear reactors, fuel processing plants, and support facilities with maximum safety and isolation. In 1974, the National Reactor Testing Station was redesignated as the Idaho National Engineering Laboratory (INEL) to reflect the broad scope of engineering activities conducted at the INEL.

The U.S. Government used portions of the Site prior to its establishment as the National Reactor Testing Station. During World War II, the U.S. Navy used about 270 mi<sup>2</sup> of the Site as a gunnery range. An area southwest of the Navy's area was once used by the U.S. Army Air Corps as an aerial gunnery range. The present INEL Site includes all of the former military area and a large adjacent area withdrawn from the public domain for use by DOE. The former Navy administration shop, warehouse, and housing area is today known as the Central Facilities Area.

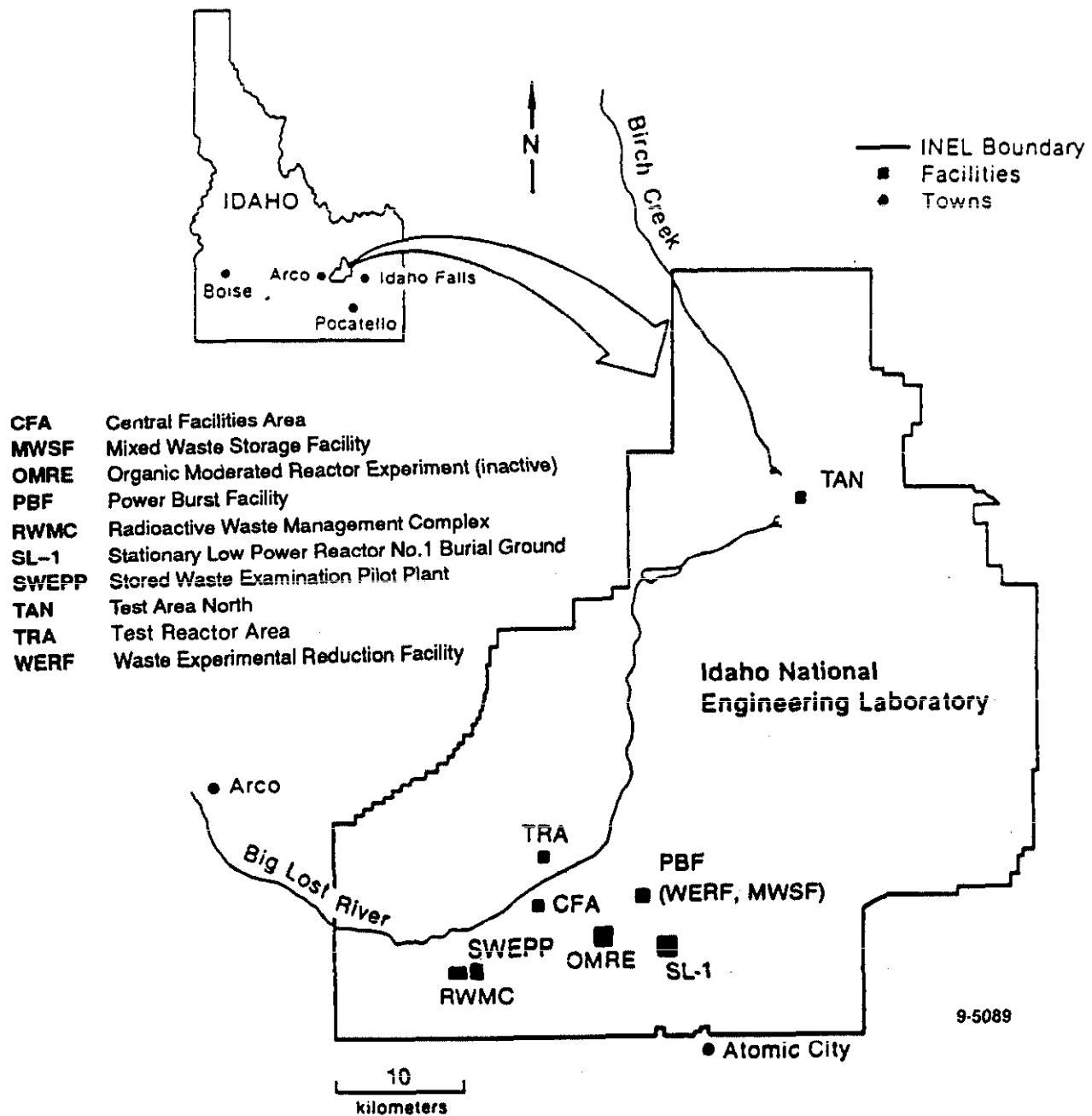


**Figure 2-1.** Facilities at the Idaho National Engineering Laboratory.

**2.1.1.2 Physiography.** The Snake River Plain is the largest continuous physiographic feature in southern Idaho (Figure 2-2). This large topographic depression extends from the Oregon border across Idaho to Yellowstone National Park and northwestern Wyoming.

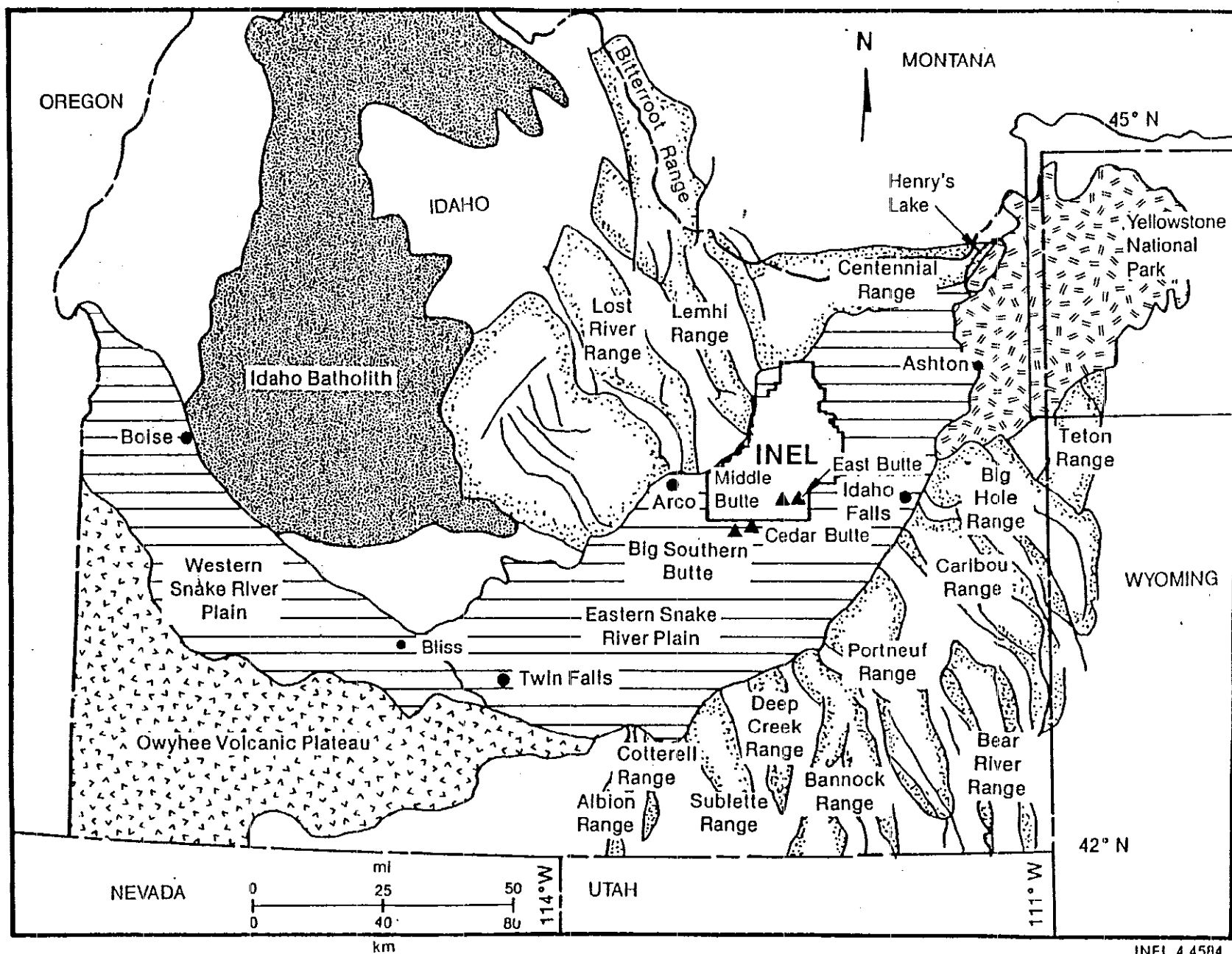
The Snake River Plain slopes upward from an elevation of about 2,500 ft at the Oregon border to over 6,500 ft at Henry's Lake near the Montana-Wyoming border. The Snake River Plain is composed of two structurally dissimilar segments, with the division occurring near Twin Falls, Idaho. West of Twin Falls, the Snake River has cut a valley through Tertiary Basin fill sediments and interbedded volcanic rocks. The stream drainage is well developed except in a few areas covered by recent thin basalt flows. East of Bliss, Idaho, the complexion of the plain changes as the Snake River carves a vertical-walled canyon through thick sequences of Quaternary basalt with few interbedded sedimentary deposits.

The INEL is located entirely on the northern side of the eastern Snake River Plain and adjoins the mountains to the northwest that make up the northern boundary of the plain. Three mountain ranges end at the northern and northwestern boundaries of the INEL: the Lost River Range, the Lemhi Range; and the Beaverhead Mountains of the Bitterroot Range (Figure 2-2). Saddle Mountain Peak, near the southern end of the Lemhi Range, reaches an altitude of 10,795 ft and is the highest point in the area.

The portion of the Snake River Plain occupied by the INEL may be divided into three minor physical provinces: a central trough that extends to the northeast through the INEL and two flanking slopes that descend to the trough, one from the mountains to the northwest and the other from a broad ridge on the plain to the southeast. The slopes on the northwestern flank of the trough are mainly alluvial fans originating from sediments of Birch Creek and the Little Lost River. Also forming these gentle slopes are basalt flows that have spread onto the plain (Figure 2-3). The landforms on the southeast flank of the trough are formed by basalt flows, which spread from an eruption zone that extends northeastward from Cedar Butte (Figure 2-2). The lavas that erupted along this zone built up a broad topographic swell directing the Snake River to its current course along the southern and southeastern edges of the plain. This ridge effectively separates the drainage of mountain ranges northwest of the INEL from the Snake River. Big Southern Butte and the Middle and East Buttes are aligned roughly along this zone; however, they were formed by viscous rhyolitic lavas extruded through the basaltic cover and are slightly older than the surface basalts of the plain.

The central lowland of the INEL broadens to the northeast and joins the extensive Mud Lake Basin. The Big and Little Lost Rivers and Birch Creek drain into this trough from valleys in the mountains to the north and west. The intermittently flowing waters of the Big Lost River have formed a flood plain in this trough, consisting primarily of sands and gravels. The streams flow (intermittently) to the Lost River Sinks, a system of playa depressions in the northeast portion of the INEL, south of the town of Howe. There, the water either evaporates, transpires, or recharges the Snake River Plain Aquifer. The sinks area covers several hundred acres and is very flat, consisting of significant thicknesses of fluvial and lacustrine sediments.

**2.1.1.3 Formation of the Snake River Plain.** Southern Idaho has been characterized by a bimodal basalt-rhyolite style of volcanism over the past 15 million years. This volcanism has occurred as two general periods. The first period consisted of the extrusion of rhyolitic lavas and tuffs interrupted by smaller basaltic outflows that have continued until recent times (Leeman 1982a). The



INEL 4 4584

Figure 2-2. Physiographic features of the INEL area.

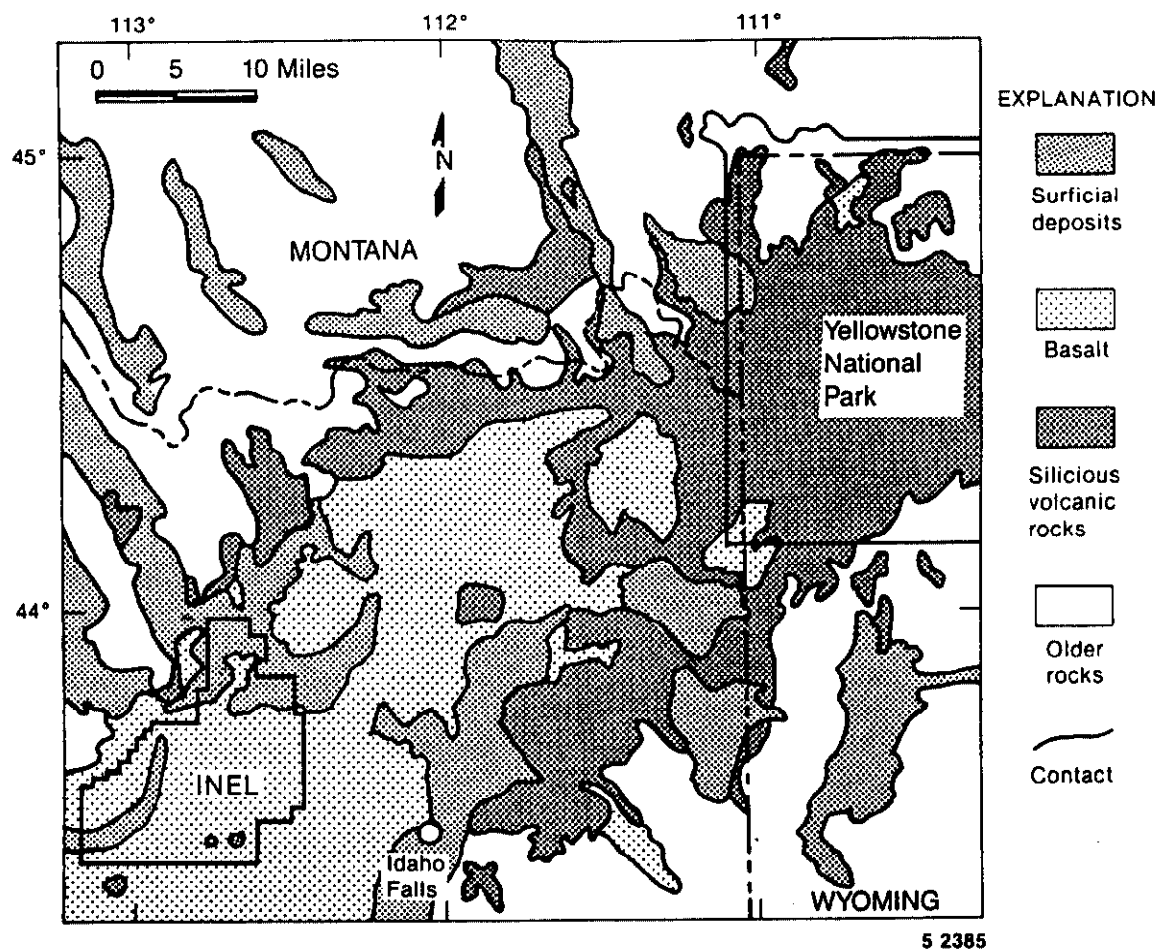


**Figure 2-3.** Geological features of the INEL area.

focus of this volcanism has progressed over time in a northeasterly trend from the Miocene to the present time and is currently located beneath the Yellowstone Plateau. The eruption of rhyolitic lavas associated with this first period has occurred at the Yellowstone Plateau as recently as 70,000 years ago (Christiansen, 1982).

The Snake River Plain is composed of two structurally dissimilar segments (Figure 2-2). The eastern Snake River Plain is considered a down-warped structure and not necessarily bounded by faults. It consists of a series of rhyolitic calderas overlain by a veneer of basalts. The eastern segment is a 60 mi-wide basin extending 200 mi from near Twin Falls, Idaho, to the Island Park Caldera north of Ashton, Idaho.

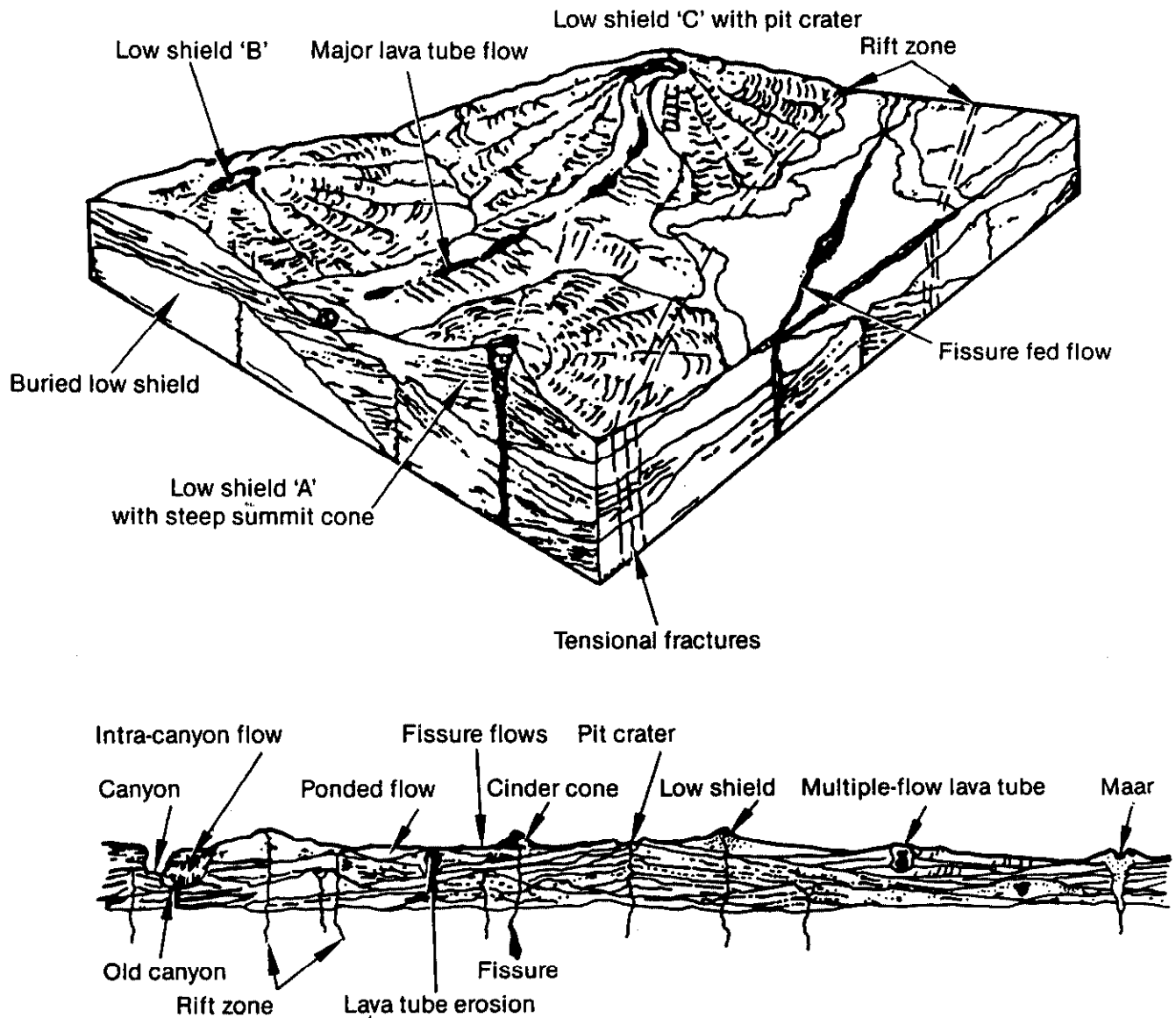
The earliest dated rhyolitic activity on the eastern portion of the Snake River Plain began about 10 million years ago in the Twin Falls area (Leeman 1982a). According to Leeman, this silicic volcanism was followed by basaltic lavas that extruded from vents along northwest-trending rift zones. The volcanic material is dominated by rhyolite ash flow tuffs and lava flows to a thickness of greater than 7,800 ft. The silicic volcanic rocks are overlain by as much as 2,000 to 3,000 ft of basaltic lava flows and interbedded sediments (Embree et al. 1982; and Robertson et al. 1974).

Basalt flows have erupted from four postulated rift zones that cross the Snake River Plain trending northwest-southeast. These rifts are defined by the linear arrangement of vents, fissures, and graben (Kuntz and Dalrymple 1979). Dating of basalt flows on and near the INEL yields eruption dates of 12,000 to 400,000 years ago. The Hells Half Acre flow, immediately adjacent to the southeastern INEL boundary, is dated at 4,100 years. The youngest basalt flows on the Snake River Plain occur along the Great Rift at the Craters of the Moon National Monument and are 2,100 years old.

**2.1.1.4 Surface Geology.** The general surface geology of the INEL is shown in Figure 2-3. Much of the surface is covered by Pleistocene and Holocene basalt flows. The second most prominent geologic feature is the flood plain of the Big Lost River. Alluvial sediments of Quaternary age occur in a band that extends across the INEL from the southwest to the northeast. The alluvial deposits grade into lacustrine deposits in the northern portion of the INEL, where the Big Lost River enters a series of playa lakes. Paleozoic sedimentary rocks make up a very small area of the INEL along the northwest boundary. Three large silicic domes and a number of smaller basalt cinder cones occur on the INEL and along the southern boundary.

**2.1.1.5 Subsurface Geology.** A number of wells have been drilled on the INEL to monitor groundwater levels and water quality. Lithologic and geophysical logs have been made for most of the wells drilled on the INEL. From these logs and an understanding of the volcanism of the Snake River Plain, it is possible to develop a reasonably comprehensive picture of subsurface geology. The INEL Site is homogeneous in terms of mode of formation and types of geologic units encountered. The exact distribution of units at any specific site, however, is highly variable.

The eastern Snake River Plain typifies a plains style of basaltic volcanism with the accumulation of basaltic flow materials by three general methods: (a) flows forming low-relief shield volcanos, (b) fissure-fed flows, and (c) major tube-fed flows with other minor flow types (Greeley 1982). These distinct flow types are often intermingled with the tube and fissure-fed flows filling in the lower regions between low-relief shield volcanos. This results in a relatively low surface gradient often with complex stratigraphic relations, as displayed in Figure 2-4. Relatively minor accumulations of basaltic



9-1552

**Figure 2-4.** Block diagram showing the relationship of low shields, major lava tube flows, and fissure flows as they relate to the plains style of basaltic volcanism (Greeley 1982).



cinders or scoria occur in plains type volcanism. This can be as relatively rare cinder cones or as thin accumulations between flows (Greeley 1982).

Basalt flows characteristically occur as layers of pahoehoe lava a few feet thick to tens of feet thick, with an average thickness on the order of 53 ft (Nace et al. 1956). The basalt flows can be interlayered with unconsolidated sediments, scoria, and breccia. Considerable variation in lithologic texture occurs between different flows as well as within individual flows.

The bases of many flows are glassy to fine grained and minutely vesicular. The midportions of flows are coarser grained with few vesicles. The upper portions of flows are fine grained with many small vesicles. This pattern is the result of rapid cooling of the upper and lower surfaces with slower cooling of the interior of the basalt flow. The massive interiors of basalt flows are generally jointed, with vertical joints in a hexagonal pattern that were formed during cooling. Basalt flows that were exposed at the surface for a significant time period have the vesicles and fractures filled with fine-grained sediments and secondary calcite. During quiescent periods between volcanic eruptions, sediments were deposited upon the basalt surfaces. These sedimentary deposits display a wide range of grain size distributions, depending on the mode of deposition -- aeolian, lacustrine, or fluvial. Because of the very irregular topography of the basalt flows, isolated depressions are common. Thus, many small pockets of sedimentary material may occur in a sequence of basalt flows. (See Figure 2-4.)

## **2.1.2 RWMC/SDA Site Description**

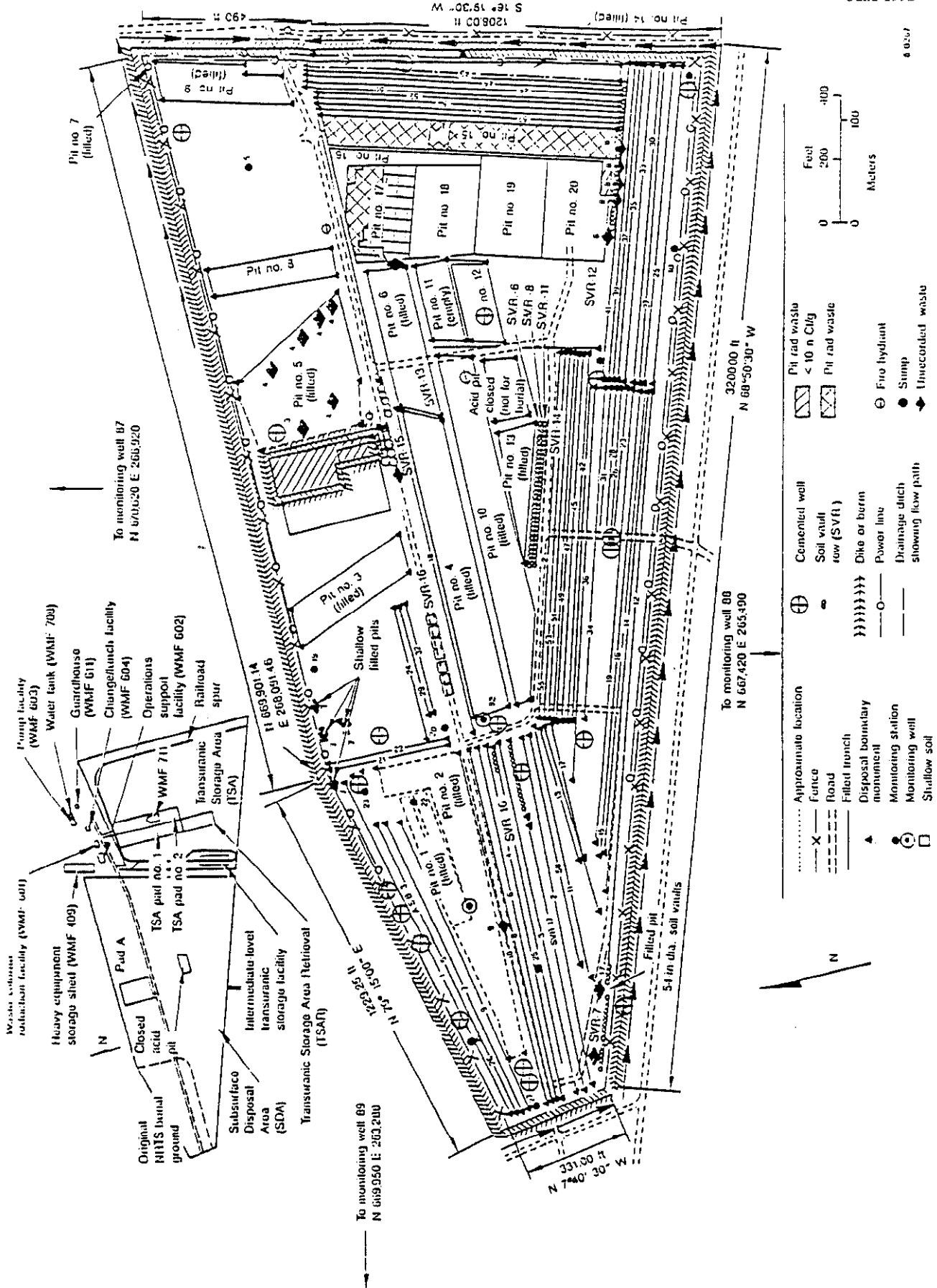
The RWMC is located in the southwest section of the INEL. It was established in 1952 as a disposal site for solid low-level waste generated by INEL operations. Its current mission is to provide waste management for the present and future needs of the INEL and to retrieve, examine, and certify waste for shipment to the DOE Waste Isolation Pilot Plant in Carlsbad, New Mexico.

The RWMC encompasses 144 acres and consists of two main disposal and storage areas: the Transuranic Storage Area and the Subsurface Disposal Area (SDA), previously known as the Burial Ground. Within these areas are smaller, specialized disposal and storage areas (Figure 2-5).

**2.1.2.1 History of the RWMC.** The SDA consists of below ground pits and trenches (Burial Ground) and one above ground disposal pad (Pad A). The first trench at the Burial Ground was opened for solid waste disposal on July 8, 1952. This trench was located in the northwest corner of the present SDA (Figure 2-5). For about 2 years, only mixed fission product waste was buried. The mixed fission product waste was contaminated with beta- and gamma-emitting radionuclides, both low-level and intermediate-level. In 1953, the Atomic Energy Commission decided that solid radioactive transuranic (TRU) waste generated by nuclear weapons production activities at the Rocky Flats Plant near Golden, Colorado, would be disposed of at the RWMC because waste disposal sites in Colorado were not acceptable. The first shipment of waste from the Rocky Flats Plant was received at the SDA in April 1954 and buried in shallow pits and trenches with no segregation of TRU waste, mixed fission product waste, and nonradioactive hazardous waste. By 1957, the 10 trenches (Trenches 1 through 10) at the 13-acre site were nearly filled.

The site was then expanded in 1957 to the 88-acre tract known today as the SDA. From 1953 to 1969 the use of large, open pits was initiated for the disposal of solid TRU wastes, and the use of

6 0267



trenches was reserved for the disposal of mixed fission product wastes. Large, bulky items contaminated with mixed fission product wastes were sometimes placed in the pits along with the TRU waste.

During the 1960s, the SDA continued to receive TRU waste for disposal in shallow land pits. During the period 1960 through 1963, the SDA also served as a burial ground for solid waste generated by other off-Site Atomic Energy Commission licensees, such as universities, hospitals, and radioisotope source manufacturers. This service stopped when commercial burial sites for waste from private industry became available.

Disposal of TRU wastes in shallow land pits and trenches at the SDA ceased in 1970 after the Atomic Energy Commission adopted a new policy for managing TRU waste. The policy required segregation and storage of all TRU waste with concentrations above 100 nCi/g. Such waste would be stored for retrieval after periods of up to 20 years. Also in 1970, the 56-acre TSA was established immediately east of the SDA for such waste management. Asphalt pads were constructed on which the TRU waste was stacked and then covered with plywood, plastic sheeting, and 2 to 3 ft of soil. Wastes stored aboveground at the TSA after 1970 are currently being retrieved, examined, and stored for future shipment to the Waste Isolation Pilot Plant.

During the SDA operational period of 1952 through 1971, approximately 3.4 million ft<sup>3</sup> of waste was disposed. Most waste disposal documentation concerning operations at the RWMC before 1971 was destroyed when the required retention period had been exceeded. Interviews with personnel who developed the Radioactive Waste Management Information System data base stated that records recovered from storage in Seattle (the National Archives and Records Service) were incomplete, with years missing. Efforts were made during the 1970s to recover these records, to no avail.

**2.1.2.2 Design Features.** The SDA is a fenced area that comprises the western part of the RWMC. Included in the SDA are pits, trenches, soil vault rows, and Pad A. The pits are excavations with a variety of dimensions. They generally have surface areas of several acres and range in depth from 5 to 15 ft. In general, the pits and trenches were excavated to bedrock and filled with waste materials. Some waste is believed to lay directly on basalt. After the waste was emplaced, the pits were backfilled with at least 3 ft of soil. During operations, soil cover was applied over the waste during weekly or daily operations, depending on the procedures for that particular year. Closure of a filled pit included applying final soil cover a few yards deep and planting stabilizing vegetation on the final cover (EG&G Idaho 1985).

**2.1.2.3 Waste Emplacement.** From 1952 to 1963, the waste was stacked in pits and trenches. From 1963 to 1969 the waste was randomly dumped into the pits to reduce labor costs and minimize worker radiation exposure. This random dumping continued until 1969, when stacking was reinstituted.

Wastes were deposited into the burial pits, trenches, and vaults in containers. Approximately 60% of the containers were steel drums (30 to 55 gal), 5% were plywood boxes, and 30% were cardboard and fiberboard containers (EG&G Idaho 1988). Large items such as vehicles and large pieces of equipment were deposited without containers. Section 2.3 provides detailed information on the volatile organic waste disposal.

**2.1.2.4 Access Roads.** Unpaved roads cross the SDA (east-west and north-south) for site access and monitoring (see Figure 2-5). Use of magnesium chloride as a dust suppressant and for

road surface enhancement was used on a trial basis in 1984 and continued in 1985 (EG&G Idaho 1985). Water for dust control is applied only on SDA roads and only during the hottest summer days.

**2.1.2.5 Surface Water Runoff Controls.** After a flood in 1962, a diversion drainage system was constructed around the perimeter of the SDA. After a flood in 1969, the dikes around the SDA were raised and exterior drainage ditches were enlarged. New dikes and ditches were designed to accommodate and withstand a major local runoff, even in the presence of deep snowdrifts. The ditches were made large enough so that heavy equipment could be used to clear snowdrifts in the ditches and prevent their blockage. In 1976, a sump pump was installed near the east perimeter fence to keep water from flowing over the trenches (EG&G Idaho 1985).

Numerous flood-control measures were taken following the flooding in February 1982. The drainage channels inside and outside the SDA were widened. Culverts were installed in the road between the SDA and the dry lake bed south of the SDA, and the southeastern SDA culvert was removed. A second sump pump was moved from the SDA north fence (east of the early waste retrieval site) and was installed at the SDA beside the sump pump near the east SDA fence (south of the access road). The second sump pump doubles the pumping capacity at the SDA location that is subject to flooding. An additional forklift-portable emergency sump pump was procured. In the spring of 1984, Flood Control Dike 1 was raised 6 ft and Dike 2 was raised 8 ft. The dike surrounding the SDA is currently at a top elevation of 5,015 ft corresponding to actual heights above the SDA of between 2 to 15 ft. There is also a smaller dike surrounding the open low-level waste pit in the SDA. Rock rip-rap was placed on both dikes. In 1985 the drain system was enhanced with the installation of a flowmeter, automatic water sampler, and two culverts. The latter provide passive flood control and were designed to meet the 100-year flood criteria (EG&G Idaho 1985).

The SDA has been regraded several times to direct surface water runoff, reduce water infiltration or soil erosion, and provide additional shielding. By the fall of 1969, all holes, crevices, and cracks were routinely filled in preparation for the spring snowmelt. In 1972, grading was instituted to improve drainage. That same year, a topographic study of the area was done to determine the areas that needed to be filled (EG&G Idaho 1985). Regrading has been periodically performed since that time.

**2.1.2.6 Utilities and Security.** Although the SDA is used strictly for disposal purposes (administrative functions are performed at the RWMC outside of the SDA boundaries), it has all vital utilities. Power for the SDA comes from the Experimental Breeder Reactor 1/Waste Management Office main feeder line that originates at the Scoville Substation in the Central Facilities Area (CFA) of the INEL. The 12.5-kV lines pass through the RWMC Administrative Area, into the TSA, and to the northeast corner of the SDA. Power is distributed here by a 20-kV pole-mounted transformer. Emergency power is provided by a 175-kW propane generator located outside of the SDA. The fire protection system for the SDA consists of an 8-in. dry fire-water line, two fire hydrants, and a post indicator valve that is kept closed.

Current fencing around the SDA consists of a newly installed chain-link fence topped with three strands of barbed wire. This new fence follows the path of the previous barbed-wire fence except that it runs along the outside of the surface water control dike surrounding the SDA. The fence has a total length of approximately 7,400 ft and contains three 30-ft gates, each centered on an existing roadway. These fences are locked and patrolled during nonoperational hours. More detailed information on utilities can be found from Figures 2-2, 2-4, and 2-5 in EG&G Idaho (1988).

### 2.1.3 Previous Investigations and Interim Measures

**2.1.3.1 Previous Investigations.** As part of the Resource Conservation and Recovery Act (RCRA) facility investigation plan for the SDA, approved April 5, 1989, EG&G Idaho conducted onsite field tests to demonstrate the effectiveness of the vapor vacuum extraction (VVE) process. A two-week test was performed during November 1989. This preliminary test was performed to check out system operation including the data accumulation system and sampling/analysis procedures.

Following the preliminary test, a four-month VVE test began on April 12 and ended on August 13, 1990. The VVE system operated a total of 2,090 hours extracting 65 million cubic feet of soil gas with 429 kg of carbon tetrachloride and 163 kg of TCE being removed from the basalts beneath the RWMC. VVE is considered a viable remedial technology for removal of VOCs from the vadose zone beneath the SDA.

**2.1.3.2 SDA Surface Contour.** From December 1987 through February 1988 existing SDA surface contour was assessed to determine the existing land irregularities and the extent of the SDA maintenance program. The current program consists of weed control; monthly surface contour evaluations to identify subsidence, cracks, and other irregularities; and filling subsidence as required to prevent ponding of water over waste disposal areas. In February 1988 SDA contour maps were developed using aerial photographs to determine surface depressions and areas with insufficient slope for proper drainage (see Figure 2-6 located in back of this document). The study results indicated that sufficient ponding of surface water on the SDA existed to cause infiltration into the buried waste.<sup>a</sup>

The objective of the SDA contouring activities is to minimize ponding of surface water, thus reducing infiltration into the SDA buried waste and migration of radioactive and hazardous constituents from the buried waste.

The contouring activities involve filling all existing surface depressions and enhancing the grade to an extent that sufficient drainage can occur without creating major elevation changes. However, these improvements alone will not totally alleviate the ponding problem. The contouring will direct most of the SDA surface water runoff into the existing drainage channels at the perimeter of the SDA, as well as the channels along the main road. The present system drains to the sampling/outlet at the extreme east end of the SDA. However, the west end SDA runoff will still drain to the west. To alleviate a ponding problem in this older area, a second sampling/outlet will be installed south of the main road at the extreme west end of the SDA. Water in the west outlet will drain to the perimeter drainage channels and to the channels along the main road.

With the above outlined improvements, a significant reduction of the surface water ponding on the SDA will result, thus greatly alleviating the infiltration problem.

---

a. Engineering Design File RWMC-318, March 24, 1988.

## 2.2 Physical Characteristics

### 2.2.1 Meteorology

Atmospheric transportation of contaminants is controlled by the following physical parameters: climate, local meteorology, local topography and large structures or buildings onsite, and contaminant source strength. This section describes the aspects of these physical parameters that are necessary to evaluate environmental and human health impacts because of atmospheric transportation of contaminants from the RWMC.

**2.2.1.1 Climate.** The climate at the INEL is influenced by the Rocky Mountains and the Snake River Plain that create a semi-arid climate with an average summer day time maximum temperature of 28°C (83°F) and an average winter day time maximum temperature of -0.5°C (31°F). Infrequent cloud cover over the region allows intense solar heating of the ground surface during the day and the low absolute humidity allows significant radiant cooling at night. These factors create large temperature fluctuations near the ground (Bowman et al. 1984). During a 22-year period of meteorological records (1954-1976), temperature extremes at the INEL have varied from a low of -41°C (-43°F) in January to a high of 39°C (103°F) in July.

The average relative humidity at the INEL ranges from a monthly average minimum of 15% in August to a monthly average maximum of 81% in February and December. The relative humidity is directly related to diurnal temperature fluctuations. Relative humidity reaches a maximum just before sunrise (the time of lowest temperature) and a minimum in the late afternoon (time of maximum daily temperature) (EG&G Idaho 1981).

The regional topography and upper-level wind patterns over North America create a semi-arid climate. Average annual precipitation at the INEL is 8.5 in. The highest precipitation rates occur during the months of May and June and the lowest rates are in July.

Snowfall at the INEL ranges from a low of about 12 in. per year to a high of about 40 in. per year, with an annual average of 26 in. Normal winter snowfall occurs from November through April, although occasional snowstorms occur in May, June, and October (EG&G Idaho 1981).

Potential annual evaporation from saturated ground surface at the INEL is approximately 36 in. Eighty percent of this evaporation occurs between May and October. During the warmest month (July), the potential daily evaporation rate is approximately 0.25 in./day. During the coldest months (December through February), evaporation is low and may be insignificant. Actual evaporation rates are much lower than potential rates because the ground surface is rarely saturated. Evapotranspiration by the sparse native vegetation of the Snake River Plain is estimated at between 6 to 9 in. per year, or 4 to 6 times less than the potential evapotranspiration. Periods when the greatest quantity of precipitation water is available for infiltration (late winter to spring) coincide with periods of relatively low evapotranspiration rates (EG&G Idaho 1981).

**2.2.1.2 Local Meteorology.** The local meteorology is influenced by local topography, mountain ranges, and large-scale weather systems. The orientation of the bordering mountain ranges, as well as the general orientation of the eastern Snake River Plain play an important role in determining the wind regime. The INEL is in the belt of prevailing westerly winds, which are normally channeled across the eastern Snake River Plain. This channeling usually produces a west-southwest or southwest wind. When the prevailing westerlies at the gradient level

(approximately 5,000 ft above land surface) are strong, the winds channeled across the eastern Snake River Plain between the mountains become very strong. Some of the highest wind speeds at the INEL have been observed under these meteorological conditions. The greatest frequency of high winds occur mainly in the spring.

Local mountain and valley features exhibit a strong influence on the wind flow under other meteorological conditions. When winds above the gradient level are strong and from a direction slightly north of west, channeling in the eastern Snake River Plain usually continues to produce southwesterly winds over most of the INEL. At the mouth of Birch Creek however, the northwest to southeast orientation of this valley channels strong north-northwest winds into the area. This "Birch Creek" wind may equal the strongest southwesterly winds recorded at other locations on the INEL (EG&G Idaho 1988).

Drainage winds also contribute to the overall wind flow over the INEL. On clear or partly cloudy nights with only high thin clouds, the valley experiences rapid surface radiant cooling. This results in simultaneous cooling of the air near the surface which causes the air to become stable and less turbulent. However, air along the slopes of mountains cools at a faster rate than air at the same elevation located over the valleys. Consequently, it becomes more dense and flows or sinks toward the valley forming a down-slope wind. When this wind reaches the valley, it still flows toward lower elevations and becomes a down-valley wind. Nocturnal down-valley flow is the second most frequent wind observed over the INEL and flows primarily out of the north-northeast.

A reverse flow, opposite in direction to that of the drainage wind, occurs during the daytime when air along the mountain slopes is heated more rapidly than air at the same elevation over the valley. Air rises along the slopes as it becomes less dense. This up-slope wind, in turn, contributes to the production of an up-valley wind. This up-valley wind is seldom detectable as a separate component of the wind until the synoptic pressure gradient becomes quite weak. Although the mountain and valley winds are predominantly "fair weather" phenomena, they can also occur under other sky cover conditions.

In addition to the relatively local drainage winds, a somewhat stronger wind has occasionally been observed. It develops when an outbreak of cold air east of the Continental Divide occurs and behaves in the same manner as the down-valley wind. If the cold air becomes deep enough, it spills over the Continental Divide and flows down across the eastern Snake River Plain. The result of this phenomenon is valley winds from the northeast.

The surface winds at the RWMC can be compared with the those of the Central Facilities Area (CFA) which are summarized graphically in the annual wind rose (Figure 2-7). The wind rose was produced from wind data at the CFA meteorological station collected from 1980 to 1982.

Pressure gradient forces related to passing synoptic weather systems, as well as local storms, all affect the winds of the INEL. These storms alter the local flow regime such that winds from any direction can be observed.

High wind-speed episodes occur in all months of the year, with the highest average hourly winds occurring during winter and spring. The passage of synoptic frontal systems involves higher and more sustained average hourly wind-speed events than those of thunderstorm gust fronts (Bowman et al. 1984).

Station: CFA  
Period: 1980-1982  
Stability: SUM  
Wind frequency by direction  
Breakdown by wind speed category

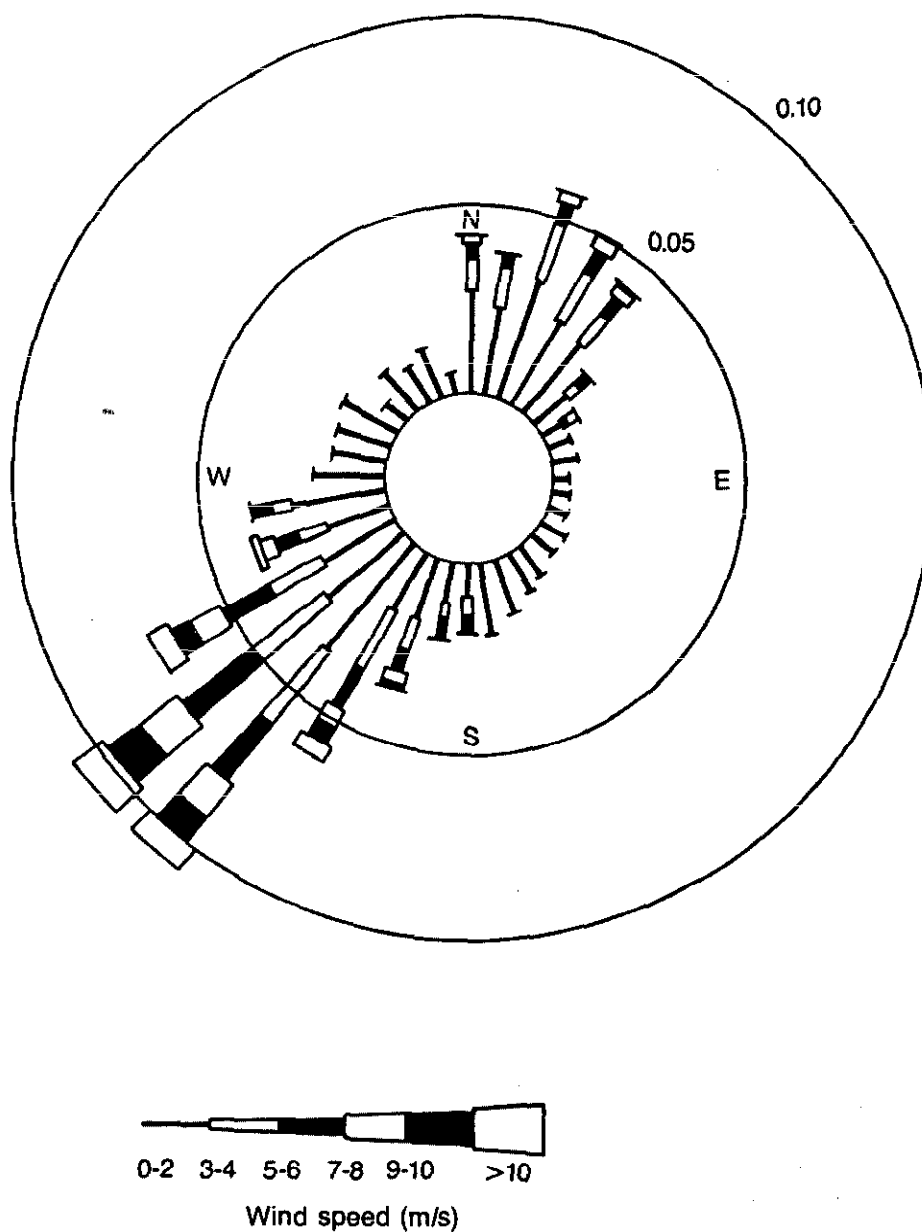


**Figure 2-7.** Wind rose for the Central Facilities Area.

8-7697



The INEL is subject to severe weather episodes throughout the year. Thunderstorms with occasional tornadoes are observed mostly during the spring and summer. The tornado risk probability at the INEL is about  $7.8 \times 10^{-5}$  per year for the INEL area (Bowman et al. 1984). An average of two to three thunderstorms occur during each of the months from June through August (EG&G Idaho 1981). Thunderstorms may be accompanied by strong, gusty winds that may produce local dust storms.

Occasionally, rain in excess of the long period average monthly total precipitation may be recorded at a monitoring station on the INEL resulting from a single thunderstorm (Bowman et al. 1984). Precipitation from thunderstorms at the INEL is generally light.

Dust devils are also common in the region. Dust devils can entrain dust and pebbles and transport them over short distances. They usually occur on warm sunny days with little or no wind. The dust cloud may be several hundred yards in diameter and extend several hundred feet in the air (Bowman et al. 1984).

The vertical temperature and humidity profiles in the atmosphere determine the atmospheric stability. Stable atmospheres are characterized by low levels of turbulence and less vertical mixing. This results in higher ground level concentrations of emitted contaminants. The stability parameters at the INEL range from extremely stable to very unstable. The stable conditions occur mostly at night during strong radiant cooling. Unstable conditions can occur during the day when there is strong solar heating of the surface layer or whenever a synoptic scale disturbance passes over the region.

**2.2.1.3 Local Topography.** The terrain in and around the INEL may affect the ambient ground-level concentrations of contaminants emitted from the RWMC. Land features located above the elevation of the source may create relatively higher ambient concentrations than features located at the same elevation as the source. The overall terrain at the INEL is flat with some small depressions and mounds, and small buttes.

**2.2.1.4 Large Structures and Buildings.** Buildings and large structures can increase the degree of turbulence in the air. The dispersion of contaminants is directly related to the degree of air turbulence. The largest buildings at the RWMC are about 30 ft tall. The low profile of these buildings will not significantly affect the degree of turbulence at the INEL. The RWMC can, therefore, be characterized as rural for dispersion analysis purposes.

## **2.2.2 Geology**

The SDA is located on the eastern Snake River Plain, a broad flat plain consisting of basaltic lava flows with thicknesses up to several thousand feet and interbeds of loess, eolian sediments, alluvial fan deposits, and lacustrine sediments. The upper 700 ft of basaltic lavas at the SDA were the result of 10 eruptive episodes occurring from about 75,000 to 600,000 years ago (Anderson and Lewis 1989; and Kuntz et al. 1980). The flows erupted from fissure vents in volcanic rift zones, the majority of which trend northwest along the northeast trending eastern Snake River Plain. The rift zones are thought to be associated with extension tectonics caused by the continuation of the Basin and Range tectonism (EG&G Idaho 1984). The basaltic lavas are underlain by rhyolitic volcanic rocks. Several of the rhyolitic domes have erupted through the basaltic pile near the southern boundary of the INEL.

The Big Southern Butte Complex is approximately 300,000 years old, and is one of several complexes believed to have erupted from rhyolitic calderas aligned in a northeast trending belt. These rhyolites apparently consisted of very viscous lavas which intruded as domes representing the waning stages of explosive silicic volcanism (Bowman et al. 1984). Descriptions of the INEL fault studies, seismology, and volcanic hazards, along with some geologic maps for the INEL, are summarized in Bowman et al. (1984).

The eastern Snake River Plain is bounded on the north and west by Cenozoic fault-block mountains of the Lost River, Lemhi, and Beaverhead ranges (Figure 2-8). These ranges are composed of Paleozoic limestones, dolomites, and shales. The fault-block ranges trend northwest-southeast and the volcanic rifts parallel the ranges and are believed to be surface expressions of extensions of the range-front faults.

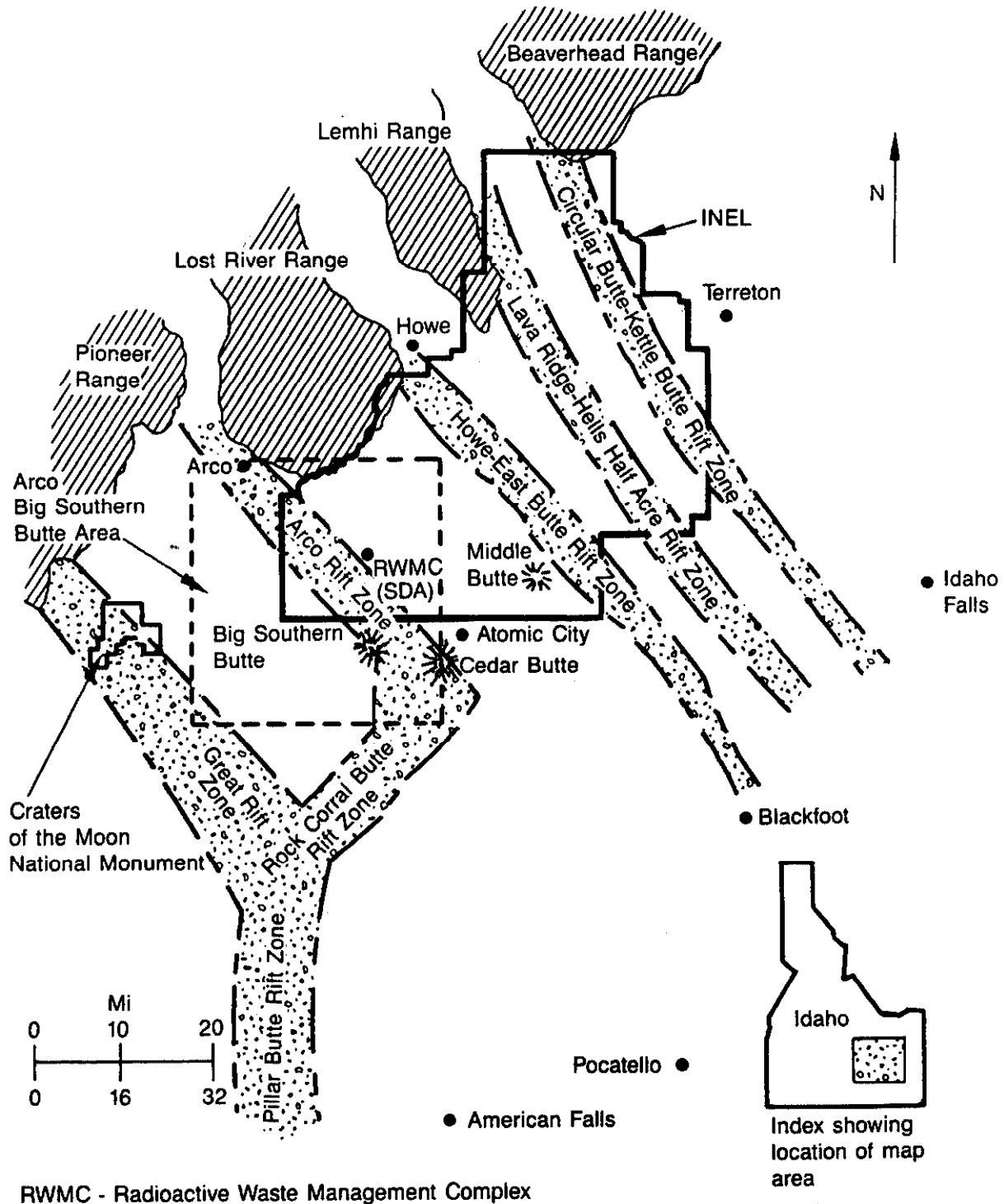
**2.2.2.1 Seismic Activity.** The seismic activity of eastern Idaho is concentrated along the Intermountain Seismic Belt, which extends more than 800 miles from southern Arizona, through eastern Idaho, to western Montana (Figure 2-9). The Idaho seismic zone, one of two zones in this belt, extends from the Yellowstone Plateau area westward into central Idaho. Minor earthquakes have occurred on the eastern Snake River Plain, east and north of the INEL [averaging about 1.0 local magnitude ( $M_L$ )].

The largest earthquake recorded for the Idaho seismic zone occurred on October 28, 1983, measuring 7.3 on the Richter scale. This earthquake resulted from movement along a range-front fault. The epicenter was approximately halfway between Challis and Mackay, and the faulting broke the surface for 25 mi along the western base of the Lost River Range. Although the earthquake was felt at the INEL, there was no structural or safety related damage to the facility. Table 2-1 lists the largest earthquakes in the eastern Snake River Plain area since 1884 (Bowman et al. 1984).

**2.2.2.2 Volcanic Hazard.** The main volcanic hazard for the SDA is from potential lava flows from source vents offsite. Kuntz (1978) identified 47 separate basaltic eruptions within the last 200,000 years in the basin where the source vents from the SDA basalts are located, the most recent being approximately 75,000 years ago. The SDA is situated in the same basin, so the potential exists for lava flows to inundate the complex from future eruptions (Kuntz 1978). The potential for rhyolitic eruptions appears to pose less of a threat to the SDA because of the intrusion of high viscosity rhyolitic domes that indicate the waning stages of silicic volcanism. The chief volcanic hazards would be the rupture of waste containers and dispersion of wastes from potential fissure eruptions within the SDA (Kuntz 1978).

**2.2.2.3 Stratigraphy at the SDA.** The basalt flows beneath the SDA are interbedded with and overlain by sediments composed primarily of fine sand, silt, and clay. The interbeds probably formed during periods of volcanic quiescence, which allowed alluvial and eolian sediments to be deposited. Three to five percent of the deposits contain rounded gravels in both surface and interbed sediments, indicating some stream deposition. Lacustrine interbed deposits, characterized by silts and clays, may have formed when lava flows dammed stream channels, creating small lakes in which the finer sediments were deposited.

The stratigraphy of the SDA has been evaluated from drilling data. The basalt flows in the unsaturated zone and upper portions of the Snake River Plain Aquifer underlying the SDA have been conceptually grouped into 10 basalt-flow groups, consisting of 22 basaltic lava flows based on



8-7696

**Figure 2-8.** Regional geology and volcanic structures near the INEL (Kuntz 1978).

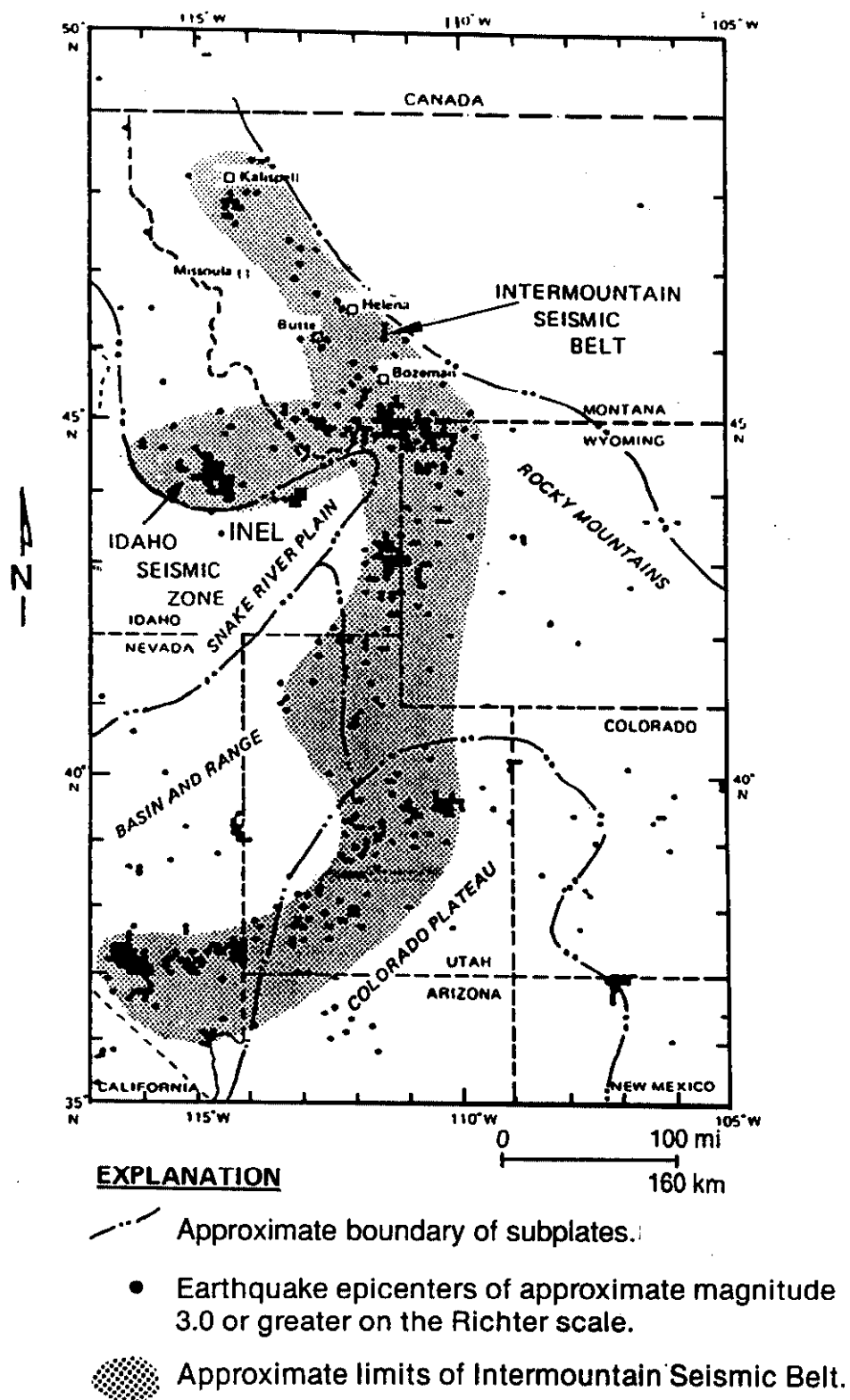


**Figure 2-9.** Intermountain seismic belt (Stickney and Bartholomew 1987).

**Table 2-1.** Largest earthquakes in regions surrounding the eastern Snake River Plain since 1884 (Bowman et al. 1984).

Date	Latitude	Longitude	Magnitude	Location
November 10, 1884	42.0	111.3	6	Bear Lake Valley <sup>a</sup>
October 5, 1909	41.3	112.7	6	Hansel Valley, Utah <sup>a</sup>
June 27, 1925	26.0	112.2	6.75	East of Helena, Montana <sup>a</sup>
March 12, 1934	41.7	112.3	6.6(M <sub>s</sub> )	Hansel Valley, Utah <sup>a</sup>
October 31, 1935	46.6	112.0	6.25	Helena, Montana <sup>a</sup>
July 12, 1944	44.7	115.2	6.1	Helena, Montana <sup>a</sup>
February 13, 1945	44.7	115.4	6.0	Seafoam, Idaho <sup>a</sup>
November 23, 1947	44.3	112.0	6.25	Southwestern, Montana <sup>a</sup>
August 17, 1959	44.3	111.1	7.1	Hebgen Lake, Montana <sup>a</sup>
August 18, 1959	44.3	110.7	6	Yellowstone Park, Wyoming <sup>b</sup>
August 18, 1959	44.3	111.6	6.25	Southwestern Montana <sup>b</sup>
March 27, 1975	44.8	110.5	6.1(M <sub>b</sub> ) <sup>c</sup>	Pocatello Valley, Idaho
			6.0(M <sub>L</sub> M <sub>s</sub> )	Idaho-Utah border <sup>a</sup>
June 30, 1975	44.8	110.6	6.1(M <sub>L</sub> ) <sup>d</sup>	Yellowstone Park, Wyoming <sup>a</sup>
			5.9(M <sub>s</sub> )	
October 28, 1983	44.05	113.89	7.3	Borah Peak, Idaho

a. Includes mainshocks (or largest swarm events) of magnitude 6.0 or greater (or M.M. intensity VIII for preinstrumental shocks from 1852 through July 1980).

b. Part of 1959 Hebgen Lake earthquake sequence.

c. M<sub>s</sub> is the magnitude of surface waves.

d. M<sub>L</sub> is the local magnitude.

core and thin-section studies (Anderson and Lewis 1989; and Kuntz et al. 1980). Basalt-flow groups unconformably overlie older flow groups or are interbedded with thin to thick layers of sediment. The basalts are intercalated with seven sedimentary interbeds, three of which have been studied previously at the SDA and are referred to as the 30-ft, 110-ft, and 240-ft interbeds (Anderson and Lewis 1989 and Barraclough et al. 1976). Figure 2-10 through 13 are geologic sections showing the generalized stratigraphy underlying the RWMC.

The uppermost basalt-flow group is covered by surface sediments ranging in thickness from 0 to 22 ft. This flow-group is composed of three to five flows, the lower two to three flows are separated from the upper flows in the western part of the SDA by the 30-ft interbed, consisting of thin and discontinuous sedimentary materials. The next basalt-flow group is separated from the uppermost flow group by the 110-ft sedimentary interbed, which varies from a trace to 30 ft thick and is continuous beneath most of the SDA. This flow group consists of three to five flows, none of which are separated by sedimentary interbeds.

The basalt-flow groups overlying and comprising the upper portions of the Snake River Plain Aquifer are separated from the above basalt-flow group by the 240-ft interbed. The 240-ft interbed is up to 33-ft thick and is continuous beneath the SDA. The basaltic flows and cinder beds that comprise the upper part of the sequence of volcanic rocks are underlain by rhyolitic ash flows and tuffs. More detailed descriptions of the lithologies can be found in Anderson and Lewis (1989) and Barraclough et al. (1976).

**2.2.2.4 Basalt Flows.** All of the basalts beneath the SDA have similar petrographic characteristics and are tholeiitic olivine basalts. These similarities suggest that the basalts erupted from the same magma source. In general, the basalts consist of olivine, plagioclase, clinopyroxene, ilmenite, magnetite, accessory apatite, trace amounts of zircon, and volcanic glass (Kuntz et al. 1980). Olivine occurs as phenocrysts and/or as a constituent of the rock matrix. Plagioclase also occurs as phenocrysts and smaller matrix crystals, often as aggregates of plagioclase laths arranged in irregular clusters. Clinopyroxene occurs as an anhedral phase of the rock matrix. Ilmenite is primarily found in slender blades and needles, and magnetite occurs most often as equant crystals with square, rectangular, or irregular shapes (Kuntz et al. 1980).

The tops and bottoms of the individual flows are characterized by clinkery, vesicular, fractured basalt. The basalts are generally dense and much less fractured in the middle of the flows. Many of the open fractures in the basalt are filled with clay particles carried by infiltrating water. The clay particles are deposited as layers on the fracture surface or in open vesicles. Flooding carries coarser (silt- and sand-sized) material into the fractures. Some vesicles and fractures are filled with calcareous fine silt and clay.

The basalts typically form ridges and valleys on the surface. There are places where the basalts may have ponded when they were trapped in topographic depressions.

**2.2.2.5 Sedimentary Interbeds.** The 30-ft, 110-ft, and 240-ft sedimentary interbeds have been studied previously at the SDA. The 30-ft interbed consists of reddish brown to dark brown silty clay. The reddish-brown color results from oxidation of iron-rich minerals. Organic-rich paleosols were encountered in several wells. In addition, baked clays occur in this interbed, overlain by a cinder zone in one well (Rightmire and Lewis 1987). The top of the 110-ft interbed contains a dark brown, organic-rich soil horizon. Basalt pebbles with iron-oxide-filled vesicles occur in this interbed. Some

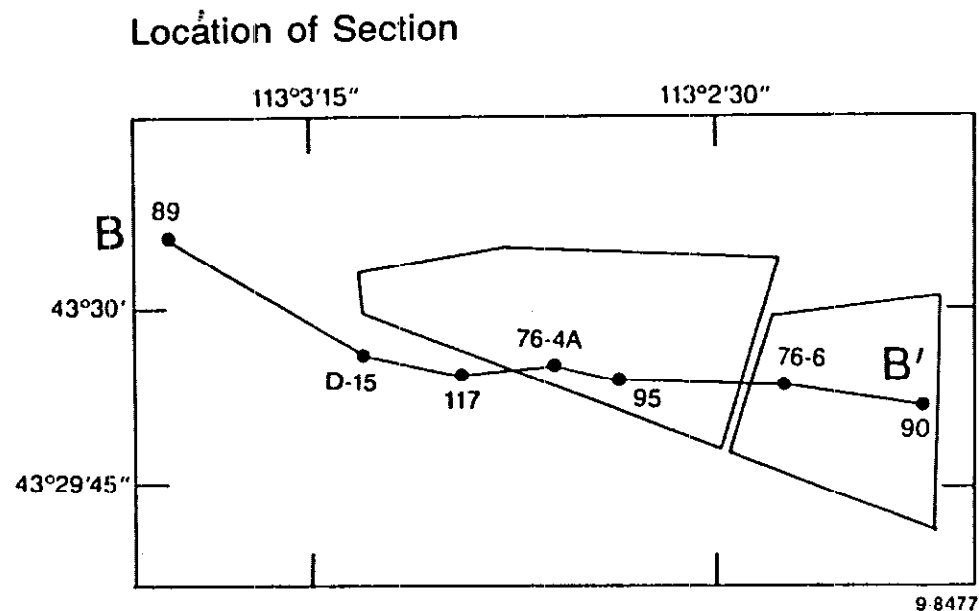
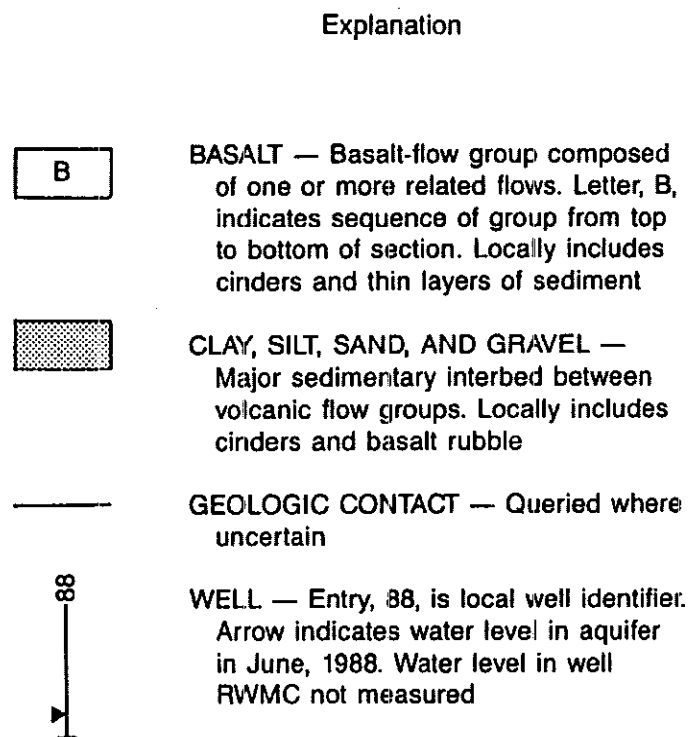


**Figure 2-10.** Geologic Section B-B' at the Radioactive Waste Management Complex (Part 1).

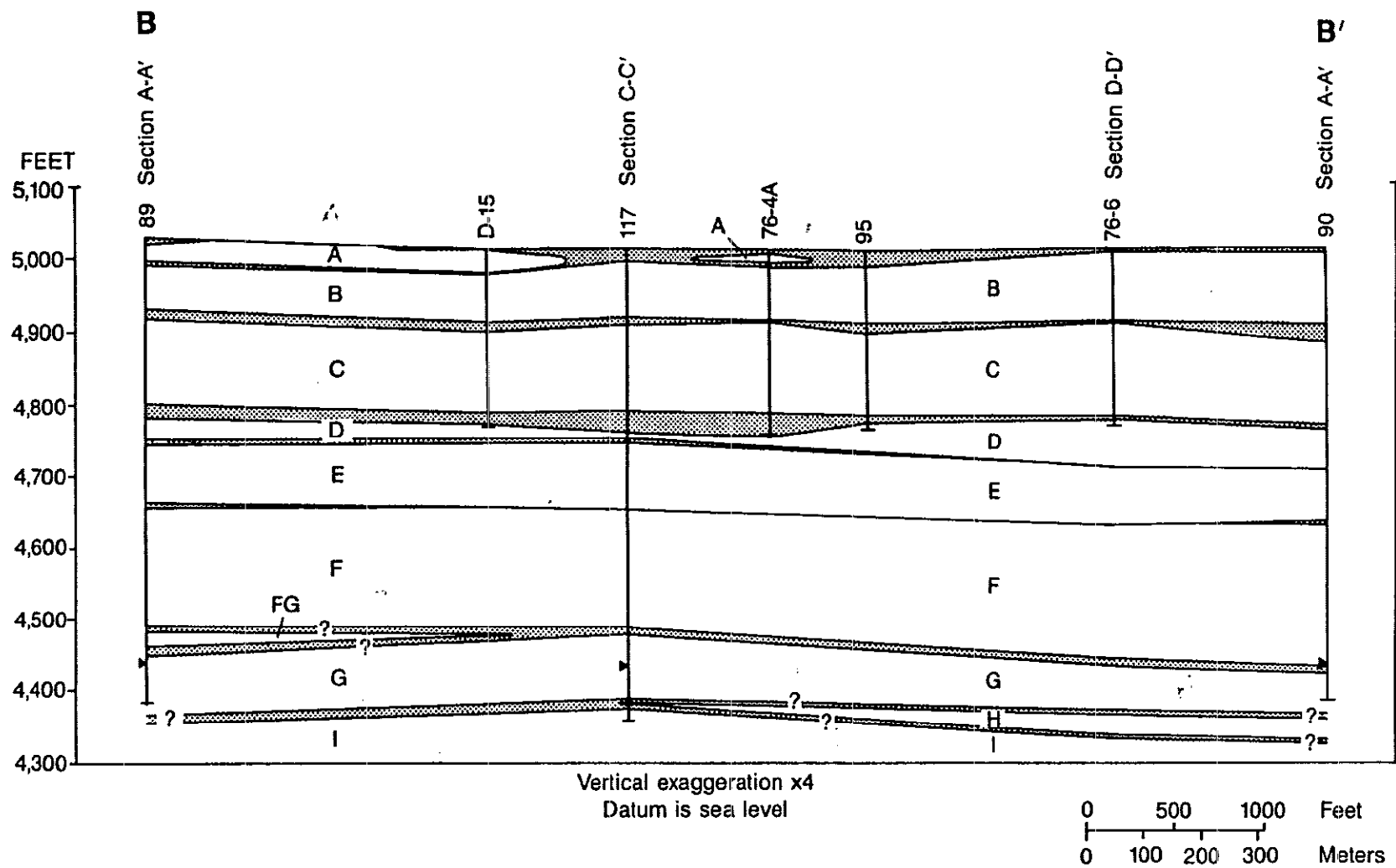
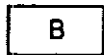


**Figure 2-11.** Geologic Section B-B' at the Radioactive Waste Management Complex (Part 2).

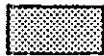
9-8481



## Explanation



**BASALT** — Basalt-flow group composed of one or more related flows. Letter, B, indicates sequence of group from top to bottom of section. Locally includes cinders and thin layers of sediment



**CLAY, SILT, SAND, AND GRAVEL** — Major sedimentary interbed between volcanic flow groups. Locally includes cinders and basalt rubble



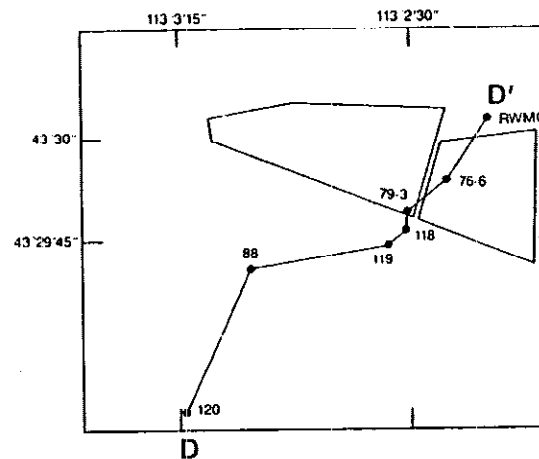
**GEOLOGIC CONTACT** — Queried where uncertain



**WELL** — Entry, 89, is local well identifier. Arrow indicates water level in aquifer in June, 1988

2-24

## Location of Section



9-8479

**Figure 2-12.** Geologic Section D-D' at the Radioactive Waste Management Complex (Part 1).

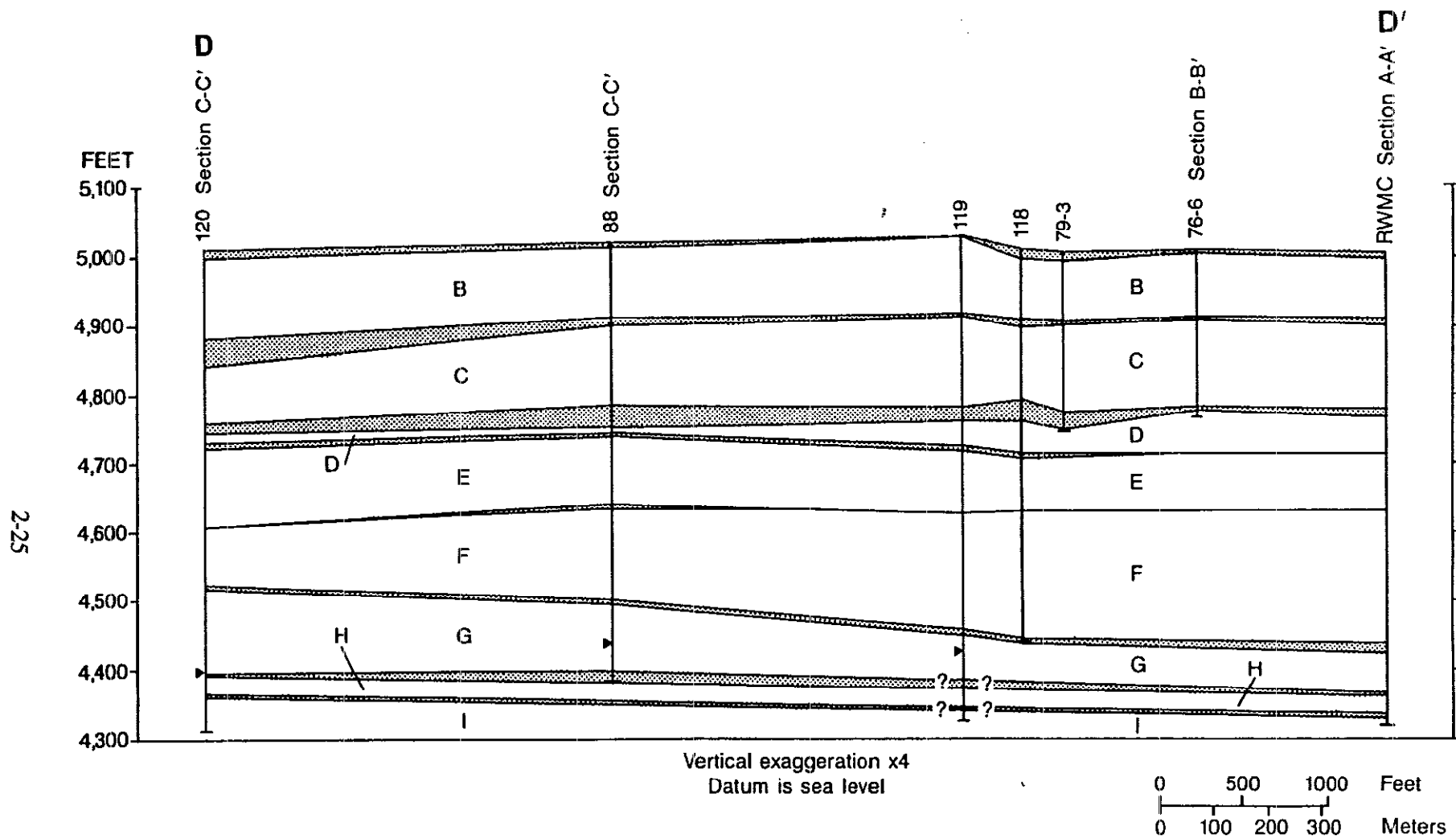


**Figure 2-13.** Geologic Section D-D' at the Radioactive Waste Management Complex (Part 2).

9-8480

of the pebbles are coated with a calcium carbonate crust, and small aggregates of opaline silica are contained in the calcium carbonate crust (Rightmire and Lewis 1987). The 240-ft interbed is typical of a stream deposit with clays, silts, sands, and gravels. Fluvial gravels make up over 50% of the interbed (Rightmire and Lewis 1987). The interbed material is uniformly oxidized throughout its thickness. At the time this interbed was deposited, the SDA area may have been the flood plain of the Big Lost River (Rightmire and Lewis 1987). More information on the composition and lithology of the interbeds is in Barraclough et al. (1976).

The structural maps shown on Figures 2-14 to 2-16 were constructed for the base of each interbed; thus, they represent the topography of the surface of the basalts on which the interbeds were deposited. A structural low may depict an alluvial flow or stream channel area, while a structural high may depict an interchannel ridge. The thickness maps (Figures 2-14 to 2-16) indicate the variations in thickness of the sediment layers. A comparison of the structural and thickness maps for each interbed indicates that the topographic lows (potential channel areas) accumulated the thickest sedimentary units (Laney et al. 1988).

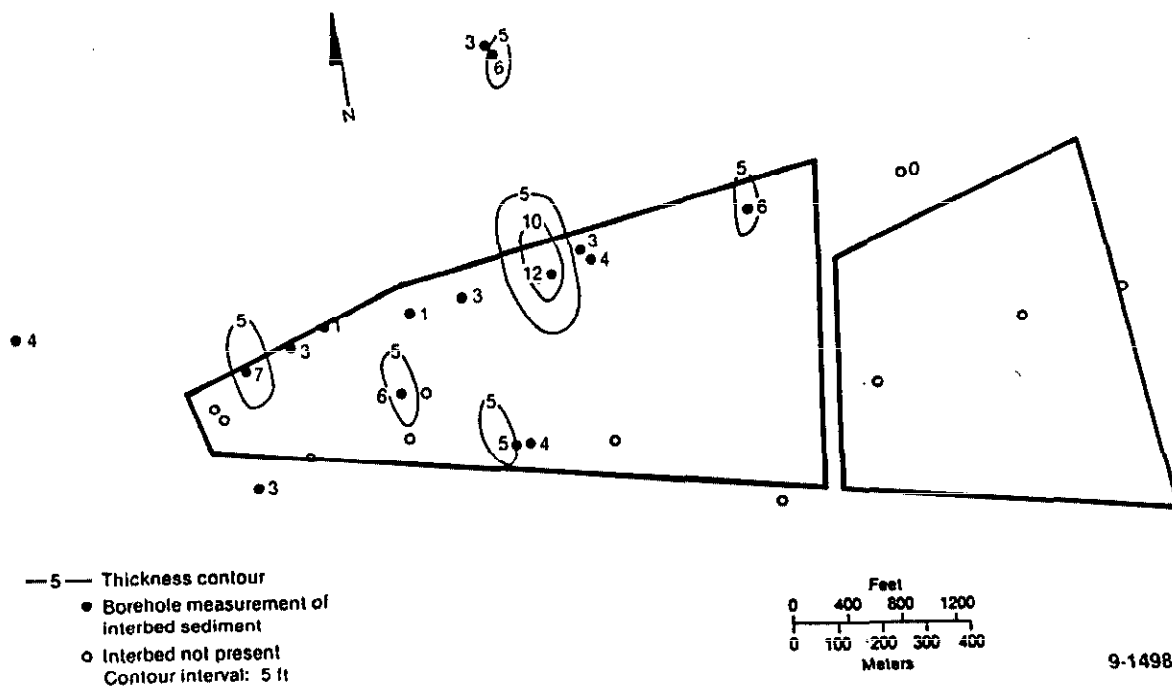
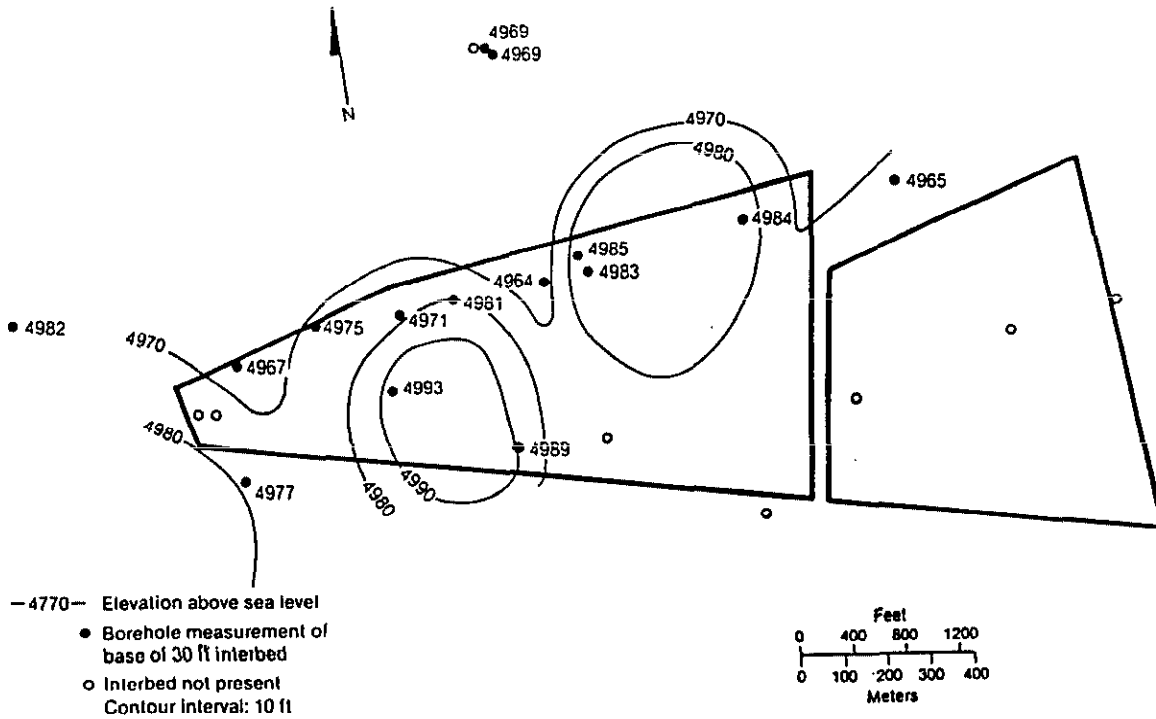
The structural and thickness maps of the 110-ft interbed best illustrate the potential alluvial flow or stream channel pattern. The maps indicate that the base of a structural high exists in the central portion of the SDA. A comparison of the maps shows that this corresponds to a thin layer of sediment. Similar interbed trends can also be seen in the structural and thickness maps of the 30-ft and 240-ft interbeds.

### **2.2.3 Surface Water Hydrology**

**2.2.3.1 Regional Surface Water Hydrology.** The INEL resides almost entirely in the Pioneer Basin, a closed topographic depression located on the Snake River Plain. The Pioneer Basin receives intermittent surface flow from three drainage basins to the north and west: the Big Lost River Basin, Little Lost River Basin, and Birch Creek Basin (see Figure 2-17) (Niccum 1973). The Big Lost River and Pioneer Basin range in elevation from about 4,700 to over 12,600 ft above mean sea level (msl). The largest runoff periods in the area of the basins at lower altitudes have historically occurred during January, February, and March. The maximum runoff from the highlands usually occurs in May or June. In Pioneer Basin, the ground thaws in March or April, preparing the soil to accept surface water by infiltration a month or two before the snowpack in the higher elevations melts (Niccum 1973).

The greatest amounts of precipitation occur on the mountain slopes of the three basins bordering Pioneer Basin. An annual maximum of 50 in. of precipitation has been recorded in the higher elevations between the Big Lost River and the Little Lost River basins. Pioneer Basin receives an average of 8 in. of precipitation annually, but variations ranging from 5 in. to over 14 in. of total annual precipitation have been recorded between 1950 and 1965 (Barraclough et al. 1976). This precipitation range affects the amount of infiltration and percolation to the water table. The relationships between natural recharge events such as rainfall and snow activity in the spreading areas have been discussed in Wood and Wylie (1991).

**2.2.3.2 Big Lost River.** The Big Lost River is the main surface water feature of the Big Lost River and Pioneer basins. The main stem of the Big Lost River is formed by the confluence of its east fork and north fork located about 22 mi northwest of Mackay Dam, which impounds the river



9-1498

**Figure 2-14.** Structural and isopach maps of 30-ft sedimentary interbed (Laney et al. 1988).

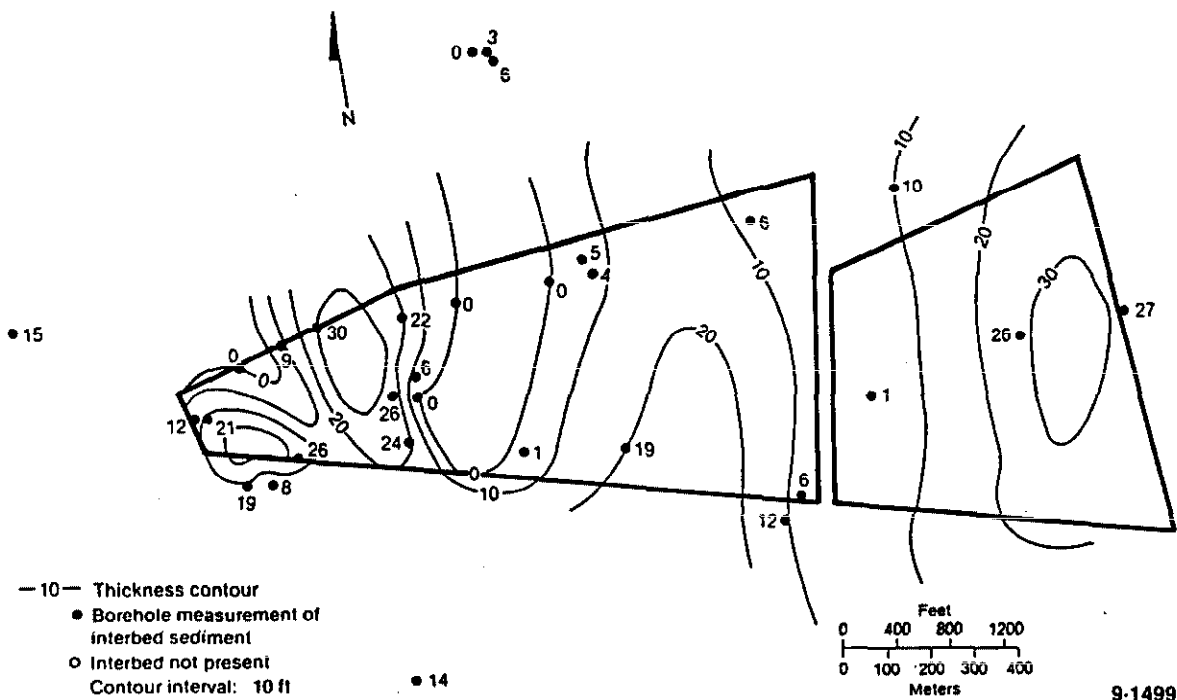
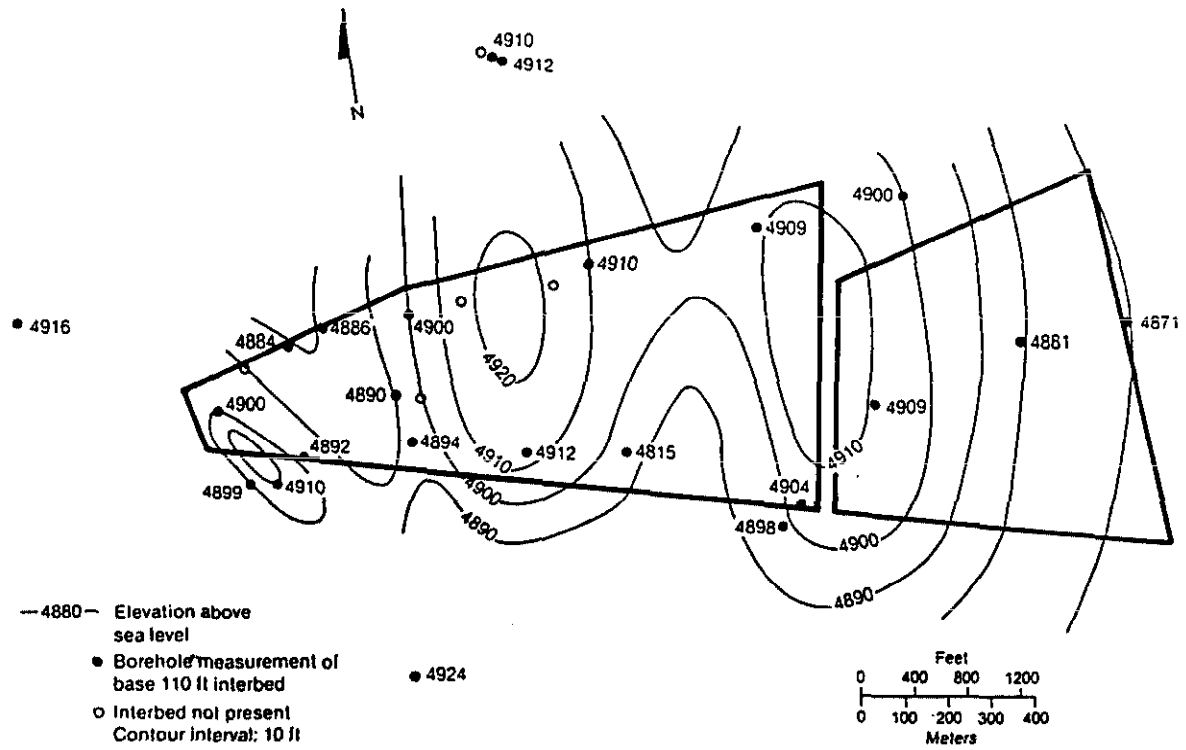


Figure 2-15. Structural and isopach maps of 110-ft sedimentary interbed (Laney et al. 1988).

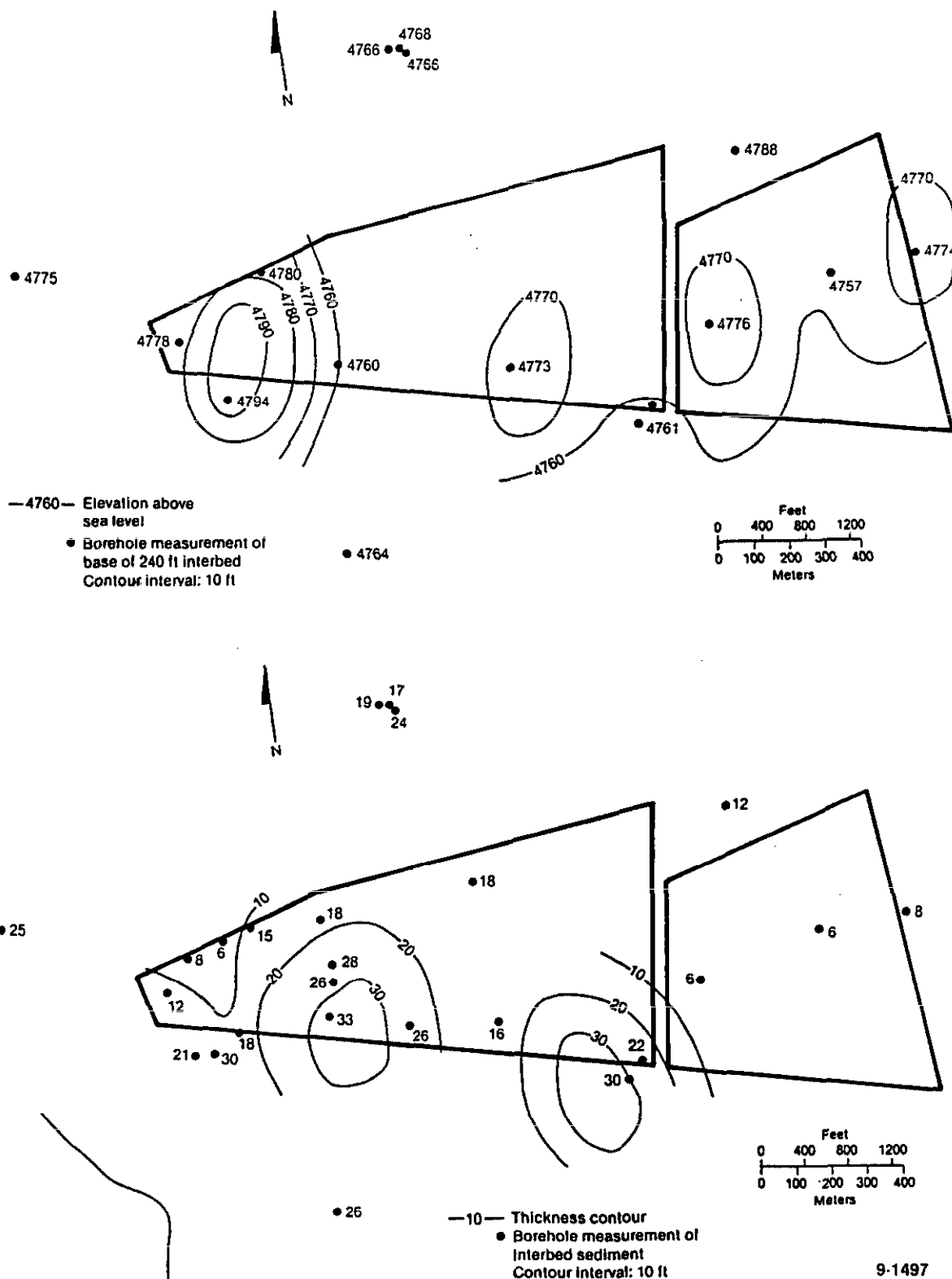


Figure 2-16. Structural and isopach maps of 240-ft sedimentary interbed (Laney et al. 1988).

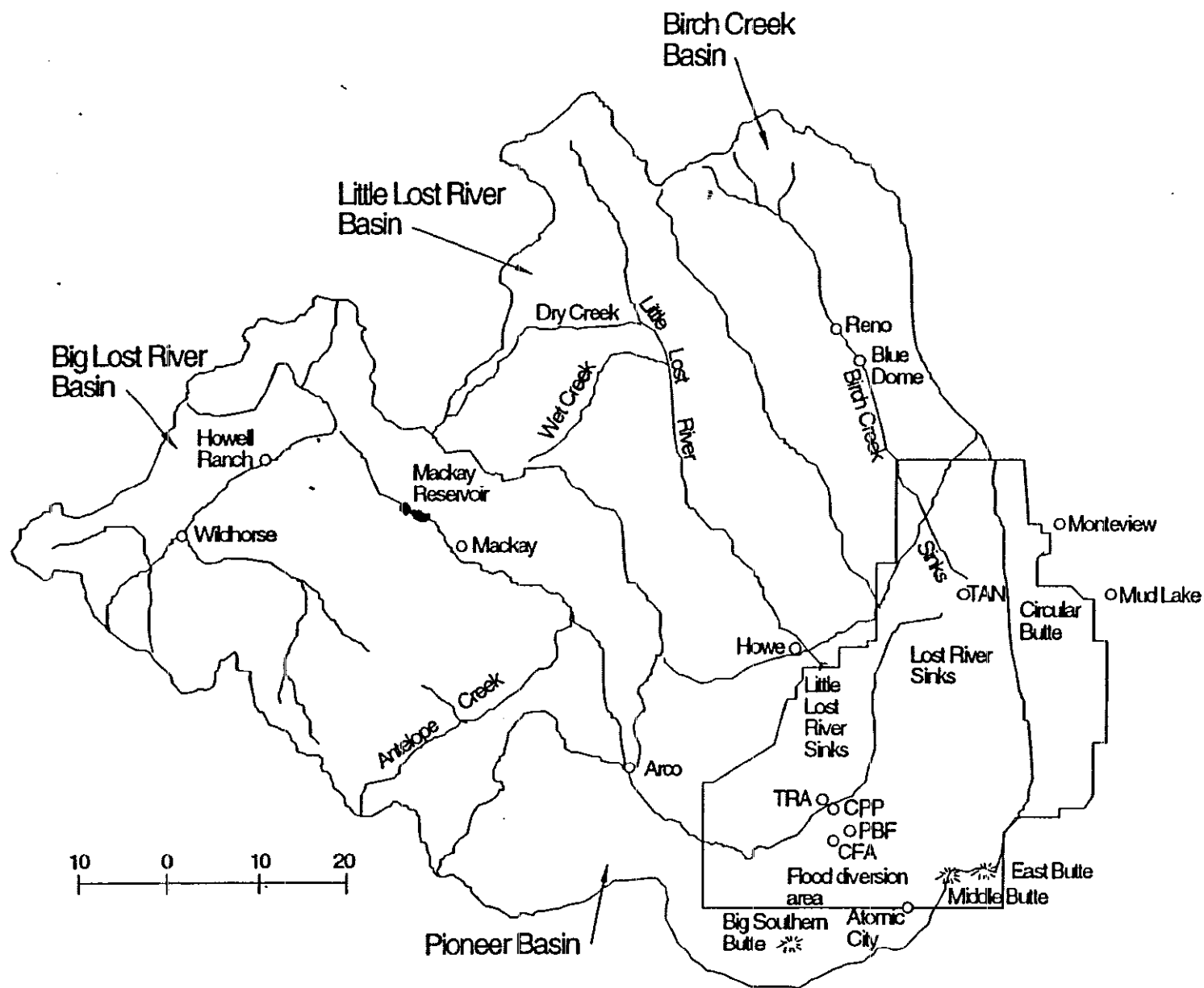


Figure 2-17. Drainage basins affecting the INEL (Niccum 1973).

approximately 4 mi northwest of Mackay (see Figure 2-18). The drainage basin above the dam has an area of 788 mi<sup>2</sup>. A significant portion of the natural streamflow is controlled by the dam, which stores runoff for irrigation (Koslow and Van Haaften 1986).

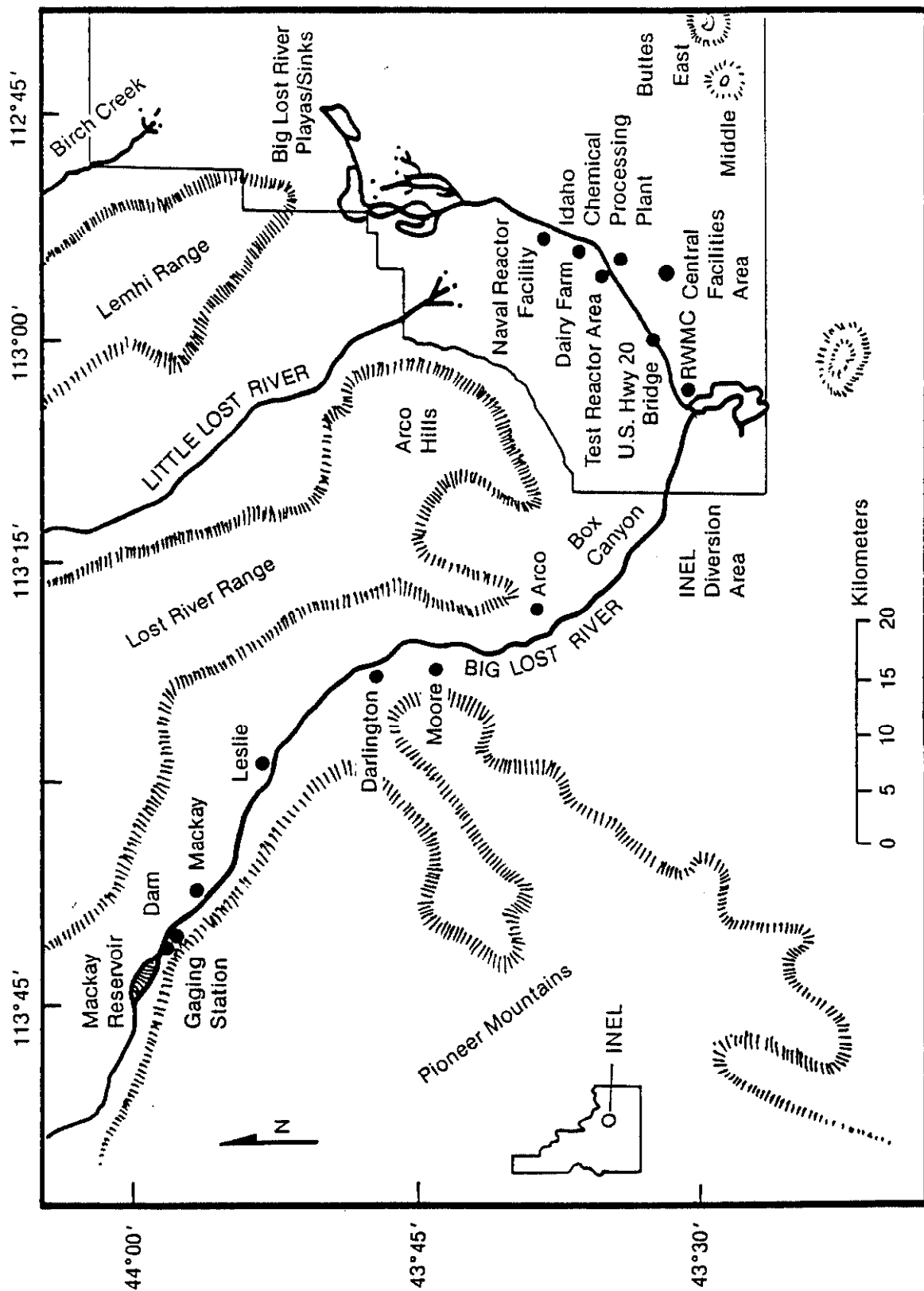
The Big Lost River flows southeast from Mackay Dam down the Big Lost River Valley past Arco into the Pioneer Basin (see Figure 2-18). Southeast of Arco, the river enters Box Canyon, a narrow canyon approximately 7 mi long with an average height of 70 ft and a width of 130 ft. The walls of the canyon are composed of fractured basalt and are nearly vertical. The river exits Box Canyon and flows to the INEL Diversion and Spreading Areas, constructed in 1958 to divert high runoff flows away from the INEL facilities. Flows not diverted at the INEL diversion dam pass northward across the INEL Site in a shallow, gravel-filled channel. This main channel branches into several channels 18 mi northeast of the diversion dam, forming four shallow sinks, referred to as the Big Lost River Sinks (Koslow and Van Haaften 1986).

The two northeast-trending tributaries of the Big Lost River generally flow through bedrock valleys and undergo minimal surface water losses to groundwater underflow until they join the main northwest trending valley. The river leaves the bedrock valley near Howell Ranch and flows over deep alluvium where infiltration rates are high (see Figure 2-19). At Arco the drainage characteristics change. The river flows over a broad, flat flood plain underlain by basalt for the first few miles below Arco (Niccum 1973). Surface drainage is confined to the Pioneer Basin in the INEL, and no surface water enters the Snake River (Koslow and Van Haaften 1986). Any Big Lost River waters not diverted for irrigation purposes are lost to evaporation or percolate to the water table, recharging the Snake River Plain Aquifer. Infiltration and depression storage losses are most significant in Box Canyon and the Big Lost River Sinks due to fractured basalt. Only in times of heavy runoff does the Big Lost River flow to its terminus at the sinks in the northwest corner of the INEL (Koslow and Van Haaften 1986).

The flow of the Big Lost River is measured at the gauging stations operated by the USGS below the Mackay Reservoir (30 mi northwest of Arco) and at the INEL diversion. The average annual discharge for 69 years of record for the Big Lost River, as measured at the Mackay gauging station, is 227,500 acre ft/y (see Figure 2-20) (Pittman et al. 1988). The main river channel flow just below the INEL diversion was 70,000 acre ft in 1974, and the INEL diversion channel flow in the same year was 32,000 acre ft (see Figure 2-21). In 1975, a total of 88,000 acre ft flowed down the main channel of the Big Lost River and 46,000 acre ft flowed through the INEL diversion channel. In 1976, only 38,000 acre ft flowed through the main channel and 18,000 acre ft flowed through the INEL diversion channel (Barracrough et al. 1981). Flow increased markedly from 1981 to 1984 with a total of 476,000 acre ft at the diversion in 1984, the highest rate yet recorded. In 1984 and 1985, flow in the main channel was maintained at 57,000 acre ft/y (Pittman et al. 1988).

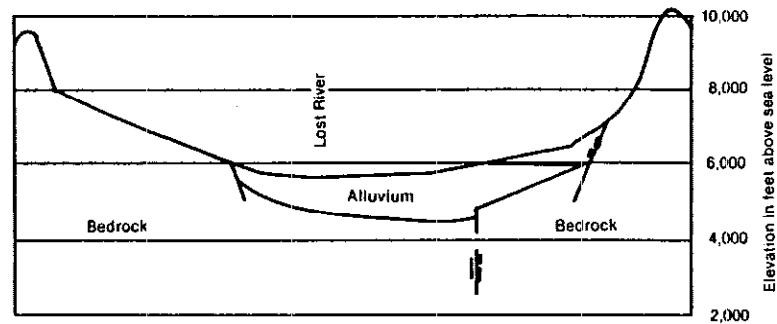
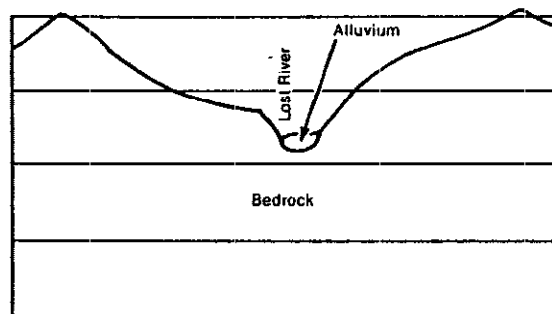
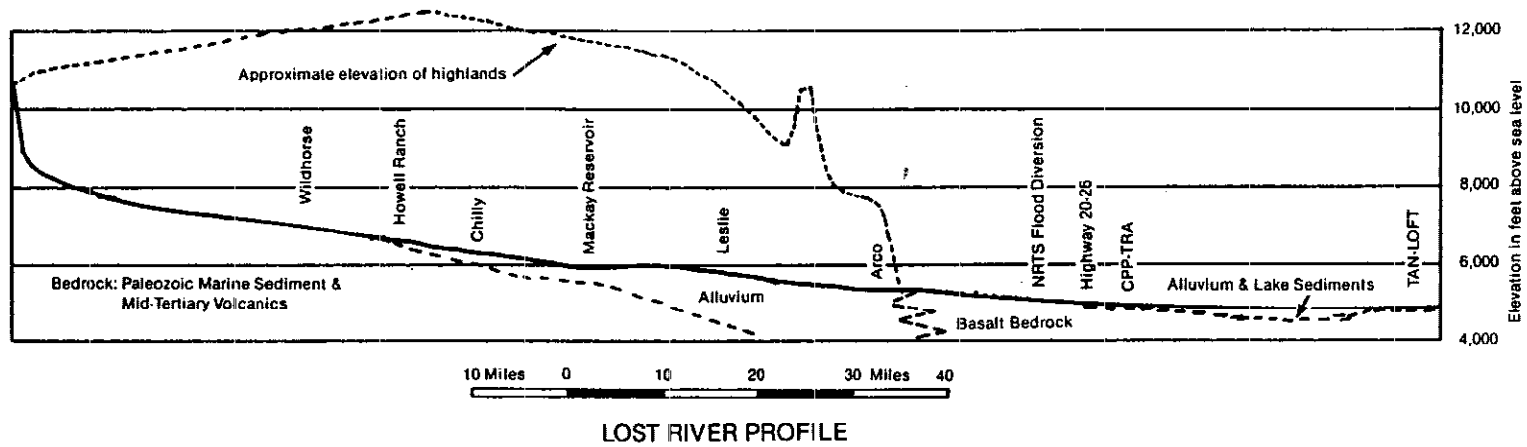
The diversion channel was excavated through several basalt ridges and intervening surface sedimentary deposits to connect the Big Lost River with a series of natural depressions. The depressions are designated as spreading areas A, B, C, and D (see Figure 2-22). Water is diverted into the diversion channel by a low earthen dam across the Big Lost River. The dam is part of a long, continuous dike extending along the north side of the river to the spreading areas. Two 6-ft-diameter corrugated metal pipes permit passage of less than 900 cfs of water through the dam into the main course of the river flowing downstream into the INEL (Lamke 1969). Flow in the river is regulated by gates on the culverts. During floods, flow in excess of that allowed to pass through the culverts is carried by the diversion channel. Flow in the diversion channel is uncontrolled at discharges that exceed the capacity of the culverts.





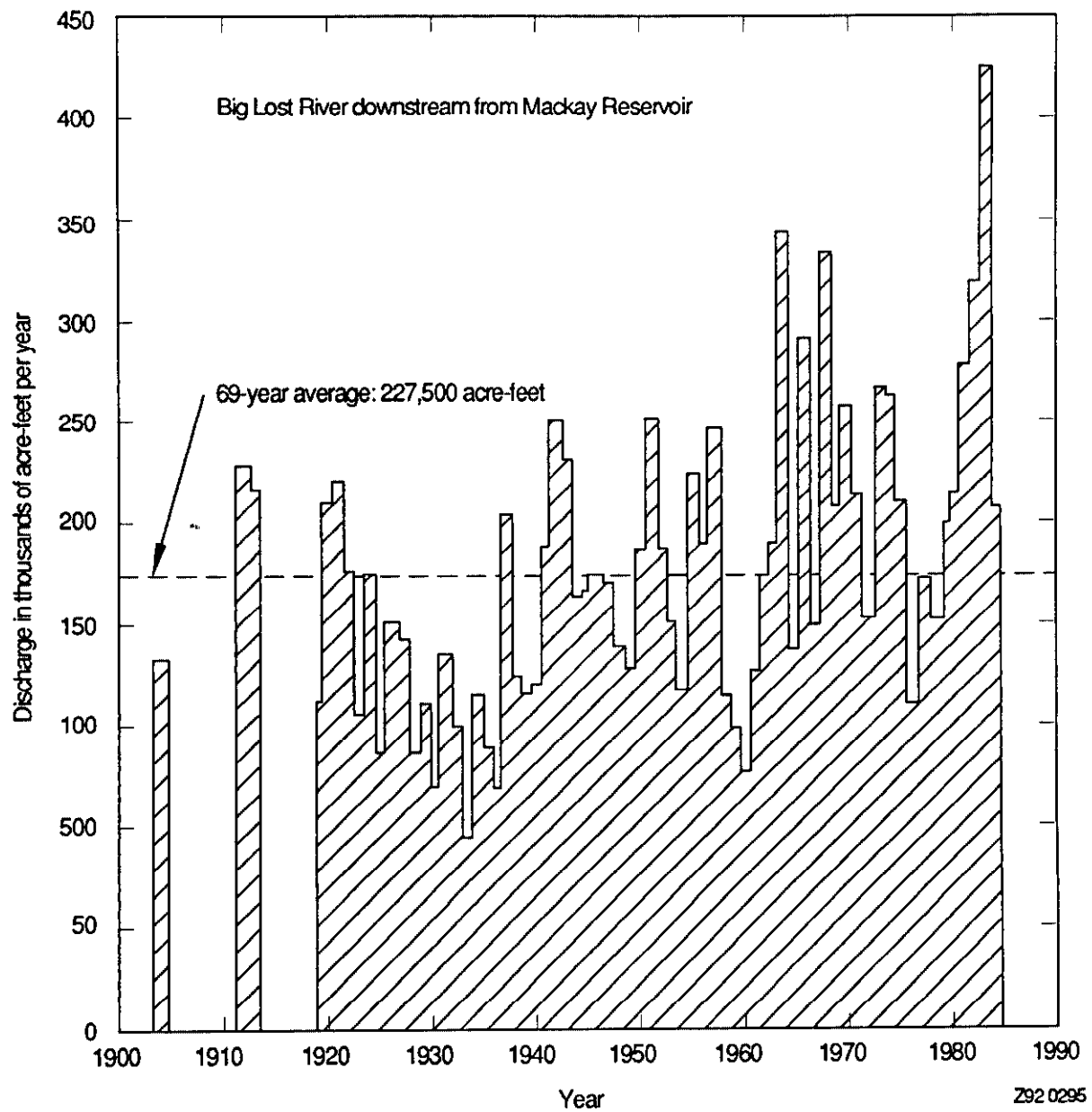
9-1565

Figure 2-18. Sites along the Big Lost River downstream from Mackay Reservoir.

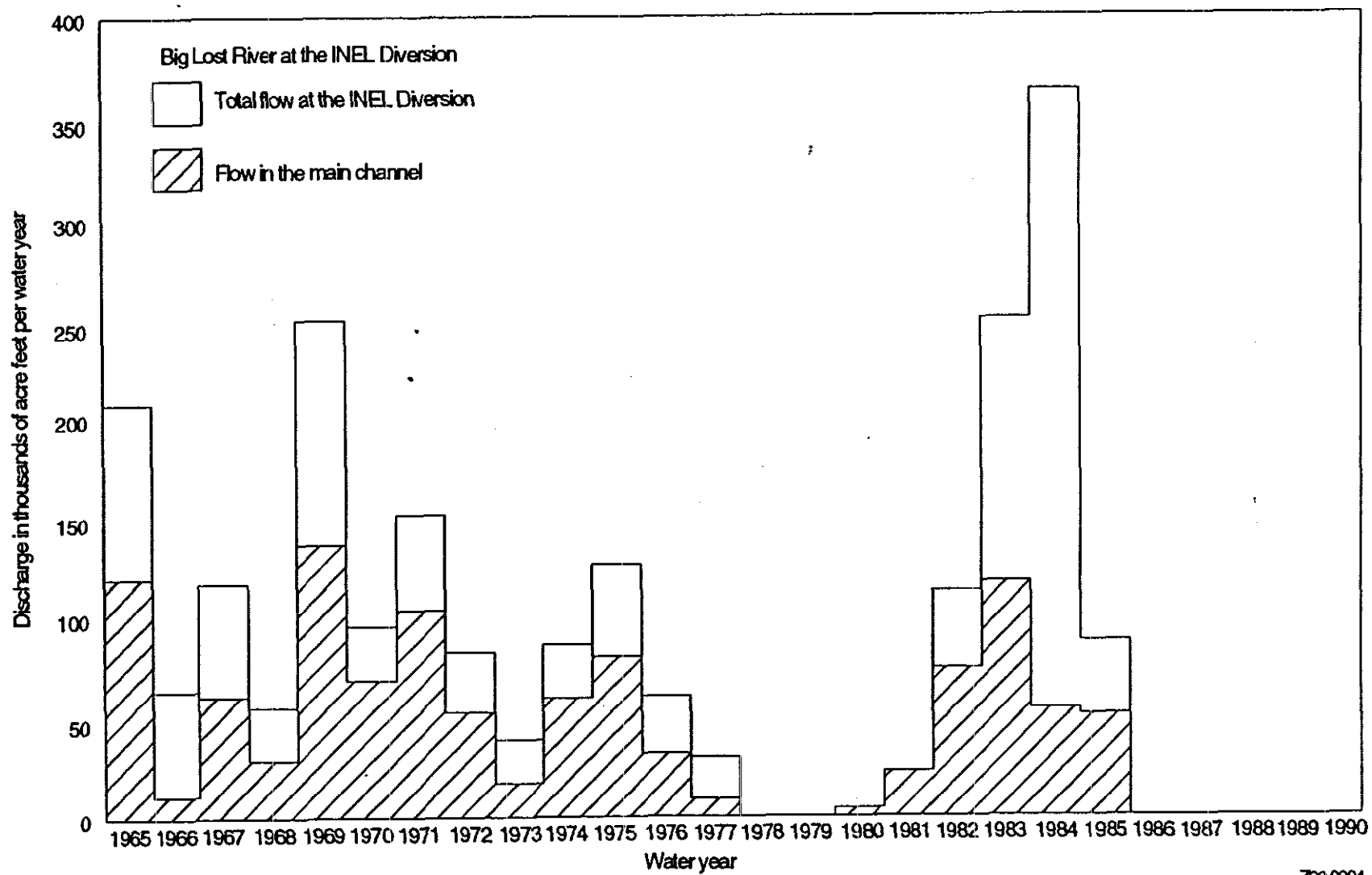


9-1568

**Figure 2-19.** Profile and sections of the Big Lost River.



**Figure 2-20.** Discharge of the Big Lost River below Mackay Reservoir (Pittman et al. 1988).



Z92 0094

Figure 2-21. Discharge of the Big Lost River at the INEL diversion channel (Pittman et al. 1988).

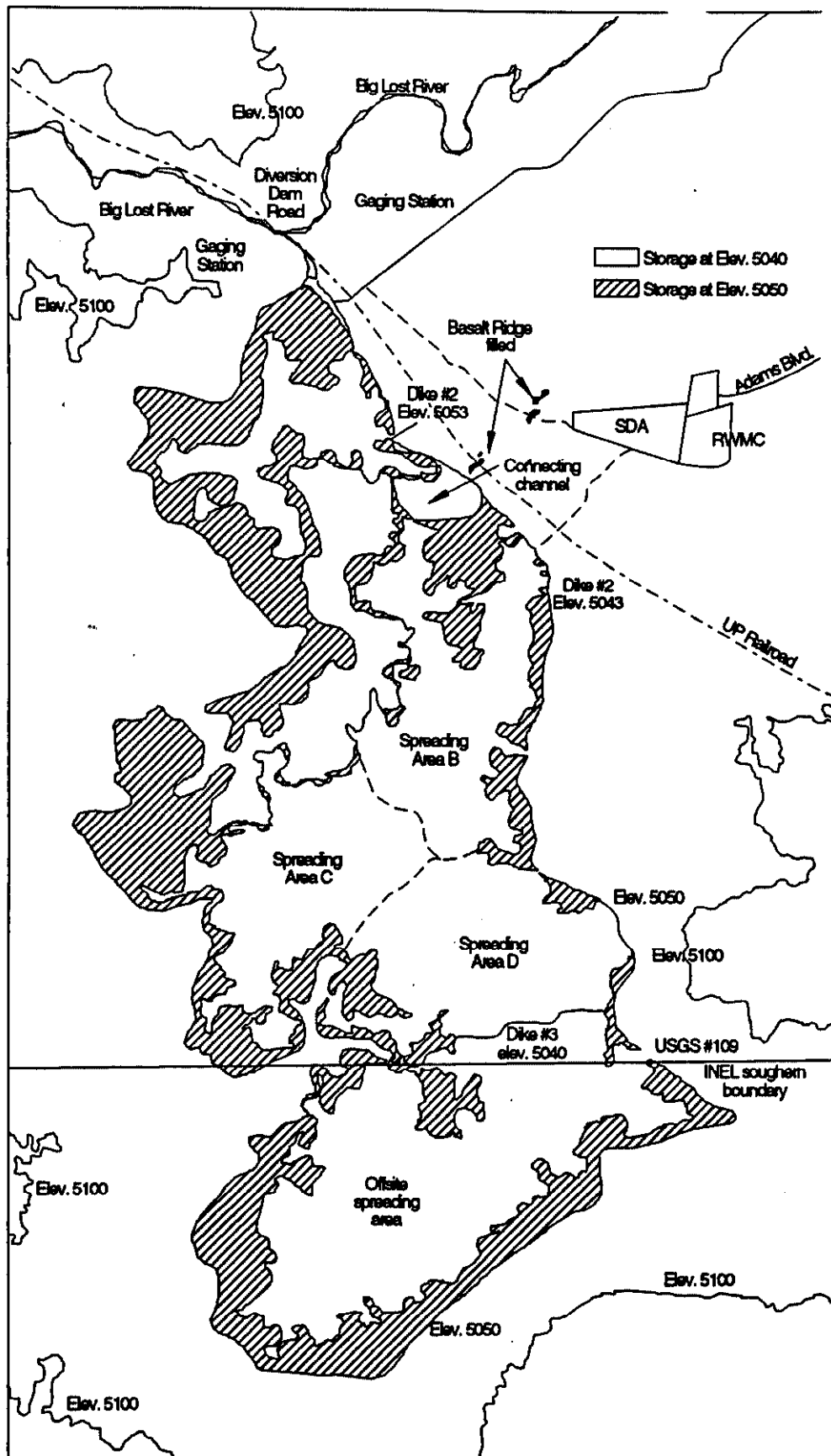


Figure 2-22. Spreading areas near the RWMC (McKinney 1985).

The diversion channel is capable of carrying 7,200 cfs from the Big Lost River into the spreading areas. Two low swales located southwest of the main channel can carry an additional 2,100 cfs, for a combined maximum diversion channel capacity of 9,300 cfs. The diversion channel extends about 0.9 mi from the point of diversion to Spreading Area A. Water flows from Spreading Area A through a short connecting channel into the three other spreading areas (Bennett 1986). The total capacity of the spreading areas is 18,200 acre ft at elevation 5,040 ft above msl and 58,000 acre ft at elevation 5,050 ft above msl (see Figure 2-22) (McKinney 1985).

The configuration of the channel is unusually rough. Resistant basalt ridges create an irregular channel bottom, which cause riffles and waterfalls at low to medium flows. The containment dike forms the east bank of the diversion channel. Basalt boulders, up to 5 ft in diameter, serve as rip-rap along the lower part of the dike. The upper part of the dike is predominately gravel. Scalloped areas, depressions, and basalt ridges form the west bank. The west-bank overflow section is sparsely to moderately covered with vegetation, chiefly sagebrush and grass (Bennett 1986).

**2.2.3.3 Surface Water Affecting the SDA.** The SDA is surrounded by higher ground to the immediate north, west, and south (see Figure 2-23). Surface water runoff from these higher elevations draws toward the SDA and eastward to the access road. Locally, the drainage patterns in the SDA are more complex due to the various containment areas and access roads. The waste disposal pit areas tend to be mounded, forcing runoff to their boundaries and toward the access roads (see Figure 2-23 and Figure 2-5). During periods of intense precipitation or flooding, ponding can occur, allowing infiltration and possible contact with buried wastes.

The SDA has flooded three times in recent years (1962, 1969, and 1982) as a result of local runoff from rapid melting of snow in the spring. Because the SDA is located in a basin, water entered the burial area and flooded some trenches and pits. During the 1962 flooding event, Trenches 24 and 25 and Pits 2 and 3 were open and were filled with water (see Figure 2-5). In 1969, water filled Pit 10, and considerable amounts entered Trenches 48 and 49. Some water possibly entered Pit 9, which was partly open. In 1982 water flowed into the southeast end of the SDA and entered Pit 16.

In February 1962, approximately 1.8 in. of rain fell on 8 in. of snow in three days (the upper 1 ft of the undisturbed ground was probably frozen). The rain caused the snow to partially melt, and an estimated 30 acre ft of water ponded in the SDA and subsequently infiltrated the subsurface (Barracough et al. 1976). Pits 2 and 3 and Trenches 24 and 25 were open at the time and filled with melt water (Barracough 1976). Some low-radiation waste boxes and barrels floated in the water and some boxes broke, spilling radioactively contaminated gloves, sample bottles, etc., into other areas within and adjacent to the SDA (EG&G Idaho 1988). In response to the flood, a system of dikes and ditches was constructed around the SDA in the latter part of 1962.

In January 1969, rainfall and snowmelt amounted to about 1.7 in. of water and an estimated 20 acre ft of water infiltrated the Burial Ground. Pit 10 was filled with water and Trenches 48 and 49 (and possibly Pit 9, which was partly open) received considerable amounts of water. Pits 9 and 10 were used for disposal of organic wastes from the Rocky Flats Plant in Colorado. The dikes established after the 1962 flood were overflowed in the 1969 flood. A more extensive dike system was constructed in 1969 to protect the SDA from runoff in the drainage basin.

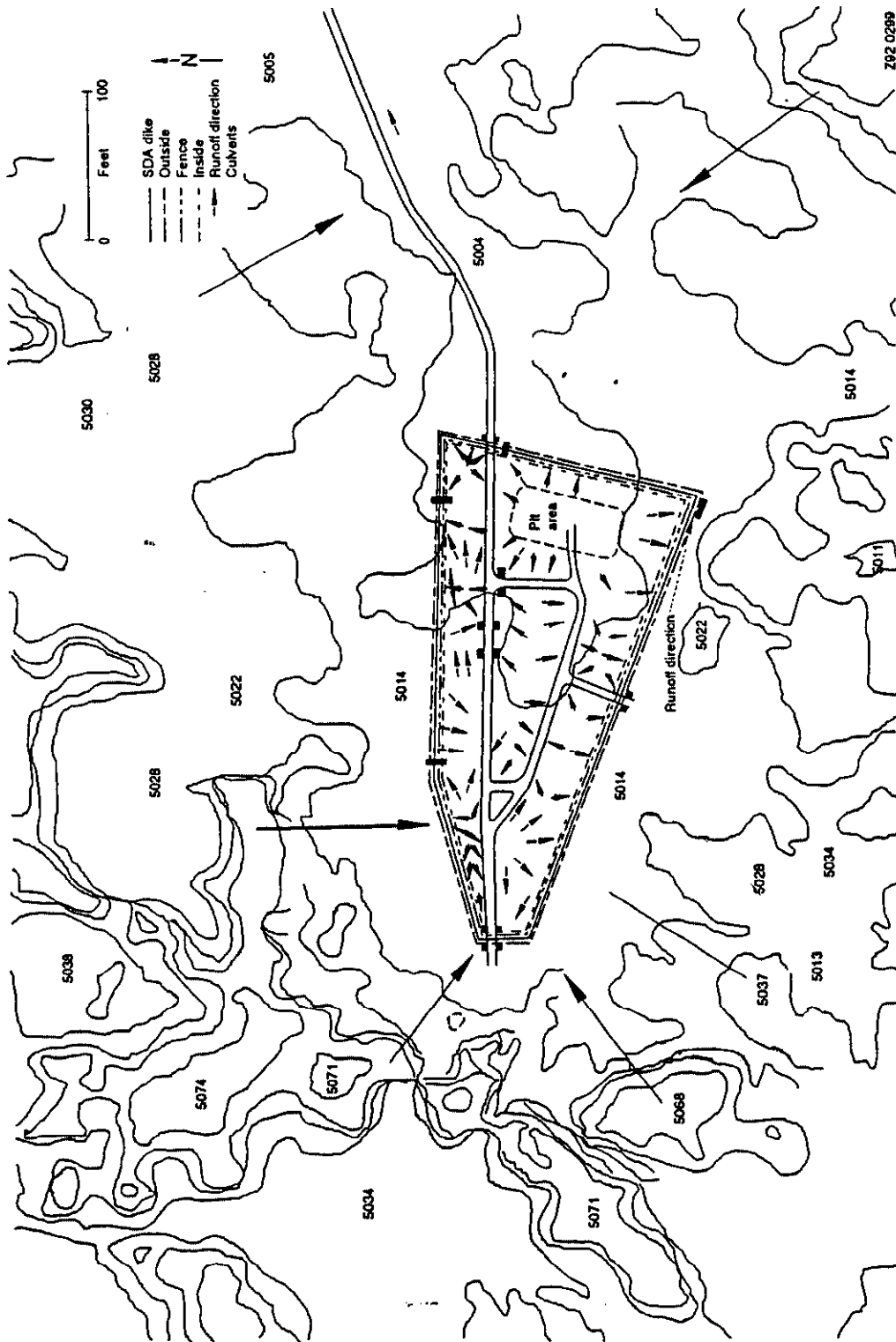


**Figure 2-23.** Surface drainage patterns at the SDA and surrounding areas.

On February 17, 1982, the dike surrounding the SDA ruptured on the southeast corner. A total volume of about 8.3 acre ft of runoff water entered the SDA, specifically into Pit 16. After workers repaired the dike and removed snow and ice blocking the SDA drainage channel, pumps were placed into Pit 16, and the run-off water was pumped into the RWMC surface water drainage system (Devries 1983). Following the dike failure, the water pooled in the SDA was sampled and analyzed for beta-gamma radiation using an alpha/beta proportional counter. On February 22, pumping was stopped because the beta-gamma count rate of the water samples from Pit 16 was increasing. Only one sample exceeded limitations in DOE Order 5480.1 for radiological releases to an uncontrolled area. That sample was taken on February 23 from Pit 16. The water of which the sample was representative did not leave the SDA because pumping was stopped the day before (Devries 1983). Pit 16 is not known to be associated with organic wastes disposed of at the SDA.

In mid-December 1983 a prolonged cold spell with temperatures consistently below freezing (32°F) and often below 0°F caused an ice buildup in Spreading Area A. Thin ice blocked the diversion channel and water began building up along Dike 1. On December 20, the water had risen to the top of the dike and began spilling over (McKinney 1985). Over the next several days, a concerted effort (EG&G Idaho personnel, DOE-ID, Morrison Knudsen Construction Management, and local contractors) relieved the blockage and raised the level of Dike 1 to avoid potential flooding. By June 1984 both Dikes 1 and 2 were raised to their present levels of 5,053 ft above msl (McKinney 1985).

The flooding events at the SDA allowed water to make contact with waste. The majority of the water generated during the flooding infiltrated the SDA subsurface. Evapotranspiration removed some flood water, but not a significant amount as compared to the infiltration (Barracough et al. 1976). Much of the available infiltration water comes in late winter or early spring when potential rates of evaporation and evapotranspiration are relatively small.

There is not enough detail in the current records to determine pulses of contamination transport that may have resulted from the flooding events. Characterization of contaminant transport is made difficult by the many variables that affect this type of analysis, such as the integrity of the drums and polybags and the amounts and specific types of waste in the pits and trenches. Detailed records for the 1962 and 1969 floods are not available. No mapping of the extent of contaminant migration was ever recorded. No aerial photographs were taken, only surface photographs.

The potential for future flooding of the SDA exists. A study conducted by the USGS (Carrigan 1972) concluded that the Big Lost River would overtop the flood-control diversion system about once every 55 years and that doubling the capacities of channels connecting the spreading areas was necessary. This added capacity would be able to handle higher flood stages estimated to occur once every 300 years. In response to the 1983-1984 near flooding of the SDA, diversion Dikes 1 and 2 were raised 8 ft by June of 1984, providing a diversion system that could contain a flood of approximately 58,000 acre ft.

Two possible sources for potential future flooding of the SDA are failure of Mackay Dam and failure of Dike 1 or Dike 2 in the spreading area. One study of the effects of a failure of Mackay Dam indicates that approximately two-thirds of the water would be lost to infiltration before reaching the INEL diversion and a significant part of the remaining one-third would be lost to depression storage (Druffel et al. 1979). Another study of a Mackay Dam failure indicates a peak water surface elevation of 5,070 ft above mean sea level (msl) (Koslow and Van Haaften 1986). Considering the diversion dam is at elevation 5,065 ft above msl and considering the topography to the north and west



of the SDA (see Figure 2-24) it seems possible that flood waters at 5,070 ft above msl could impact the SDA. No flood analysis to date has definitively exempted the SDA from the impact of flood water. A breach in Dike 1 or Dike 2 could possibly inundate the SDA; the flow from the area of the dikes would be from the west to the east onto the SDA (see Figures 2-23 and 2-24). Flow would move east from the SDA along the access road, with ponding likely to occur in this area. The potential magnitude of such a flood is a matter of conjecture, considering the many variables involved. Since the dikes have been raised and the spreading area volumes increased, a breach at a time of maximum water levels could inundate the SDA with substantial amounts of water.

**2.2.3.4 Surface Water Use.** Surface water is present at the SDA only during periods of heavy rainfall and snow melt, which generally occur in January. The SDA water needs are met by groundwater supplied by a production well in the RWMC administration area; the surface water runoff is not used for domestic or industrial purposes, but it may be used by animals and plants. Surface water in the diversion system to the west of the SDA attracts wildlife and waterfowl to the area.

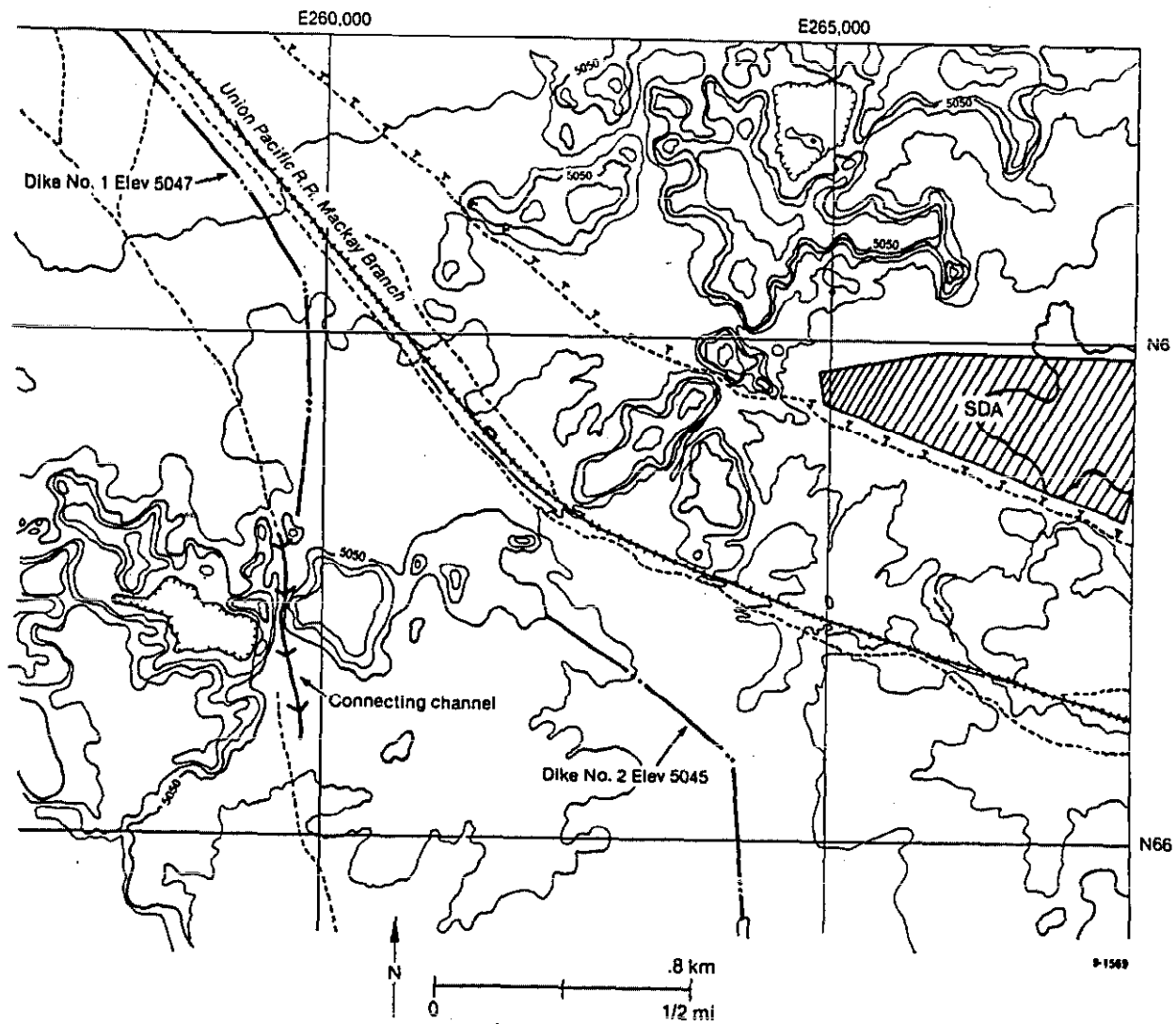
## **2.2.4 Groundwater Hydrology**

**2.2.4.1 Regional Groundwater Hydrology.** The INEL is located on the eastern edge of the Snake River Plain, which overlies the largest potable water aquifer in Idaho. The Snake River Plain Aquifer is a sequence of basaltic lava flows intercalated with alluvium and lakebed sedimentary deposits. The aquifer is approximately 200 mi long, 30 to 60 mi wide, and covers an area of about 9,600 mi<sup>2</sup>. The depth to the water table from land surface ranges from about 200 ft in the northeast corner of the INEL to approximately 1,000 ft in the southeast corner, a distance of about 42 mi. The average regional slope of the aquifer is about 0.2% from the northeast to the southwest with local variations. The thickness of the aquifer is difficult to estimate, but based on limited deep drilling activities at the INEL in 1978 and 1979, the aquifer may be 400 or more feet thick.

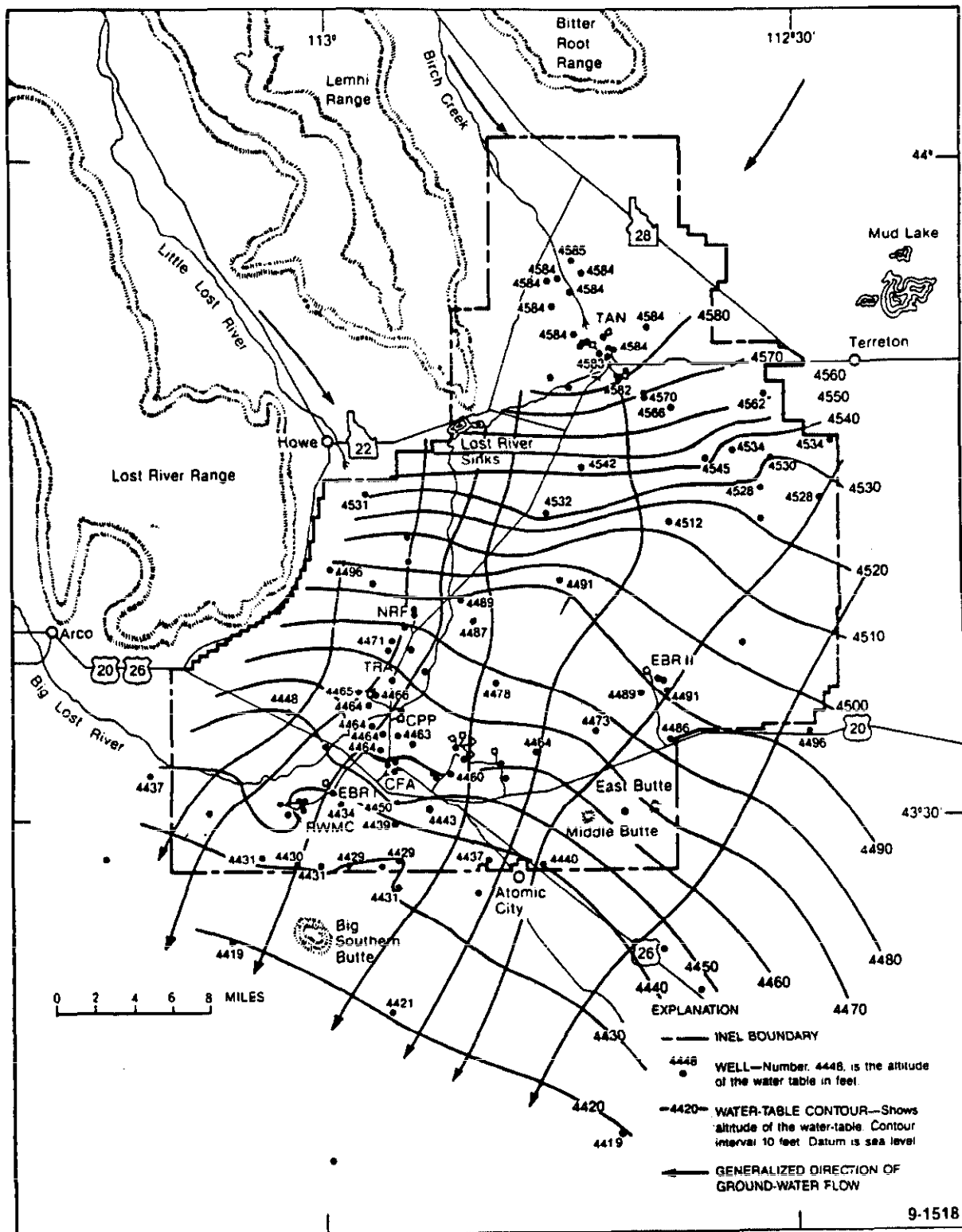
Water enters the regional aquifer from the west, north, and east. Most of the inflow occurs as underflow from alluvial-filled valleys along tributaries of the Snake River on the east side of the plain, from mountain ranges on the north, and from the alluvial valleys of Birch Creek, Little Lost River, and Big Lost River on the west. Little recharge occurs through the surface of the plain except for flow in the channel of the Big Lost River, its diversion areas, precipitation, and some surface irrigation.

The configuration of the water table indicates that water in the Snake River Plain Aquifer moves regionally from the northeast to the southwest, approximately parallel to the longitudinal axis of the plain (see Figure 2-25). The aquifer contains approximately  $2 \times 10^9$  acre ft of water, of which about  $5 \times 10^8$  acre ft might be recoverable (Robertson et al. 1974). The aquifer discharges about  $6.5 \times 10^6$  acre ft of water annually through springs in the area from Twin Falls to Hagerman, Idaho (Figure 2-25). The discharges from the springs significantly contribute to the flow of the Snake River downstream from Twin Falls, Idaho. Groundwater used for surface irrigation totals about  $1.5 \times 10^6$  acre ft annually. Average flow rates of groundwater within the aquifer, while meaningful only as approximations, indicate a range from 4 to 20 ft per day (Robertson et al. 1974).

**2.2.4.2 Site Specific Hydrologic Conditions.** Several groundwater monitoring wells, soil and a groundwater production well have been drilled or augured in or near the SDA. The location of wells and boreholes at the RWMC are shown on Figure 2-26. The wells drilled within the SDA do not penetrate the Snake River Plain Aquifer. These wells monitor the perched water zones and go



**Figure 2-24.** Location of Dikes 1 and 2 and topographic features in the vicinity of the SDA.



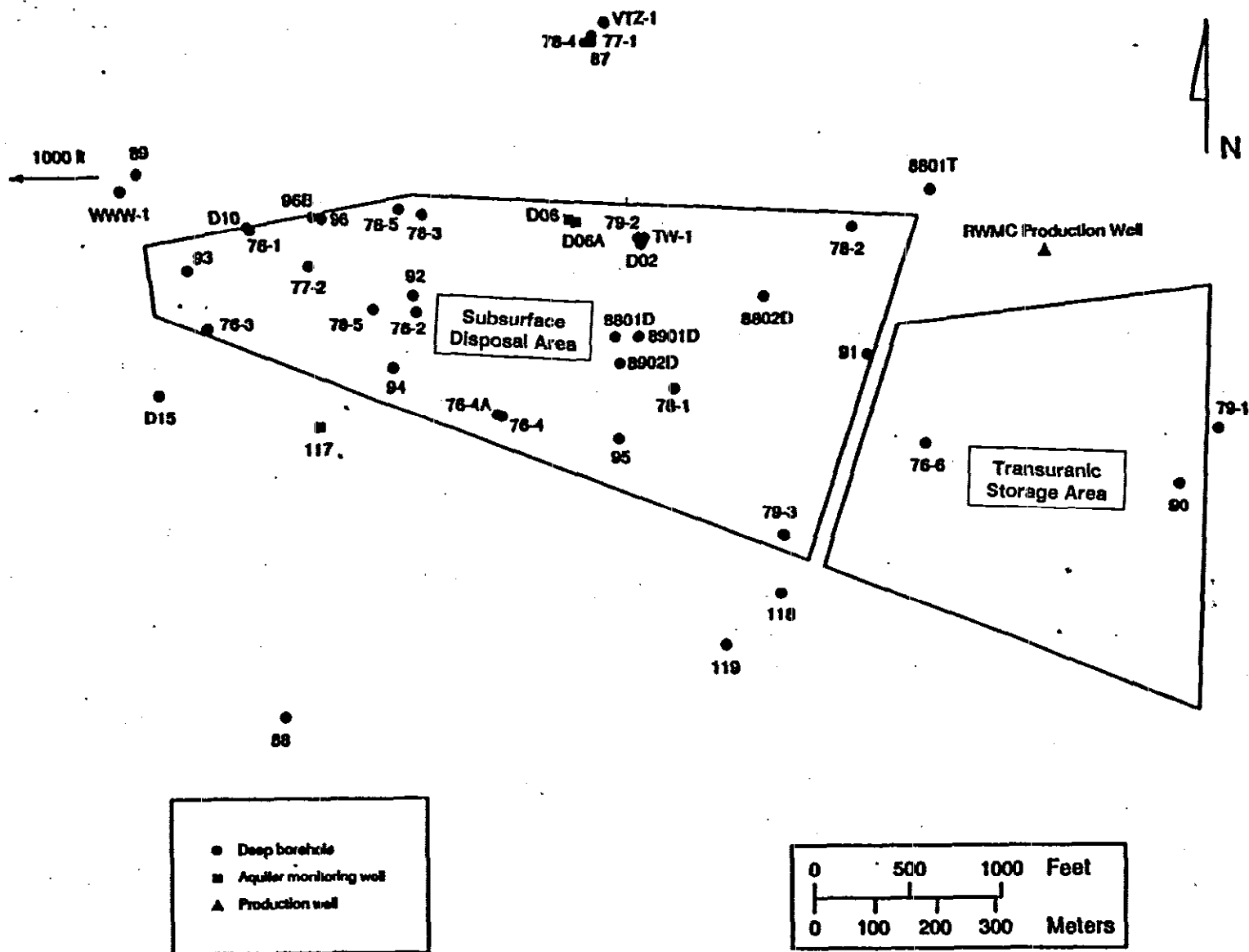


Figure 2-26. Locations of wells drilled at the RWMC (depths from 50 to 700+ ft below land surface).

to a maximum depth of about 300 ft below land surface. All groundwater monitoring wells completed in the Snake River Plain Aquifer are located outside the boundaries of the SDA. Figure 2-27 shows the location of the monitoring wells near the SDA. Table 2-2 shows the total depths and the well construction details for the monitoring wells near the SDA. The depth to the water table below the SDA is approximately 580 ft from the ground surface.

Figure 2-25 presents the generalized direction of groundwater flow below the INEL. This direction parallels that of the regional groundwater flow in the Snake River Plain Aquifer which is from the northeast to the southwest. A more complete reference on groundwater conditions can be found in Wood (1989) and Wood and Wylie (1991). Figure 2-25 shows groundwater movement in the southwestern portion of the INEL, and the direction of groundwater flow near the SDA and the Big Lost River diversion area in July 1978. The groundwater beneath the SDA is influenced by recharge from the diversion areas to the west and south of the SDA, as well as by the Big Lost River to the north. Figure 2-28 shows the groundwater below the SDA in 1984 flowing to the northeast, counter to the regional direction of flow. Figure 2-29 shows the groundwater below the SDA 1984 again flowing in the direction of regional flow. Data used to construct these figures were obtained from well locations shown on Figure 2-27 except for well 117, 119, and 120 which were constructed after 1984. Local groundwater data indicate that a reversal such as this commonly occurs after periods of snowmelt and heavy rainfall that create more flow in the Big Lost River and, as a result, into the INEL diversion areas. Water levels in some groundwater monitoring wells at the SDA rise within a few months following periods of water flow in the spreading areas (Wood 1989). The SDA also lies in a topographically low area that receives some runoff waters that may recharge the aquifer. These sources of aquifer recharge complicate local groundwater elevations, gradients, and associated rates and directions of flow. The local recharge due to topography is minimal and has probably little or no effect on the water table. For the most part, when recharge from the diversion areas is not affecting the water table, the direction of flow beneath the SDA is to the south and southwest. Normal seasonal groundwater elevation fluctuations not related to recharge from the spreading areas are minimal relative to the effects of recharge from the diversion areas.

As an example of fluctuations in groundwater elevations, Figure 2-30 show hydrographs for seven water wells located near the SDA. The hydrographs are arranged by well location and the year the well was drilled. Figure 2-31 shows water levels for Wells 87, 88, 89, and 90, which were drilled in 1971 and 1972 and are located just outside the boundaries of the SDA.

During the 1970s the water levels in the Wells 87, 88, and 90 tracked essentially the same path, all showing a gradual decline in water levels, which was probably associated with a decline in the regional water table during this time (Wood 1989). Well 89 is the exception to this showing fluctuations in water levels of about 8 ft from 1972 to 1977 (Figure 2-30). These fluctuations correlate to small discharges to the spreading areas during the same time periods (Wood 1989). Starting in the latter part of 1982 and continuing to 1989, there was a large rise in water levels recorded in wells shown in Figure 2-30. The highest water level occurred in 1984 with Well 88 showing a 70-ft rise in groundwater elevation. This rise corresponds to the highest discharge year on record (Wood 1989). The apparent anomalous behavior of water levels can be explained in part by the use of diversion areas that previously had never been flooded. After 1984, the wells show a decline in water levels, with the exception of Well 89, which showed a small rise in the water table associated with a small discharge to the spreading areas in 1987.

The general character of water in the Snake River Plain Aquifer below the INEL varies. The western part of the INEL, where the SDA is located, is underlain by a calcium-, magnesium-, bicarbonate-, and carbonate-dominated water. This reflects the fact that recharge areas to the north and west of the INEL are mainly composed of limestone and dolomite. The groundwater on the east

## Wells Used in Study and Spreading Areas A, B, C and D

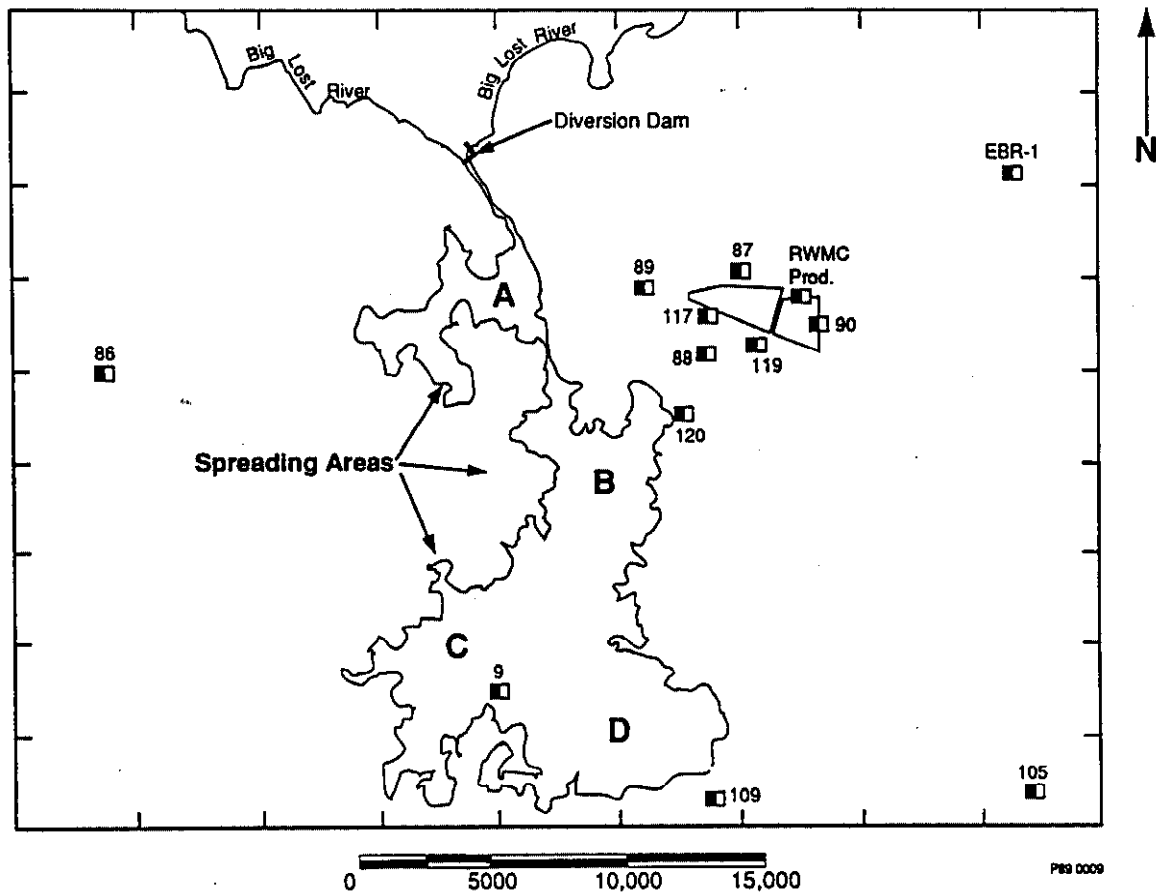
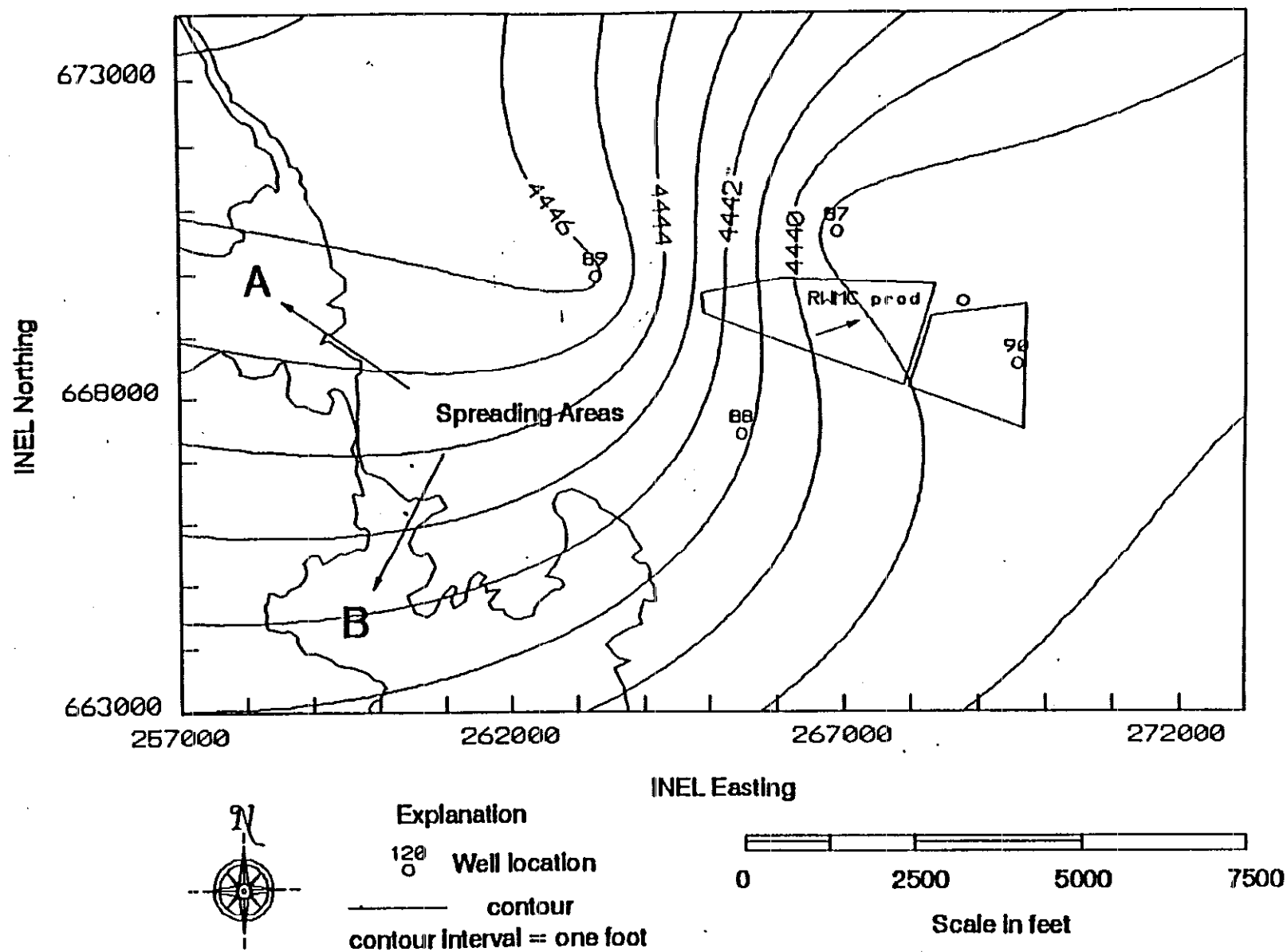


Figure 2-27. Location of groundwater monitoring wells near the SDA.

**Table 2-2.** Summary of well construction details for groundwater monitoring wells near the SDA (Wood 1989).

Well name	Year drilled	Total depth	Casing construction				Well logs		Depth to water when drilled
			Material	Cased interval	Screened and/or open interval(s)	Screen type	Geologist log	Geophysical logs	
EBR-1	1949	1075	Steel	0-750	600-750 750-1075	Perforated open hole	No	No	596.00
RWMC Production Well	1974	685	Steel	0-660	590-610 625-635	Perforated Perforated	Yes	Yes	?
USGS-87	1971	640	Steel	0-585	585-607 caved to 607	Open hole	Yes	Yes	582.70
USGS-88	1971	635	Steel	0-587	587-635	Open hole	Yes	Yes	583.65
USGS-89	1972	646	Steel	0-576	576-646	Open hole	Yes	Yes	590.64
USGS-90	1972	626	Steel	0-580	580-609 caved to 609	Open hole	Yes	Yes	574.62
USGS-117	1987	655	Steel/SS	0-555	555-653	Perforated	Yes	Yes	581.30
USGS-119	1987	705	Steel	0-639	639-705	Perforated	Yes	Yes	600.80
USGS-120	1987	705	Steel/SS	0-638	638-705	Perforated	Yes	Yes	611.45



**Figure 2-28.** Elevation of the water table for the Snake River Plain Aquifer for the region near the RWMC, 3rd quarter 1984 (USGS 88 data not plotted).



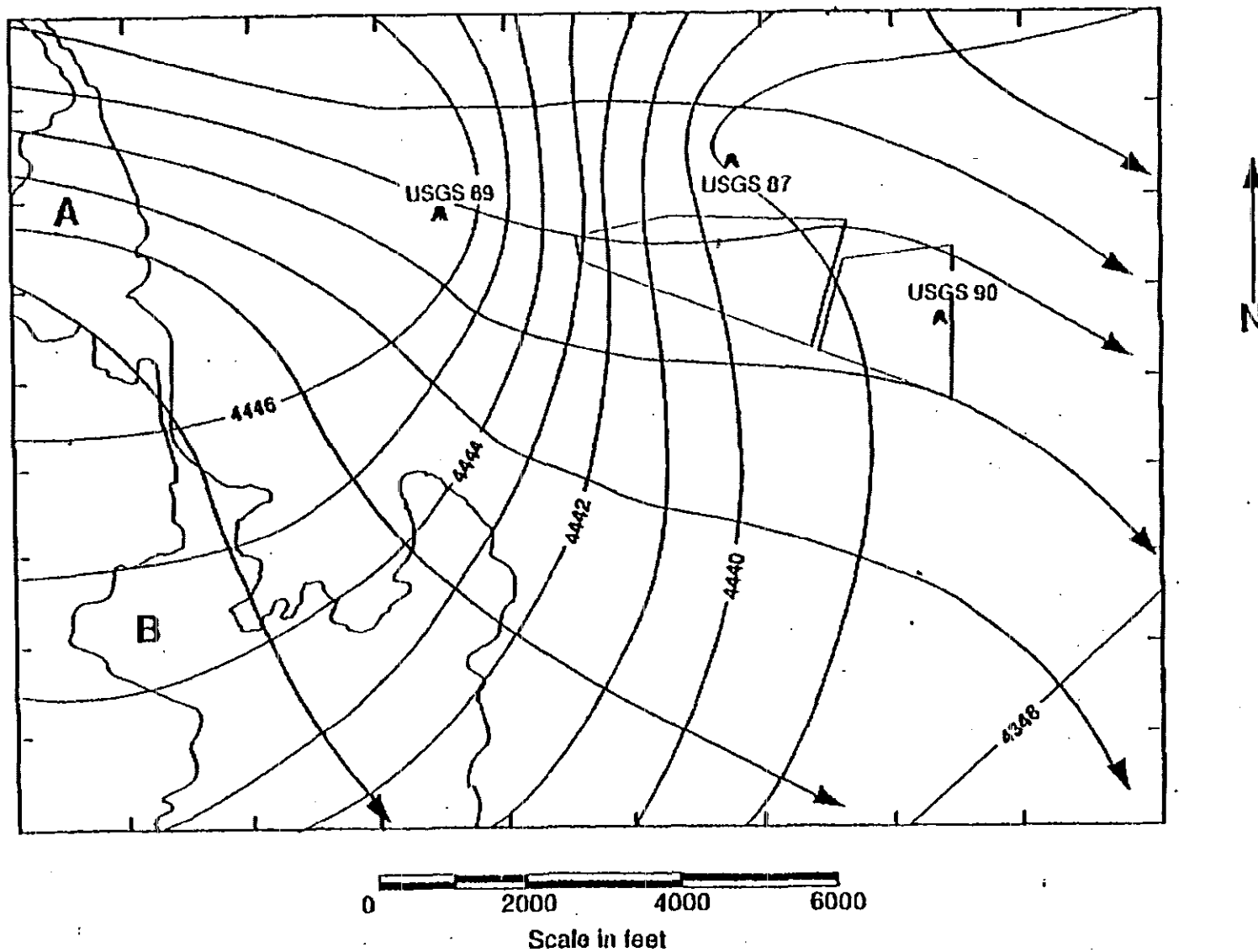


**Figure 2-29.** Altitude of the water table for the Snake River Plain aquifer and general direction of groundwater movement, 3rd quarter of 1984 (well 88 data not plotted).

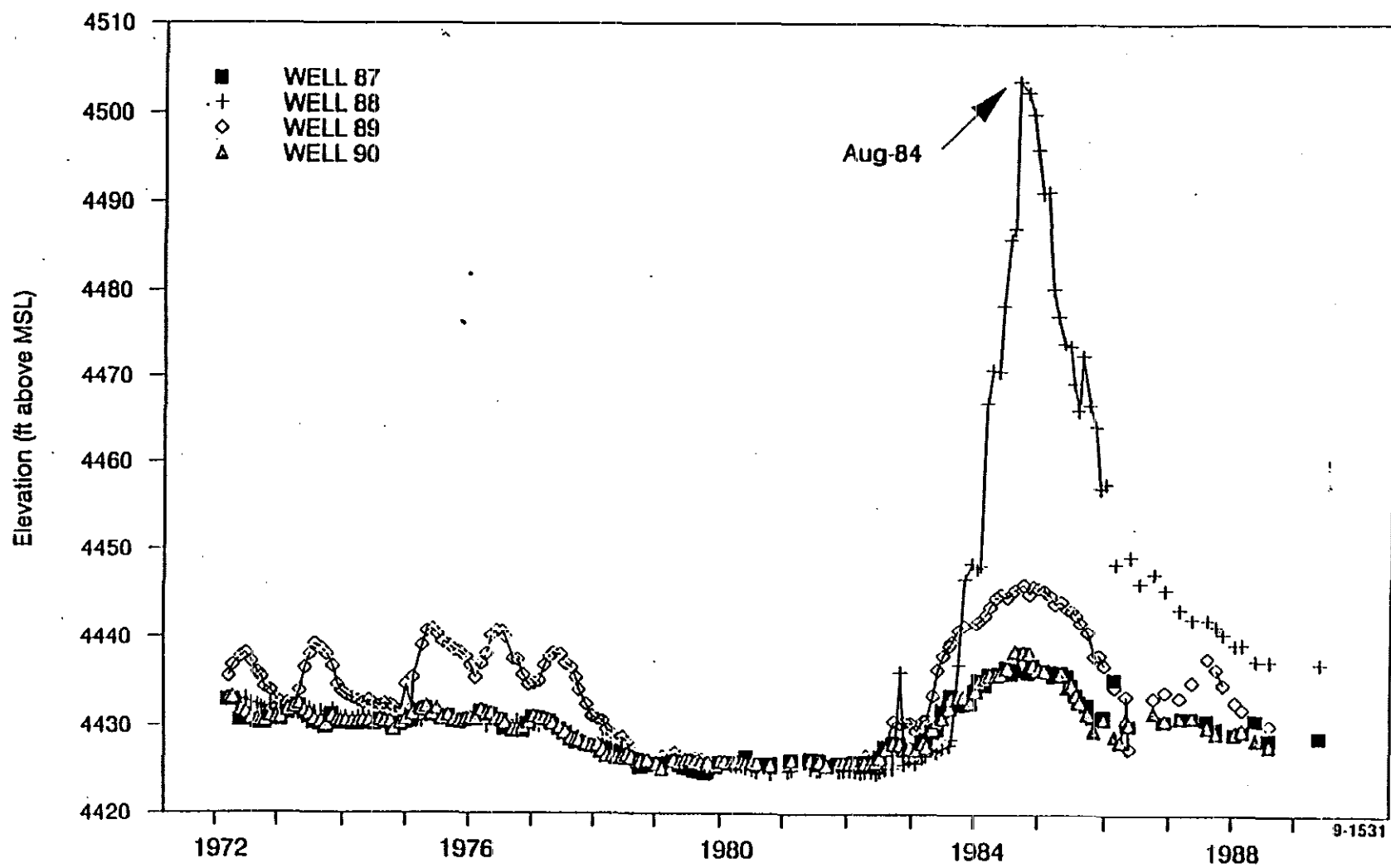


Figure 2-30. Well hydrographs for USGS Wells 87, 88, 89, and 90 from 1972 through 1989 (Wood 1989).

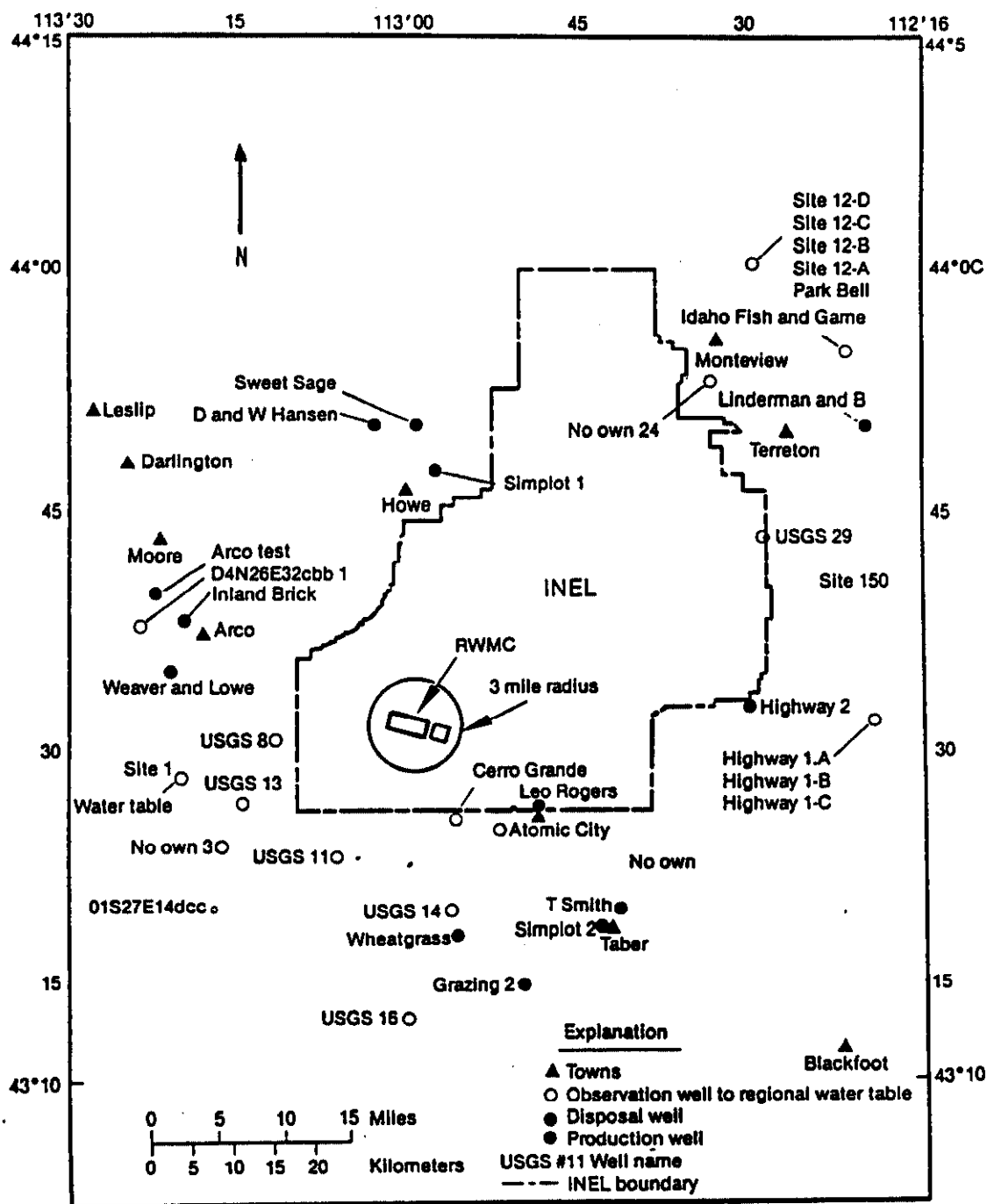


Figure 2-31. Name and location of selected wells near the INEL.

side of the INEL contains more sodium and potassium, indicating that the recharge to that part of the aquifer originates in the silicic volcanic-dominated mountains to the north and northeast of the site (Lewis and Jensen 1984). The groundwater from the Snake River Plain Aquifer below the INEL is relatively low in total dissolved solids (an average of slightly more than 200 mg/L) (EG&G Idaho 1988). The low mineralization reflects the moderate to abundant precipitation in the mountainous source areas, the absence of extensive deposits containing soluble minerals, and the low solubility of the basalt that forms the principal aquifer system. The water in the aquifer is generally of high quality, and with modest treatment can be made suitable for most uses. The specific conductivity for normal average aquifer water ranges from  $2.5 \times 10^{-4}$  to  $3.3 \times 10^{-4}$  mho/cm for the years 1976 through 1979 (EG&G Idaho 1981).

The Snake River Plain Aquifer is the only source of water used at the INEL. Pumpage rates and their effect on aquifer water levels are closely monitored by the USGS. Pumping has a very limited and localized effect on annual water-level changes in the aquifer in the vicinity of the RWMC Production Well because the amount of groundwater pumped is small in proportion to the total aquifer storage and recharge (Barracough et al. 1981). Water usage during 1986 from the RWMC Production Well totaled 5,000,000 gal and in 1987 totaled 3,400,000 gal.

**2.2.4.3 Groundwater Use.** The primary uses of groundwater at the RWMC include fire safety, drinking water, and showers for workers. This groundwater is supplied by the RWMC Production Well located northeast of the SDA (Figure 2-26). The Production Well operates at 80% of design capacity under the following conditions:

- Capacity: 240 gpm
- Inside well diameter: 10 in.
- Depth of well: 685 ft
- Static water level below top of well: 581 ft
- Pumping water level below top of well: 586 ft
- Pumping water level above top of well: 35 ft
- Total pumping head including line loss: 645 ft.

According to Goldstein and Weight (1982), "The RWMC Production Well was drilled in 1974 using the cable tool method, to a depth of 685 ft. Initially, the well was drilled to a depth of 562 ft. An 18-in. casing was set to a depth of 198 ft with a 14-in. casing set inside the 18-in. casing from the land surface to 562 ft. The space between the 18-in. casing and the borehole wall, and the annular space between the 14-in. and 18-in. casings was then filled with cement. The well was then drilled an additional 123 ft, and was completed as a 14-in. open hole. A 10-in. casing was then suspended from the surface to a depth of 658 ft and perforated in two zones--between 590 and 610 ft and between 625 and 635 ft. A 24-hour pump test was run from November 23 to November 24, 1974. The RWMC Production Well was pumped at variable rates of about 100, 200, 350, and 400 gal/minute. Water-level drawdown ranged from 3 to 5.5 ft depending on the pumping rate. The specific capacity of the well, after pumping four hours at 412 gal/minute, was 75 gal/minute per foot of drawdown."

The well pump and associated piping system supplies water to the RWMC by maintaining at least a 16-ft water level in a water storage tank located above ground in the northeast corner of the site. The storage tank is a standard carbon steel tank designed to supply 250,000 gal of water to the fire and domestic water pumps at the RWMC (EG&G Idaho 1988). The annual volumes of water pumped from the RWMC Production Well from 1986 to 1988 ranged from approximately 3 to over 5 million gal (Table 2-3).

Drinking water samples are collected monthly from the RWMC Production Well and from other active INEL production wells under a general program to monitor the drinking water at the INEL. In addition to the production well monitoring conducted by the Radiological and Environmental Sciences Laboratory, the USGS extensively monitors groundwater at the INEL and at selected locations beyond the boundaries of the INEL (Hoff et al. 1987). A groundwater production well at Experimental Breeder Reactor 1 (Well EBR-1) located approximately 2 mi northeast of the SDA is one of the wells monitored (Figure 2-27). Water production wells that are monitored include those scattered from the INEL south to Aberdeen, Idaho. Those wells within 20 mi downgradient from the SDA to the south-southwest (offsite) include Crossroads, Wheatgrass, Finger's Butte, and Quaking Aspen Butte. All are located on Bureau of Land Management lands and supply water for livestock and irrigation. The wildlife in this area also use water supplied by these production wells. These wells are located on Figure 2-31. According to EPA guidelines, all wells that are within a 3-mi radius of the SDA and draw water from the Snake River Plain Aquifer are considered important, unless they are separated from the SDA by a discontinuity in the aquifer, which is not the case here. The only other groundwater production well within 3 mi of the SDA besides the RWMC Production Well is Well EBR-1 (Figure 2-27).

**2.2.4.4 Hydraulic Properties.** Horizontal hydraulic conductivity values in the Snake River Plain Aquifer basalts range from 0.1 ft per day in dense portions of basalt flows to 10,000 ft per day in cinder or scoria zones, in fractures, and along interflow contacts (Barracough et al. 1976). In general, the greatest hydraulic conductivity is observed at basalt flow contacts where irregular fractures, cinder zones, and surface irregularities are prevalent (Robertson et al. 1974).

The upper limit of hydraulic conductivity is among the highest for any known aquifer. However, over a distance of a few feet, hydraulic conductivity can range widely. Although vertical hydraulic conductivity is usually less than horizontal conductivity in basalt, significant vertical conductivity does exist largely because of the presence of vertical fractures. This is demonstrated when surface water from the Big Lost River and associated diversion areas migrate vertically and produce a measurable recharge to the aquifer (Barracough et al. 1976). Overall aquifer permeability is related to intercrystalline pore spaces, fractures, fissures, and other interconnected voids.

Aquifer tests conducted within a basaltic zone about 100 ft thick near the Test Area North area of the INEL indicate an average horizontal permeability of about 20 darcies (equivalent to hydraulic conductivity of about 55 ft per day or 17 m per day); and vertical permeability of about 6 darcies (equivalent to hydraulic conductivity of about 15 ft per day or 4.5 m per day) (Barracough et al. 1976). Although that basalt may not be the same as the basalt strata directly beneath the SDA, it demonstrates a ratio of horizontal conductivity to vertical conductivity of 3.7 to 1 (Barracough et al. 1976).

**Table 2-3.** Annual volume of water pumped from the RWMC Production Well from 1986 to 1988.<sup>a</sup>

Reporting time period	Volume pumped (thousands of gallons)	Yearly total (thousands of gallons)
1986 (yearly total)	5,094	5,094
January 1987	309	--
February 1987	516	--
March 1987	210	--
April 1987	85	--
May 1987	207	--
June 1987	111	--
July 1987	106	--
August 1987	620	--
September 1987	866	--
October 1987	564	--
November 1987	50	--
December 1987	57 <sup>b</sup>	3,701
January 1988	113	--
February 1988	214	--
March 1988	355	--
Second Quarter 1988 (April-June)	550	1,232 (to June/30)

a. EG&G Idaho 1988

b. More current information is not readily available

Figure 2-32 shows generalized transmissivity contours for the Snake River Plain Aquifer beneath the INEL. Results from pumping tests conducted in the water wells near the SDA are shown on Table 2-4. These tests provide information on the aquifer characteristics near the SDA including the hydraulic conductivity of the aquifer, which ranged from 0.04 to 3,200 ft/d, and the transmissivity of the aquifer, which ranged from 4.05 to 211,000 ft<sup>2</sup>/d (30.3 to 1.6 x 10<sup>6</sup> gal/d/ft) (Wood 1989). These pumping tests were done with small diameter wells that only penetrate a short distance below the water table (Wood 1989). The differences between the transmissivities presented on Figure 2-32 and the values given in Table 2-4 stem from two widely different estimation methods. The tabular data were from analysis of pumping test whereas the contours in the figure resulted from model calibration. Subsequent studies have shown the model resulted in plumes that moved more rapidly than the actual plume.

Based on regional studies of the transmissivity at the INEL, the transmissivity near the RWMC is estimated to be approximately 173,000 ft<sup>2</sup>/d (1.3 x 10<sup>6</sup> gal/d/ft) (Robertson et al. 1974). Estimates of the effective porosity of the aquifer range from 5 to 15% with 10% being the most accepted value (Robertson et al. 1974). This porosity estimate is a spatial average over a large volume since the aquifer is composed of massive basalt with an effective primary porosity of only a few percent and fractures and cinder zones with very high secondary porosity (Wood 1989).

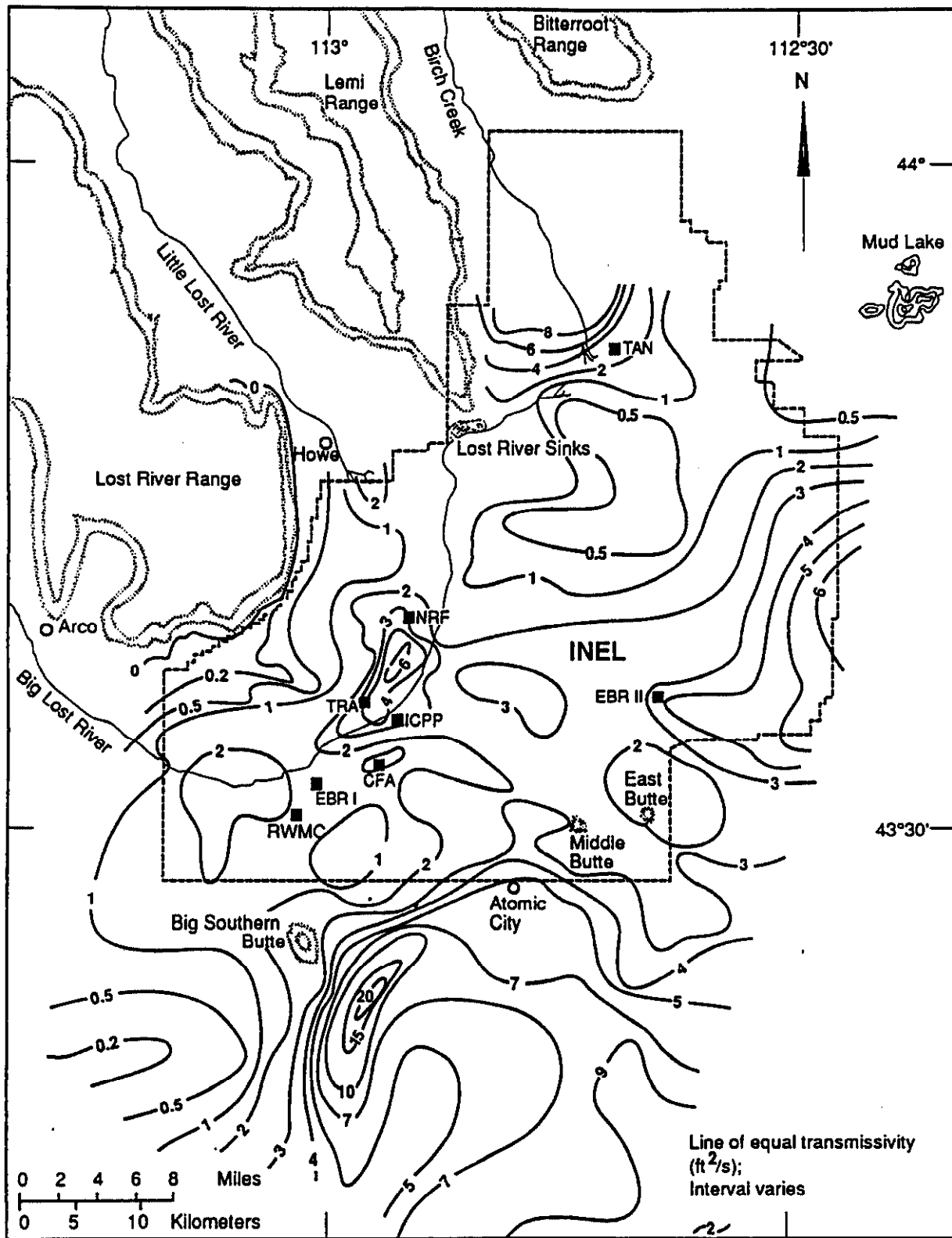
### 2.2.5 Vadose Zone

The vadose zone at the SDA consists of a soil layer ranging from 0 to 22 ft thick and underlying basalt flows located at and below the land surface to the saturated zone approximately 580-ft below ground. The basalt flows are frequently separated by interbeds of sedimentary deposits. There are 22 individual basalt flows and at least seven sedimentary interbeds underlying the SDA above the water table (Anderson and Lewis 1989). Major interbeds occur at average depths of 30, 110, and 240 ft. There are several other interbeds below the 240-ft interbed, however, most of the available data on the vadose zone at the SDA are for depths shallower than 250 ft. The majority of the wells were completed at depths shallower than 250 ft, and no boreholes have been drilled to depths greater than 310 ft at the SDA.

**2.2.5.1 Soils.** INEL soils are derived from Cenozoic felsic volcanic and Paleozoic sedimentary rocks from nearby mountains. The soils in the northern portion of INEL are generally composed of fine-grained lake and eolian (wind-carried) deposits of unconsolidated clay, silt, and sand. Generally, the soils at the southern INEL (where SDA is located) are shallow, consisting of fine-grained eolian soil deposits with some fluvial gravels and gravelly sands.

**2.2.5.2 Soil Characteristics.** In general, soils at SDA have moderate water-holding capacity, although some areas of SDA have shallow soils with low water-holding capacity (Bowman et al. 1984). These soils are predominantly derived from loess deposits. Some SDA soils may also be derived from stream deposits of the Big Lost River.

The surficial deposits at the SDA range in thickness from 0 to over 22 ft (Figure 2-33). The irregularities in the soil thicknesses generally reflect the surface of the underlying basalts. A soil column of SDA (Figure 2-34) displays a few common features of the soils in the area. These features include pebble layers, freeze thaw textures, glacial loess deposits, and palette caliche horizons. The stratigraphy of surficial deposits and soil characteristics at SDA are being evaluated in ongoing



P89 0019

**Figure 2-32.** Generalized transmissivity contours for the Snake River Plan Aquifer.



**Table 2-4.** Well parameters for wells near the SDA based on tests conducted by the USGS.

Well	Date	Discharge rate (gpm)	Saturated thickness (ft)	Maximum drawdown (ft)	Specific capacity (gpm/ft)	Transmissivity (ftc/d)	Hydraulic conductivity (ft/d)	Analytical method
Well 87 <sup>a</sup>	07/14/87	2.20	24 (approx.)	0.13	16.90	700	30	Theis
Well 88 <sup>a</sup>	07/08/87	5.00	51 (approx.)	28.70	0.17	23.40 3.11	0.46 0.061	Jacobs Theis
Well 89 <sup>a</sup>	07/21/87	4.41	56	6.32	0.70	52.90	0.95	Jacobs
	07/22/87	4.39	56	6.69	0.66	55.30	0.99	Jacobs
Well 90	07/15/87	3.81	34 (approx.)	0.53	7.20	733	22	est. Theim
Well 117 <sup>a</sup>	12/17/87	6.79	72	20.35	0.34	15.7	0.22	Theis
Well 119 <sup>a</sup>	12/16/87	3.15	104	68.81	0.046	4.05	0.04	Theis
Well 120	12/15/87	20.7	94	0.01	2070	211,000	3,200	est. Theim
RWMC Production Well	07/24/74	412.0	30	5.50	75	7,600	254	est. Theim

a. Pumping test data evaluated by the U.S. Geological Survey (USGS 1989).

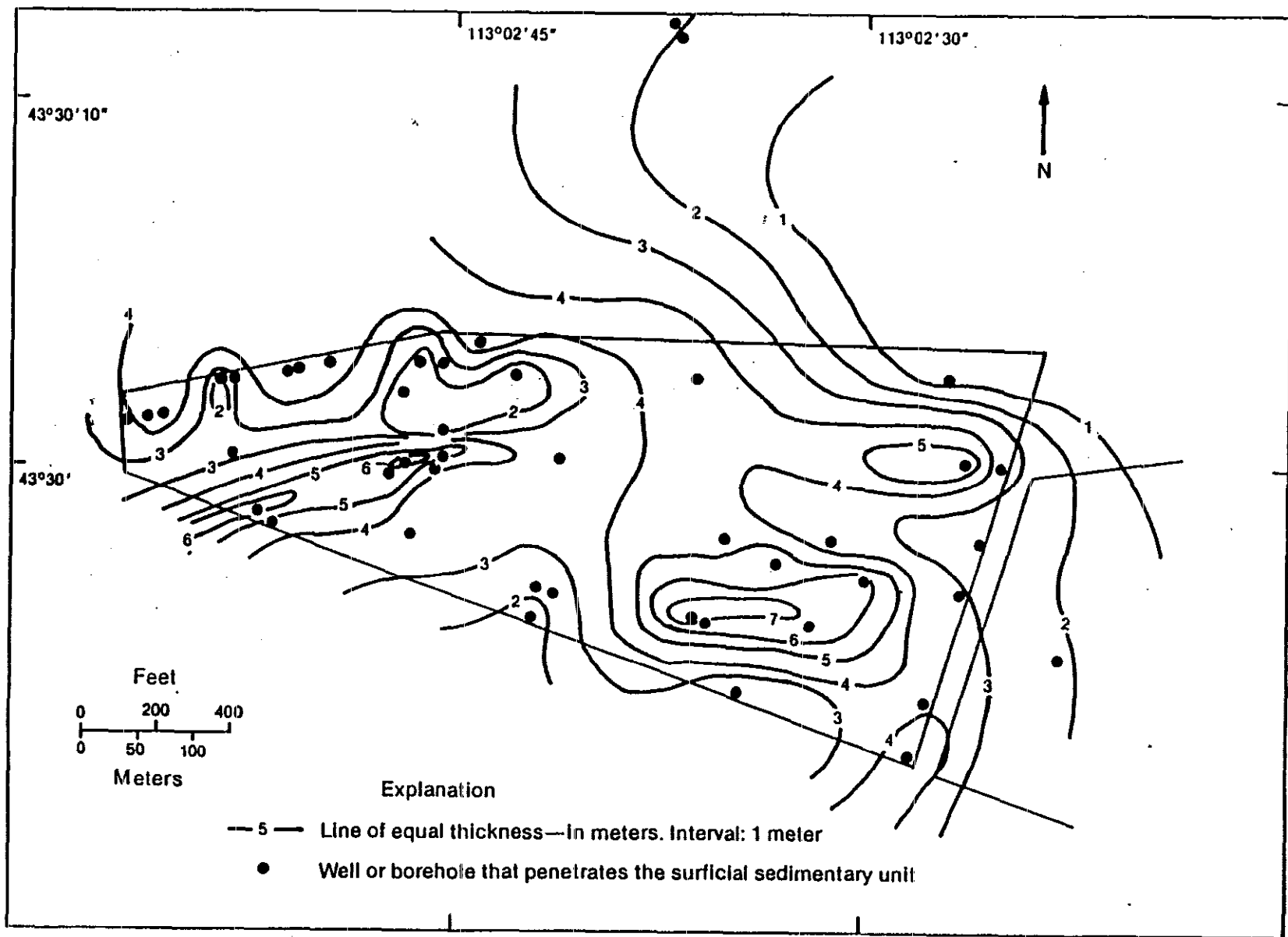


Figure 2-33. Isopach map of surficial sediments at the SDA (Rightmire and Lewis 1987).

9-1306

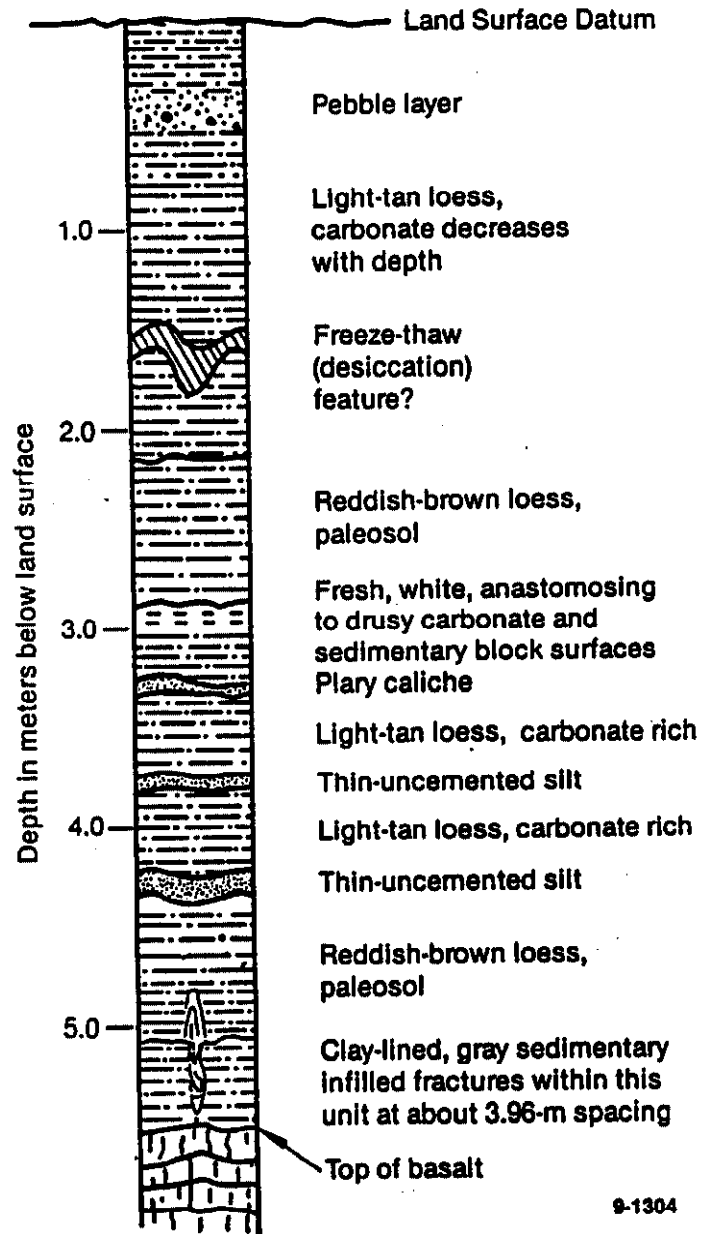


Figure 2-34. Representative soil column at the SDA (Rightmire and Lewis 1987).

subsurface investigation projects. The vertical hydraulic conductivities, bulk densities, porosities, and moisture content for a representative group of soil samples from the SDA are given in Table 2-5 (Barracough et al. 1976). The particle size distribution, clay minerals content, and cation exchange capacity for the same group of soil samples characterized in Table 2-5 are presented in Table 2-6 (Binda 1981). The particle size distribution and mineralogy for a selected group of four soil samples collected from the southeast corner of the SDA are shown on Tables 2-7 and 2-8. The clay mineralogy and cation exchange capacity of these same samples are shown in Table 2-9. The majority of the sampled material (71.1 to 94.8%) was silt and clay. Illite and illite/smectite layer clays are predominant in all four samples collected (Rightmire and Lewis 1987).

**2.2.5.3 Features Affecting Contaminant Transport.** The surficial soils overlying the basalt range in depth from 0 to about 22 ft. The pits for waste disposal were excavated to basalt or to within a few feet of basalt. The trenches used for waste disposal were not as deep as the pits. However, because of the variation in soil depth across the SDA, waste in the trenches may be within a few feet of basalt, although efforts were made to leave a minimum of 2 ft of soil above the basalt in the bases of the pits and the trenches. Despite the possibility of a thin soil layer at the bases of the pits and trenches, the soil characteristics may have some effect on retarding VOC migration out of the pits and trenches because of the high content of silt and clay in the surficial soils.

The information and potential effects of soil characteristics on the migration of radionuclides and organic and inorganic chemicals draws on the information presented above for undisturbed soils at the SDA and RWMC. The 88-acre SDA consists of numerous pits and trenches used for waste disposal, and Hubbell and Higgs<sup>a</sup> estimated that 39% of the soil in the vicinity of the waste burial areas has been disturbed. As a result, the soil characteristics in and around the waste pits and trenches may vary from those presented for undisturbed soil samples.

Several features of the soils at the SDA can affect the rate, direction, and volume of radionuclide and chemical contaminant transport, including:

- Vertical and lateral hydraulic conductivity
- Clay content
- Cation exchange capacity
- Organic matter content
- Matrix potential
- Evapotranspiration
- Microbial activity.

The SDA soil has a high clay content (approximately 36%) and a high silt content (approximately 56%). As a result, the soil has a very low vertical hydraulic conductivity, approximately 0.01 ft/d ( $4.7 \times 10^{-6}$  cm/s) (Barracough et al. 1976), which should retard the downward migration of vapor or liquids from the buried wastes. In addition, the clay may retard the migration of radionuclides and chemicals through adsorption.

---

a. Hubbell, J. M. and B. D. Higgs, 1989, Memo: Estimate of Disturbed Soil at the Subsurface Disposal Area, JMH-23-89.

**Table 2-5.** Various physical characteristics of soil and sediment samples from the RWMC wells.<sup>a</sup>

Well number	Depth interval		Specific gravity	Bulk density (g/cm <sup>3</sup> )	Porosity (%)	Moisture content (%)	Vertical hydraulic conductivity (m/day)
	Top (ft)	Bottom (ft)					
92	2.6	5	2.65	1.87	34.3	12.9	5.5 x 10 <sup>-4</sup>
94	6.5	8.25	2.67	2.02	30.5	16.4	2.7 x 10 <sup>-4</sup>
95	10	12.5	2.66	1.70	41.0	13.2	7.9 x 10 <sup>-3</sup>

a. Barraclough et al. 1976

**Table 2-6.** Properties of soil and sediment samples from the RWMC wells.<sup>a</sup>

Well No.	Depth interval		Particle size distribution portion <sup>b</sup>			Clay minerals percent moisture			Cation exchange
	Top (ft)	Bottom (ft)	Clay	Silt	Sand	Kaolinite	Illite	Montmorillionite	Capacity (meg/100 g)
92	2.5	5	21.2	48.8	30.1	2	5	5	14
94	6.5	8.25	38.7	56.5	4.8	3	9	4	23
95	10.0	12.5	38.5	55.6	5.9	1	4	3	17
Median <sup>c</sup>			35.9	56.0	7.3	2	7	6	21

a. Binda 1981.

b. Clay <0.004 mm  
 Silt 0.004 - 0.062 mm  
 Sand 0.062 - <2.00 mm

c. Median of eight samples.

**Table 2-7.** Particle size distribution for subpit samples (in percent of analyzed sample).<sup>a</sup>

Sample <sup>b</sup> number	Depth (meters)	Clay <0.004mm	Silt 0.004- 0.0625mm	Sand - very fine 0.0625- 0.125mm	Sand fine 0.125-0.25mm	Sand medium 0.25-0.5mm	Sand coarse <sup>c</sup> 0.5-1mm
EWR-1-4	0.91	53.3	38.5	4.8	2.3	0.9	0.1
EWR-1-3	1.22	41.0	30.1	11.0	17.7	0.2	0
EWR-1-2	1.52	54.7	40.1	4.1	0.7	0.2	0.1
EWR-1-1	1.83	23.5	69.8	6.0	0.6	0	0.1

a. Analyzed by the USGS Hydrologic Laboratory, Denver, Colorado.

b. All samples from surficial deposits.

c. No particles coarser than 1 mm observed.

**Table 2-8.** Mineralogy for subpit samples (in percent of analyzed sample)<sup>a</sup>

Sample <sup>b</sup> number	Depth (meters)	Quartz	Potassium feldspar	Plagiocase	Çalcite	Pryoxene (idioxide)	Clay minerals	Total percent
EWR-1-4	0.91	27	≤5	11	1	4	70	113+ <sup>c</sup>
EWR-1-3	1.22	29	≤6	10	0	9	55	103+
EWR-1-2	1.52	15	≤3	6	41	≤9	25	87+
EWR-1-1	1.83	29	5	12	13	≤9	40	99+

a. Analyzed by the USGS Hydrologic Laboratory, Denver, Colorado.

b. All samples from surficial deposits.

c. Due to high percentage of clay minerals.



**Table 2-9.** Clay mineralogy of selected surficial sediment samples (in percent of total clay minerals/percent of original bulk samples)<sup>a</sup>

Sample	Depth (meters)	Chlorite	Illite	Mixed layer clays (illite/smectite)	Smectite	Kaolinite	Cation exchange capacity <sup>b</sup>	Carbonate content (as CaCO <sub>3</sub> ) percent
EWR-1-4	0.91	03/0	25/6	45/32	13/9	6/4	27	0
EWR-1-3	1.22	03/0	16/0	48/26	15/9	6/3	27	2.3
EWR-1-2	1.52	03/0	9/6	31/8	24/6	9/2	11	36.1
EWR-1-1	1.83	03/0	12/2	30/12	26/10	12/5	11	10.8

a. Analyzed by the USGS Hydrologic Laboratory, Denver, Colorado.

b. In milliequivalents per 100 g.

The clay minerals predominantly found are illite and montmorillonite. Illite has a moderate cation exchange capacity and montmorillonite has a high cation exchange capacity. The clay content, mineralogy, and cation exchange capacity of the soils at the SDA imply that moderate retardation of migrating cations is possible (Brady 1974).

The natural organic matter content of soils strongly influences the retardation of contaminants being transported through the soil because natural organic compounds, which tend to have high surface areas, adsorb contaminants. The light color of much of the soil column (light tan loess) implies that the soil is low in natural organic matter (see Figure 2-34).

The presence of microbes in the soil capable of degrading organic contaminants could also affect overall contaminant transport. Information on microbial activity in the soil at the SDA is not currently available.

Other characteristics that may affect the transport of chemicals, in both liquid and vapor phases, in the soil are the thickness of the evapotranspiration zone and soil matrix potentials. Preliminary evaluation of data collected at the SDA indicates that, at a minimum, evapotranspiration affects the top 4 to 5 ft of soil (Laney et al. 1988). McElroy and Hubbell (1989) calculated hydraulic gradients from soil matrix potentials measured in the surficial sediments. Upward hydraulic gradients were observed at depths shallower than 3.9 ft and downward hydraulic gradients were observed below 10.8 ft. Between the depths of 3.9 and 10.8 ft, there was both upward and downward moisture movement depending on the relative dryness or wetness in the surficial sediments at each monitoring location (McElroy and Hubbell 1989).

**2.2.5.4 Basalt Flows.** The composition of the basalt flows underlying the SDA is discussed in general in Section 2.2.2.4 and in detail in Kuntz et al. (1980). A discussion of the stratigraphy of the basalt-flow groups and the interbedded sedimentary deposits is presented in Section 2.2.2.3.

**2.2.5.5 Sedimentary Interbeds.** Descriptions of the previously studied sedimentary interbeds underlying the SDA are presented in Section 2.2.2.5 and in several references (Barracough et al. 1976; Laney et al. 1988; and Rightmire and Lewis 1987). In addition, the stratigraphy of the basalt-flow groups and sedimentary interbeds is discussed in Section 2.2.2.3.

Saturated vertical hydraulic conductivity values have been measured in laboratory studies for the 110-ft and 240-ft sedimentary interbeds (Barracough et al. 1976). Measurements were taken on 22 cores from 10 wells in or near the SDA. The values ranged from  $2.2 \times 10^{-5}$  to 9.8 ft/d ( $6.7 \times 10^{-6}$  to 3.0 m/d) for the 110-ft interbed, and  $2.6 \times 10^{-6}$  to 8.9 ft/d ( $8.0 \times 10^{-7}$  to 2.7 m/d) for the 240-ft interbed (Figure 2-35). Porosity values for these cores ranged up to 53%. In the wells tested, the 110-ft interbed is more permeable than the 240-ft interbed because it is composed of coarser-grained sediments.

Water infiltrating the basalts probably flows through fractures. Therefore, the discontinuity of the fractures in the basalts and the generally lower hydraulic conductivities of the sediments may limit the vertical movement of water through the interbeds (Barracough et al. 1976). However, McElroy

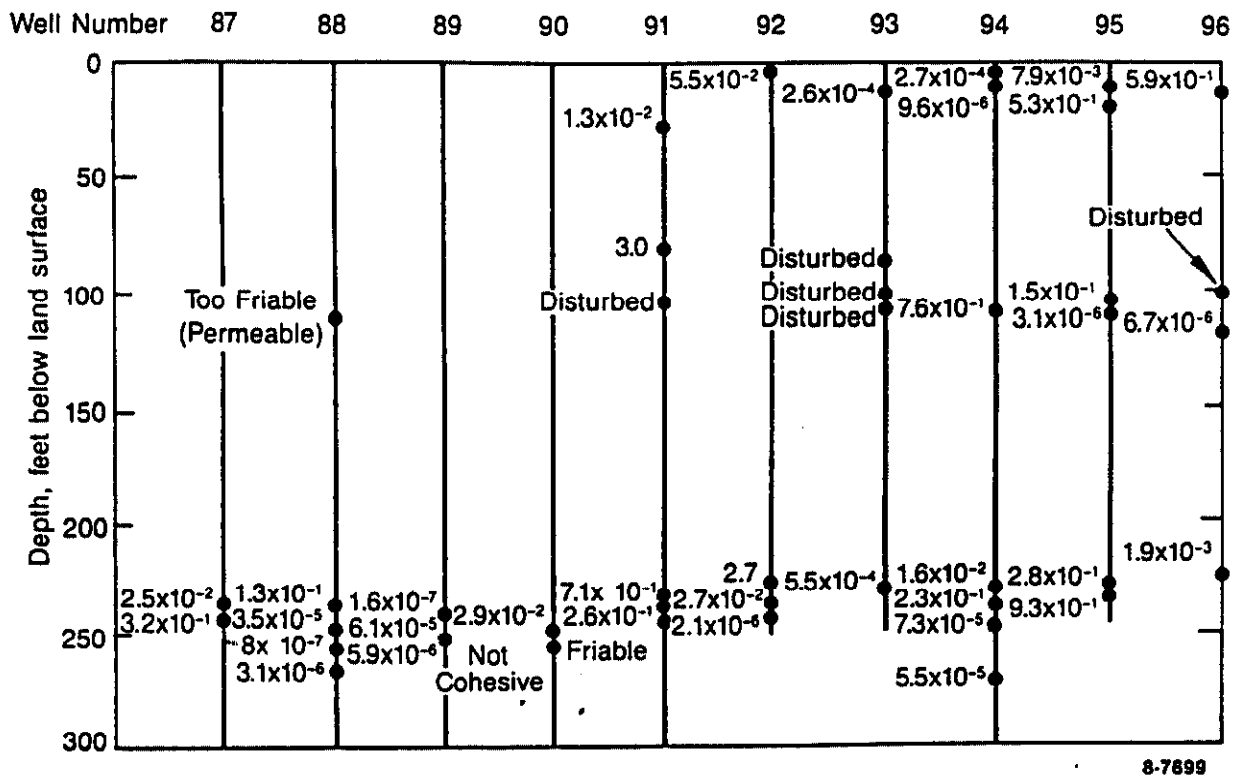


**Figure 2-35.** Laboratory-determined vertical hydraulic conductivities in m/d sediment samples from 10 wells in or near the RWMC (Barracough et al. 1976).

and Hubbell (1989) found that the matrix potentials and calculated hydraulic gradients in the 110-ft and 240-ft interbeds indicated that there was downward movement of water through the sedimentary units.

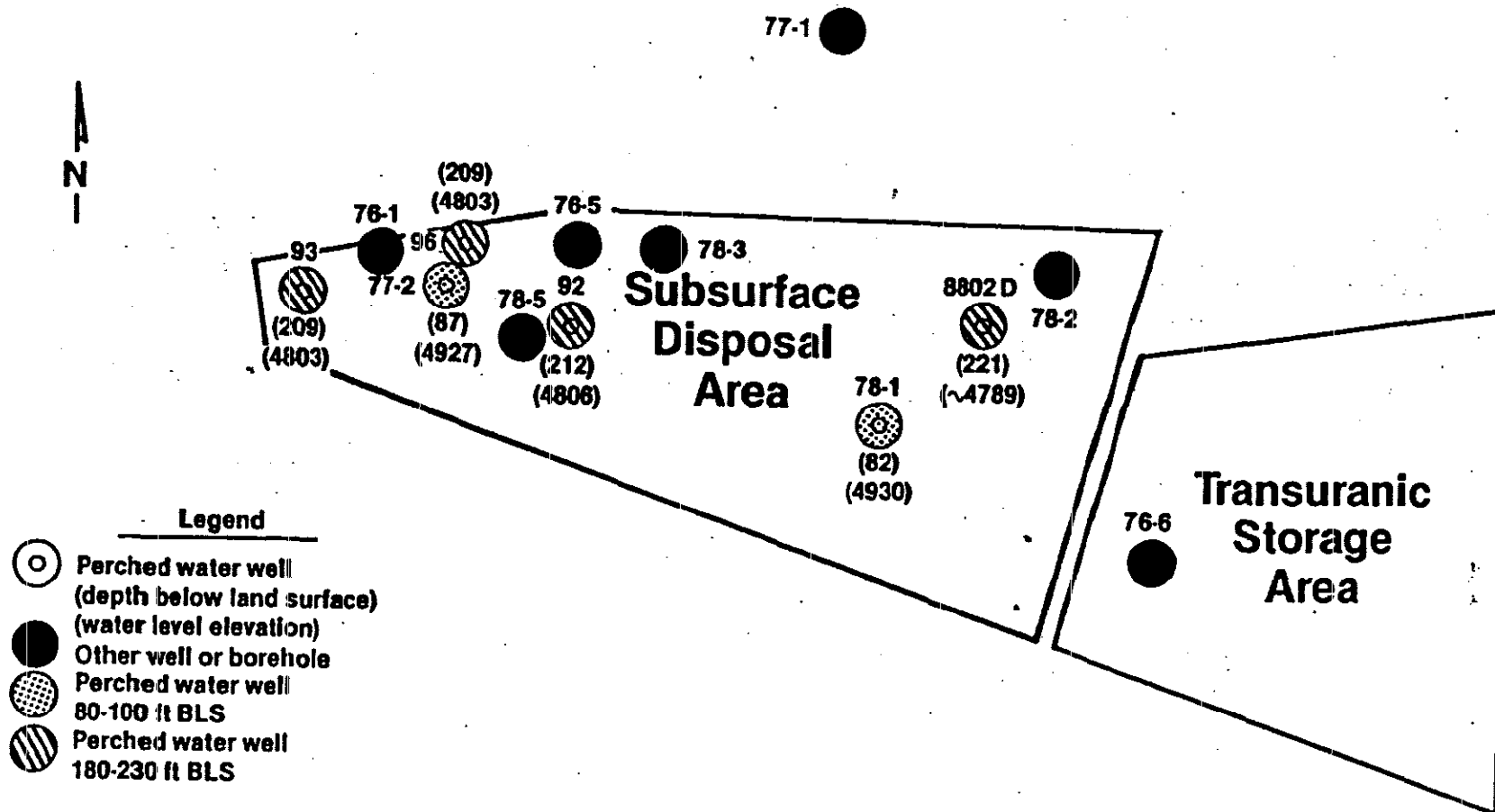
**2.2.5.6 Perched Water Zones.** Perched water occurs where variations in permeabilities result in discontinuous saturated lenses with unsaturated conditions above and below (Freeze and Cherry 1979). These saturated conditions can vary temporally and spatially, since they are affected by variations in recharge events. For the RI/FS program, as in recent work at the SDA (Hubbell 1989), perched groundwater will be discussed only for those zones in which standing water can be monitored in a piezometer or well. Perched water zones, as defined above, have only been encountered in six of the wells drilled at the RWMC (Figure 2-36), and conditions in several of these wells have been observed to vary.

The intervals of 80-100 ft and 180-220 ft below land surface seem to have the highest potential for perched groundwater (Hubbell 1990). However, the saturated intervals are not laterally or vertically extensive and contain relatively small volumes of water. Hubbell (1990) reports recharge rates of 200 to 800 mL/mo for the one well (Well 92) which is monitored regularly.

Subsurface investigations were conducted to identify potential pathways and rates of migration of radionuclide wastes from the SDA (Barraclough et al. 1976, Burgus and Maestes 1976, Humphrey and Tingey 1978, and Humphrey 1980). Several boreholes were drilled in the course of these investigations and wet or saturated zones were encountered at various depths. Standing water was encountered in Well 92 at 212 ft and in Well 77-2 at 87 ft. However, perched water was suspected in the following boreholes: 76-1 at 30 ft; 76-5 at 30, 85, and 95 ft; 76-6 at 65 ft; and 77-1 at 230 ft. Technical difficulties encountered during drilling prevented the field personnel from determining whether or not the wet zones were indeed perched water zones. The locations of these boreholes are shown on Figure 2-36.

The lateral extent of perched groundwater in the SDA is known to a limited extent. Seven of 45 wells drilled at the RWMC have detected perched groundwater. Two wells have detected standing water at approximately 85 ft below land surface with the remaining wells detecting standing water at varying depths between 180 to 220 ft bls. There is some evidence that water may be traveling from the spreading areas toward the SDA at approximately 220 ft depth (above the 240 ft interbed). The water level in Well 92 is shown in Figure 2-37. This is the only perched water well that has been actively monitored. Rapid decreases in the water level (Figure 2-37) reflect when water was removed for analyses. This water level shows the influence of being sampled over 23 times. Hubbell 1989 discusses water level fluctuations in this well by greater detail. This data suggests that the water level recovers slowly following sampling and that the water level in this well does not get any higher than approximately 4,800 ft. To provide further information on the spatial distribution of the perched water zones, three additional confirmatory boreholes were drilled in 1978 (Humphrey and Tingey 1978). These three boreholes included Wells 78-2, 78-3, and 78-5. Well 78-2 was installed in the northeast section of the SDA, Well 78-3 was drilled to the east of Well 76-5; and Well 78-5 was located west of Well 92 (see Figure 2-38 for borehole locations). All three boreholes failed to intercept any perched water zones.

Water infiltrates into the subsurface at or near the SDA by a combination of mechanisms, including direct precipitation, seasonal runoff of snowmelt, and infrequent flooding events at the



9-0779

Figure 2-36. Perched water wells at the RWMC (Hubbell 1989).

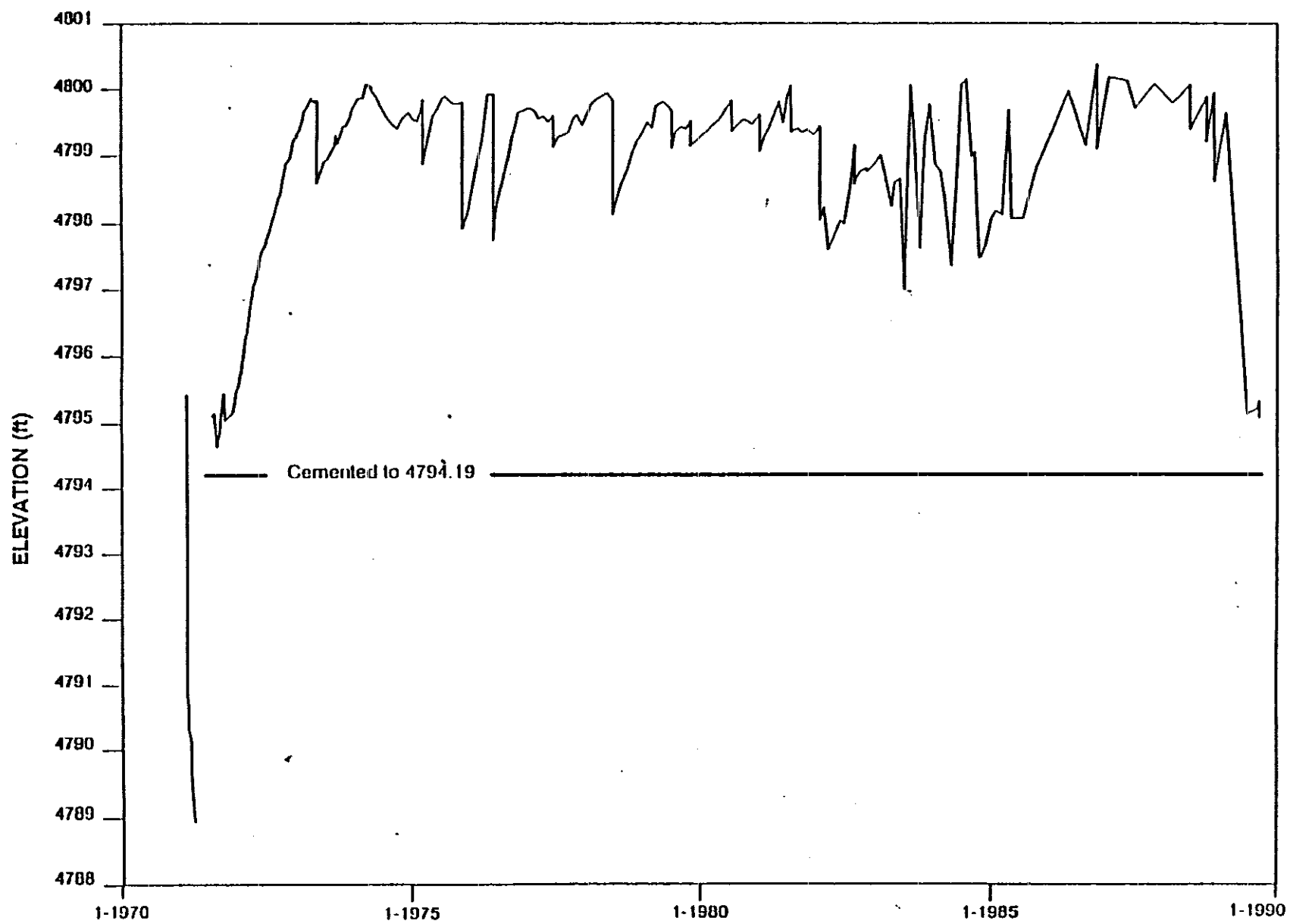
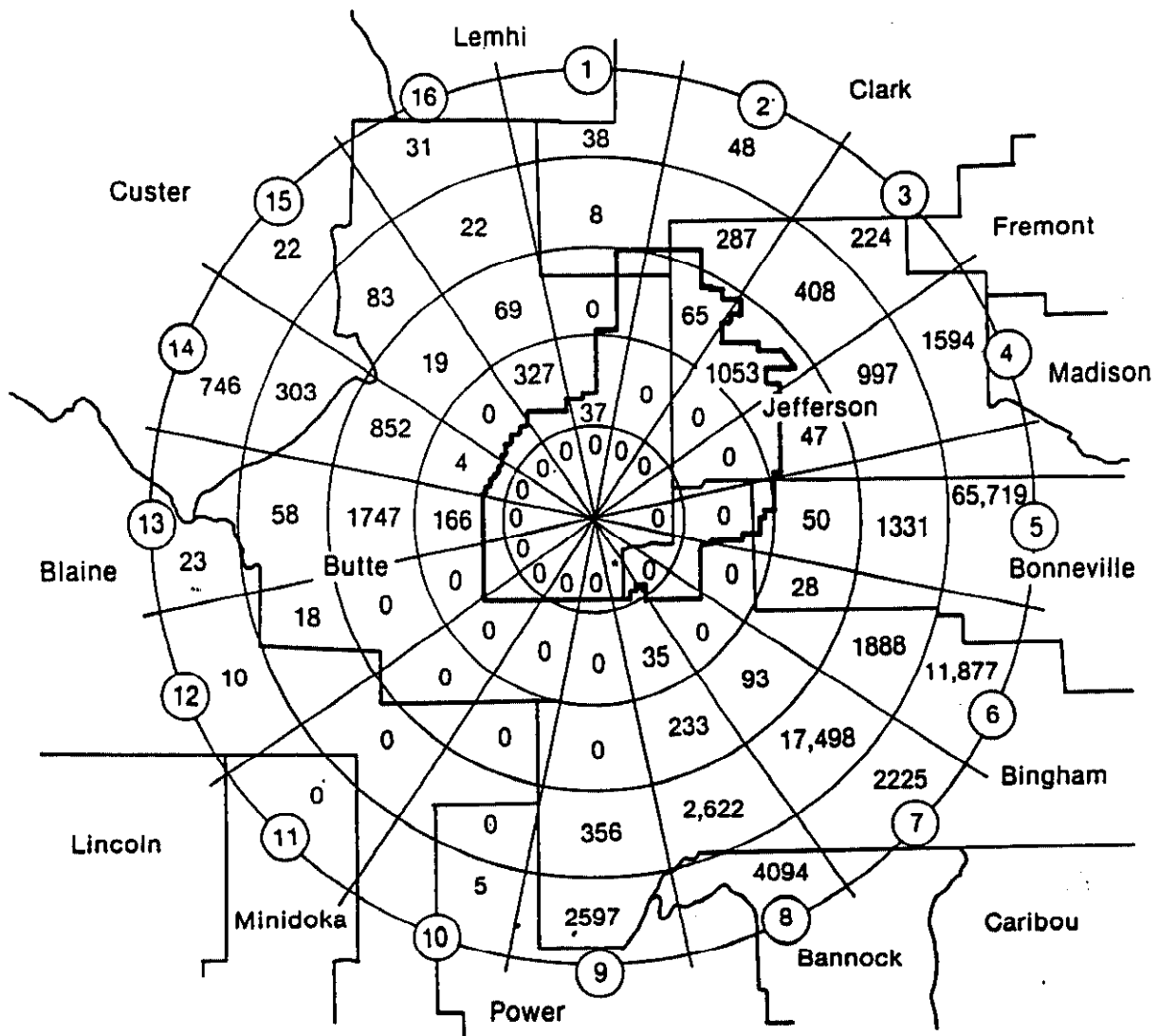


Figure 2-37. Water level elevation in Well 92, 1990 (Hubbell 1989).



\*The computer listing of six persons living in this area is erroneous, because of the program's assumption that persons within a given  $\text{mi}^2$  section are uniformly distributed in that area. No persons reside in this area.

INEL 4 4892

**Figure 2-38.** Population distribution centered near the SDA.

diversion areas of the Big Lost River. It is not well established which of these mechanisms has the greatest effect on the occurrence of perched groundwater. Hubbell (1989) indicates that seasonal runoff of snowmelt has the greatest potential for substantial recharge, because of the large volumes of water and the low potential for evapotranspiration. However, Rightmire and Lewis (1987) propose that the perched groundwater observed beneath the SDA was primarily due to lateral flow of water infiltrating through the diversion areas, based on stable isotope and chemical data.

## **2.2.6 Demography and Land Use**

**2.2.6.1 Population at the INEL.** The INEL economically influences a large area of southeastern Idaho, primarily the six counties of Jefferson, Madison, Bonneville, Butte, Bingham, and Bannock. Population growth since the 1980 census has varied for these six counties. The highest growth rates have occurred in Madison and Jefferson counties, and a loss of population has occurred in Butte County. The 1980 county population, projected 1989 county population and percent change for the six primary counties and other counties within a 50-mi radius of the INEL are shown in Table 2-10. In general, many counties experienced either a rapid increase or decrease after the mid-1980s and then a slower but gradual increase after the mid-1980s. Population density by county is shown in Table 2-10.

In FY 1989, the INEL employed an average of approximately 10,378 persons with 7,610 working at Site facilities and the remainder at facilities located in Idaho Falls (Table 2-11). Approximately 99 employees work at the RWMC daily over a 24-hour period on a four day work week. These personnel support ongoing operations at the SDA, TSA, and Stored Waste Examination Pilot Plant.

The greatest human traffic near the SDA is found at the Experimental Breeder Reactor No. 1 (EBR-1), which is located almost 2 mi to the northeast of the SDA. EBR-1 is a museum open to visitors during the summer months. Approximately 10,578 people visited EBR-1 in 1987. The main access to the INEL is U.S. Route 20, which runs across the INEL from southeast to northwest. Vehicle access to EBR-1 and the SDA are via a road off U.S. 20, 2.5 mi northeast of EBR-1. The closest U.S. Route 20 approach to the SDA is approximately 3-1/2 mi to the northeast.

**2.2.6.2 Surrounding Populations.** In 1985, a computer code was developed by the Radiological and Environmental Sciences Laboratory of DOE-ID for estimating population distribution within an 50 mi radius of INEL facilities. The baseline location population was determined by using 1980 census data and 7.5-minute USGS quadrangle maps. Dwellings were located on the topographical maps and assigned an average of 3 residents per unit based on the 1980 census household size for southeast Idaho. A population estimate was entered for each section (one square mile). Exact city and town populations were entered in the appropriate sections. The estimate was then adjusted to match census division totals. The number of persons per section was entered into a data base file. Population is, therefore, assumed to be uniform across each section. The code reads the file by geographic coordinates and calculates the population within 22.5-degree radiating sectors that are divided into 16-km (10-mi) increments for a total of 80 sections (Figure 2-38).

The results of this computer code formed the basis (baseline) for population projections for the INEL. The total population figure for each individual section was updated. Population projection



**Table 2-10.** County population surrounding the INEL.<sup>a</sup>

County	Square miles	1980 population	1989 projected population	Population per square mile	Percent change
Bannock	1,112	65,421	71,374	64.2	9.1
Bingham	2,096	36,489	40,333	19.2	10.5
Bonneville	1,840	65,980	74,645	40.6	13.1
Butte	2,236	3,342	3,182	1.4	-4.8
Jefferson	1,093	15,304	17,505	16.0	14.4
Madison	468	19,480	23,493	50.2	20.6
Other counties within 50-mi radius					
Blaine	NA	9,841	13,774	NA	36.1
Clark	NA	798	715	NA	-10.4
Custer	NA	3,385	5,194	NA	53.4
Lemhi	NA	7,460	7,374	NA	-1.2
Power	NA	6,844	6,858	NA	0.8

a. Idaho Department of Employment, Bureau of Research and Analysis.

**Table 2-11.** Employment by area for the INEL during FY 1989.

Area	Average employment
Argonne National Laboratory-West	736
Central Facilities Area	1,098
Idaho Chemical Processing Plant	1,531
Naval Reactors Facility	2,787
Waste Experimental Reduction Facility, Power Burst Facility, and Special Power Excursion Reactor Test	106
Test Area North	745
Test Reactor Area	508
Radioactive Waste Management Complex	<u>99</u>
Total	<u>7,610</u>

by county for 1989 was obtained from the Idaho Department of Employment, Bureau of Research and Analysis.

There are no permanent residents at the INEL (EG&G Idaho 1981). Figure 2-38 presents a population summary in the INEL vicinity based on the 1980 census. From Sectors 10-12 in Figure 2-38, there may be as many as 635 people living downgradient (defined as the southwest direction of regional groundwater flow) of the SDA. All these people live more than 32 km (20 mi) from the SDA.

The SDA is in Butte County, which includes the majority of the western portion of the INEL. The total Butte County population is 3,342. Arco is the only major town in Butte County and it has 1,241 residents. The county population density is 1.4 persons/mi<sup>2</sup> (see Table 2-10).

The closest towns to the SDA are Butte City (population 93) and Atomic City (population 141). Butte City is approximately 12 mi to the northwest and Atomic City is approximately 12 mi to the southeast of the SDA. Neither town is located downgradient of the SDA.

**2.2.6.3 Surrounding Land Use.** The INEL has been committed to energy research and development and was designated a National Environmental Research Park in 1975. Approximately 95% of the 890 mi<sup>2</sup> area has been withdrawn from the public domain. The remaining 5% is controlled by the DOE. A series of Public Land Orders dating to 1946 has established the present uses of the INEL. Lands originally under the control of the Bureau of Land Management were withdrawn from the public domain under three principal Public Land Orders. Six other Public Land Orders pertaining to INEL lands have been issued. These orders primarily concern the managerial transfer responsibilities (Bowman et al. 1984). Land in Sectors 10-12 downgradient of the SDA (see Figure 2-39) is predominantly controlled by the Federal Government (DOE and the Bureau of Land Management) and the State of Idaho. Only about 4% is private (Bowman et al. 1984).

Approximately 330,000 acres of the INEL are open to grazing by cattle or sheep. Figure 2-40 presents a map of grazing areas relative to the RWMC and the SDA. These areas at the INEL are mutually agreed to by the DOE and the Department of the Interior. Grazing permits are administered through the Bureau of Land Management. Grazing is prohibited within 2 mi of any nuclear facility and livestock populations are controlled. No dairy cows are allowed in the area (Bowman et al. 1984).

Crops grown in Sectors 10-12 within 50 mi of the INEL include alfalfa, hay, and grains (Bowman et al. 1984). Livestock in these sectors, approximately 22,000 animals, include cattle, beef cows, and sheep; no dairy cows are raised in these sectors (Bowman et al. 1984).

## **2.2.7 Biota**

**2.2.7.1 Flora.** The 500,000 acres of the INEL are located on the eastern end of the basaltic Snake River Plain in a desert community that is typical of the Great Basin Region. This area is dominated by big sagebrush, green rabbit brush, bluebunch wheatgrass, and Indian ricegrass (McBride et al. 1978 and Cholewa and Henderson 1983). The INEL is a mosaic of over 20 vegetation communities and almost 400 plant species (Table 2-12). Sagebrush provides the largest

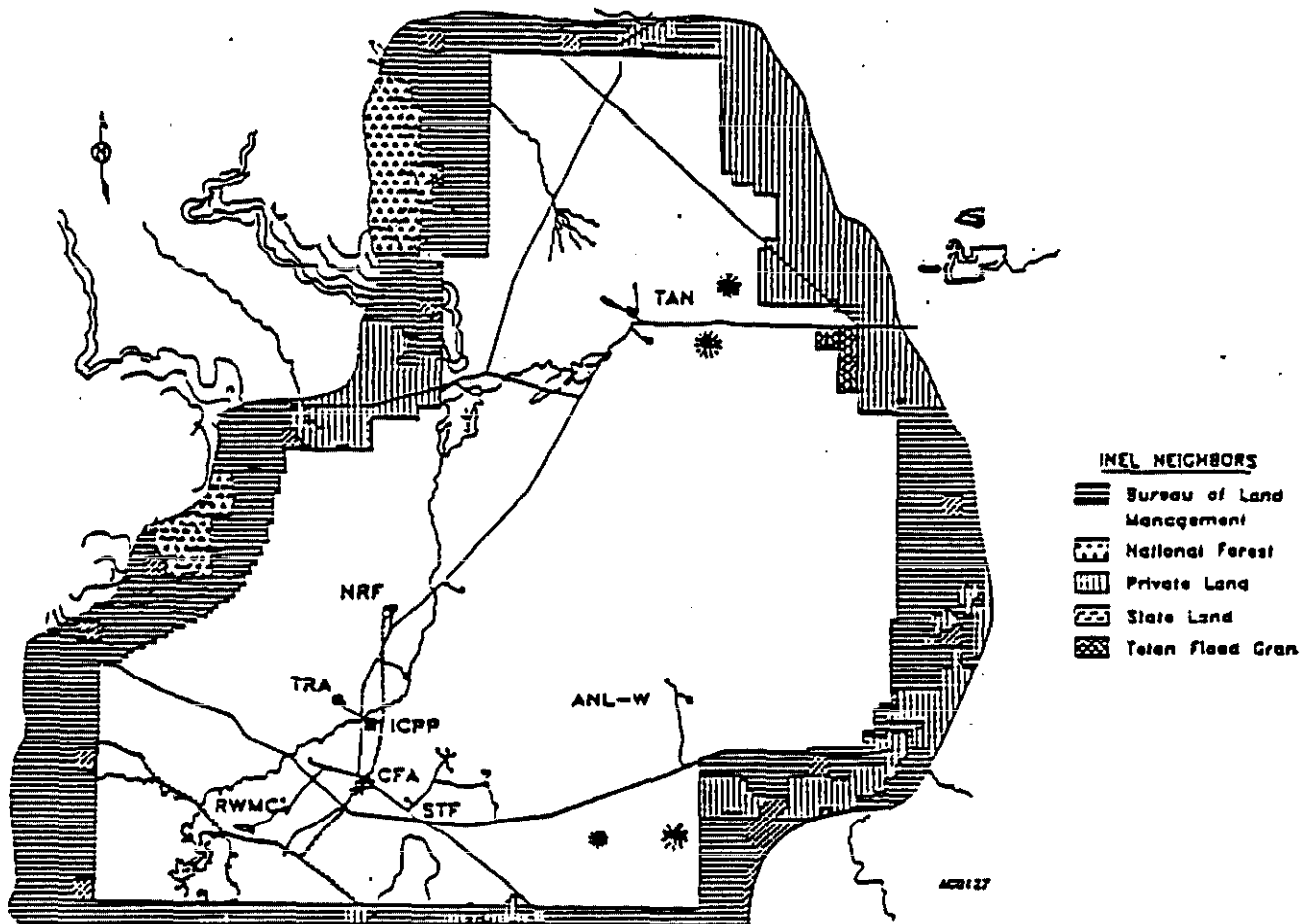
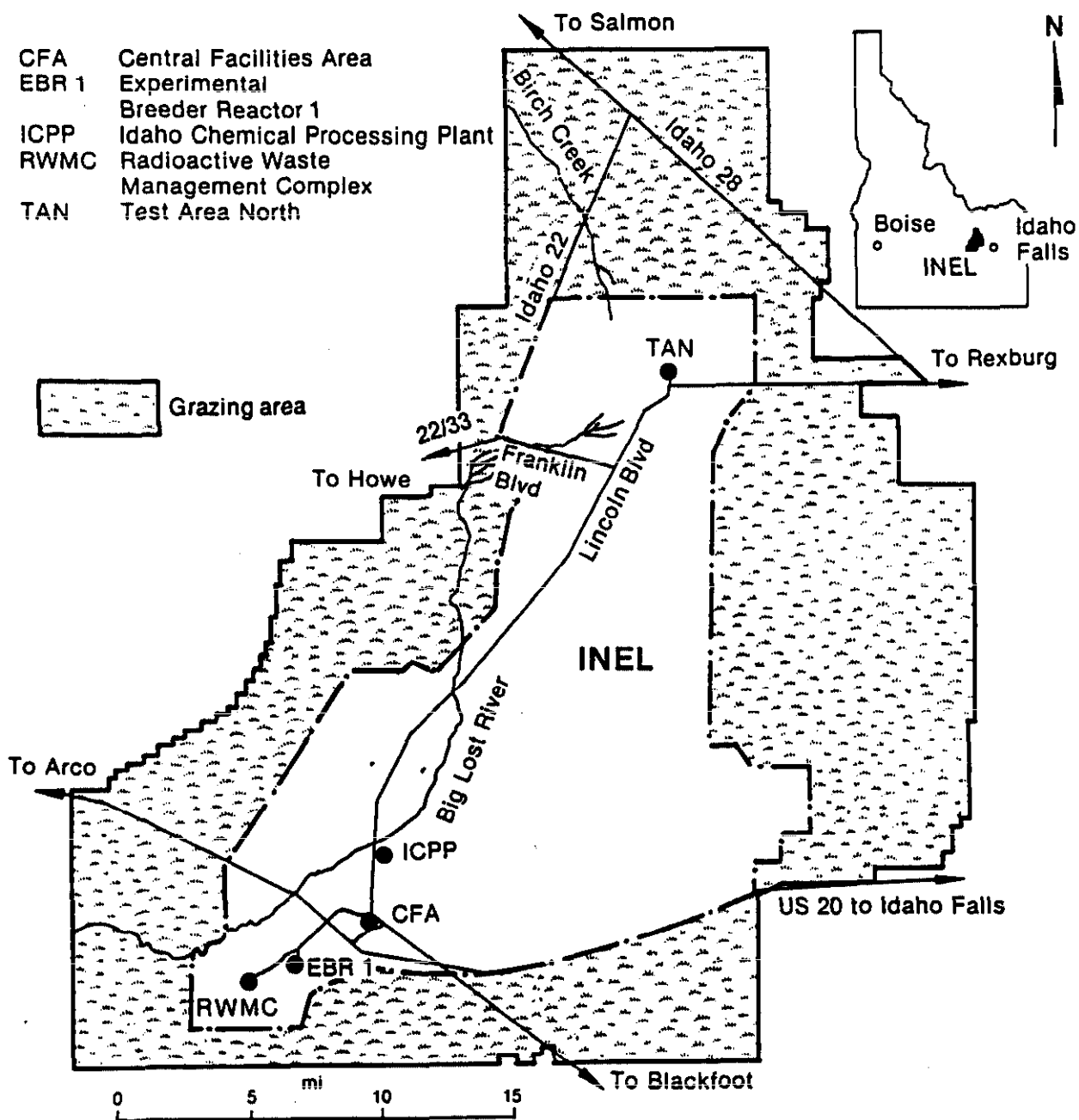


Figure 2-39. Land ownership surrounding the INEL.



INEL 4 4612

Figure 2-40. Permitted grazing areas at the INEL.

**Table 2-12.** Representative plant and animal species at the INEL.<sup>a</sup>

Common name	Scientific name
Flora	
Cactacea (cactus family)	
Pin cushion cactus	<i>Corypantha missouriensis</i>
Chenopodeaceae (Goosefoot family)	
Winterfat	<i>Ceratoides lanata</i>
Shadscale saltbush	<i>Atriplex confertifolia</i>
Nuttall saltbush	<i>Atriplex nuttalli</i>
Compositae (Composite of Sunflower family)	
Big sagebush	<i>Artemisia tridentata</i>
Low sagebush	<i>Artemisia arbuscula</i>
Rabbitbrush	<i>Chrysothamnus spp.</i>
Hawksbeard	<i>Crepis spp.</i>
Yellow salsify	<i>Tragopogon dubius</i>
Wild lettuce	<i>Lactuca serriola</i>
Thistle	<i>Cirsium spp.</i>
Gray horsebrush	<i>Tetradymia canescens</i>
Dandelion	<i>Taraxacum officinale</i>
Cruciferae (Mustard family)	
Bladder pod	<i>Lesquerella kingii</i>
Cupressaceae (Cypress family)	
Juniper	<i>Juniperus spp.</i>
Cyperaceae (Sedge family)	
Sedge	<i>Scirpus spp.</i>
Gramenaceae (Grass family)	
Bluebunch wheatgrass	<i>Agropyron spicatum</i>
Thickspike wheatgrass	<i>Agropyron dasystachyum</i>
Crested wheatgrass	<i>Agropyron cristatum</i>
	<i>Agropyron desertorum</i>
Indian ricegrass	<i>Oruzopsis hymenoides</i>
Neddle-and thread grass	<i>Stipa comata</i>
Squirreltail grass	<i>Sitanion hystrix</i>
Blue grass	<i>Poa spp.</i>
Great Basin wild rye	<i>Elymus cinereus</i>
Wild barley	<i>Hordeum jubatum</i>
Cheatgrass	<i>Bronius tectorum</i>

**Table 2-12.** (continued).

Common name	Scientific name
Hydrophyllaceae (Waterleaf family)	
Phacelia	<i>Phacelia inconspicua</i>
Juncaceae (Rush family)	
Rush	<i>Juncus spp.</i>
Leguminosae (Pea family)	
Painted milk vetch	<i>Astragalus ceramicus</i>
Wooly pod milk vetch	<i>Astragalus purshii</i>
Milk vetch	<i>Astragalus gilviflorus</i>
Milk vetch	<i>Astragalus kentrophyta</i>
Polygonaceae (Buckwheat family)	
Oxytheca	<i>Oxytheca dendroidea</i>
Salicaceae (Willow family)	
Willow	<i>Salix spp.</i>
Plains cottonwood	<i>Populus deltoides</i>
Scophulariaceae (Figwort family)	
Speedwell	<i>Veronica sp.</i>
Typhaceae (Cattail family)	
Cattail	<i>Typha latifolia</i>
Fauna	
Amphibians and Reptiles	
Anura (Amphibians)	
Great Basin Spadefoot toad	<i>Spea intermontana</i>
Squamata (Reptiles)	
Short-horned lizard	<i>Phrynosoma douglassi</i>
Sagebrush lizard	<i>Sceloporus graciosus</i>
Gopher snake	<i>Pituophis melanoleucus</i>
Western rattlesnake	<i>Crotalus viridis</i>
Birds	
Ciconiiformes (heron, bitterns, and relatives)	
White-faced ibis	<i>Plegadis chilhi</i>

**Table 2-12.** (continued).

Common name	Scientific name
<b>Anseriformes (ducks)</b>	
Mallard	<i>Anas platyrhynchos</i>
Pintail	<i>Anas acuta</i>
American widgeon	<i>Anas americana</i>
Northern shoveler	<i>Anas clypeata</i>
American green-winged teal	<i>Anas acuta</i>
Readhead	<i>Aythya americana</i>
Lesser scaup	<i>Aythya affinis</i>
Common goldeneye	<i>Bucephala clangula</i>
Bufflehead	<i>Bucephala albeola</i>
Ruddy duck	<i>Ozyura jamaicensis</i>
Hooded merganser	<i>Mergus strepera</i>
<b>Falconiformes (hawks and falcons)</b>	
Osprey	<i>Pandion haliaetus</i>
Bald eagle	<i>Haliaeetus leucocephalus</i>
Ferruginous hawk	<i>Buteo regalis</i>
Rough-legged hawk	<i>Buteo lagopus</i>
Red-tailed hawk	<i>Buteo jamaicensis</i>
Swainson's hawk	<i>Buteo swainsoni</i>
Golden eagle	<i>Aquila chrysaetos</i>
Merlin	<i>Falco columbarius</i>
Peregrine falcon	<i>Falco peregrinus</i>
Gyr Falcon	<i>Falco rusticolus</i>
Prairie falcon	<i>Falco mexicanus</i>
American kestrel	<i>Falco sparverius</i>
<b>Galliformes (grouse and pheasants)</b>	
Gray partridge	<i>Perdix perdix</i>
Chukar	<i>Alectoris chukar</i>
Ring-necked pheasant	<i>Phasianus colchicus</i>
Blue grouse	<i>Dendragapus obscurus</i>
Sage grouse	<i>Centrocercus urophasianus</i>
<b>Gruiformes (rails and coots)</b>	
American coot	<i>Fulica americana</i>
<b>Charadriiformes (shorebirds)</b>	
Long-billed curlew	<i>Numenius americanus</i>
Common snipe	<i>Gallinago gallinago</i>
<b>Columbiformes (doves and pigeons)</b>	
Mourning dove	<i>Zenaida macroura</i>



**Table 2-12.** (continued).

Common name	Scientific name
<b>Striniformes (owls)</b>	
Burrowing owl	<i>Athene cunicularia</i>
Long-eared owl	<i>Asio otus</i>
<b>Passeriformes (perching birds)</b>	
Horned lark	<i>Eremophila alpestris</i>
Barn swallow	<i>Hirundo rustica</i>
Black-billed magpie	<i>Pica pica</i>
American robin	<i>Turdus migratorius</i>
Sage thrasher	<i>Oreoscoptes montanus</i>
Brewer's sparrow	<i>Spizella breweri</i>
Sage sparrow	<i>Amphispiza belli</i>
Western meadowlark	<i>Sturnella neglecta</i>
Brown-headed cowbird	<i>Molothrus ater</i>
<b>Mammals</b>	
<b>Chiroptera (bats)</b>	
Little brown bat	<i>Myotis lucifugus</i>
Long-eared bat	<i>Myotis evotis</i>
Small-tooted myotis	<i>Myotis leibii</i>
Big brown bat	<i>Eptesicus fuscus</i>
Townsend's big-eared bat	<i>Plecotus townsendii</i>
<b>Lagomorpha (rabbits)</b>	
White-tailed jack rabbit	<i>Lepus townsendii</i>
Black-tailed jack rabbit	<i>Lepus californicus</i>
Nuttall cottontail	<i>Sylvilagus nuttallii</i>
Pygmy rabbit	<i>Sylvilagus idahoensis</i>
<b>Rodentia (rodents)</b>	
Yellow-bellied marmot	<i>Marmota flaviventris</i>
Townsend's ground squirrel	<i>Spermophilus townendii</i>
Richard's ground squirrel	<i>Spermophilus richardsonii</i>
Least chipmunk	<i>Eutamias minimus</i>
Great Basin Pocket mouse	<i>Perognathus parvus</i>
Ord's kangaroo rat	<i>Dipodomys ordii</i>
Western harvest mouse	<i>Reithrodontomys megalotis</i>
Deer mouse	<i>Peromyscus maniculatus</i>
Northern grasshopper mouse	<i>Onychomys leucogaster</i>
Bushy-tailed wood rat	<i>Neotoma cinerea</i>
Montane vole	<i>Microtus montanus</i>
Sage vole	<i>Lagurus curtatus</i>
Pocket gopher	<i>Thomomys sp.</i>

**Table 2-12.** (continued).

Common name	Scientific name
<b>Carnivora (carnivores)</b>	
Badger	<i>Taxidea taxus</i>
Bobcat	<i>Lynx rufus</i>
Coyote	<i>Canis latrans</i>
Long-tailed weasel	<i>Mustela frenata</i>
Mountain lion	<i>Felis concolor</i>
Spotted skunk	<i>Spilogale gracilis</i>
<b>Artiodactyla (even-toed ungulates)</b>	
Mule deer	<i>Odocoileus hemionus</i>
Pronghorn	<i>Antilocapara americana</i>

a. Based on surveys of the INEL performed by EG&G Idaho, and Arthur et al. 1983.

habitat on the INEL and is important to many animal species. Juniper communities occur in the northwest and southeast portions of the INEL (Figure 2-41). These communities are generally associated with increasing elevation and are found near East and Middle Buttes and in the foothills of the Lemhi Range. Although these communities are restricted in their distribution, they provide important nesting habitat for raptors (Craig 1989) and are used by a variety of passerines.

Crested wheatgrass seedlings are common throughout the INEL. These have flourished on the INEL since the 1950s when they were planted on disturbed sites (Marlette and Anderson 1983). A grass community dominated by Indian ricegrass also occurs in a relatively narrow band near the eastern border of the INEL. Previously an old burn site, it contains other disturbance species such as needle-and-thread, squirreltail, halogeton, and Russian thistle, which probably colonized the area after the burn (Cholewa and Henderson 1983).

Irrigated farmland intersperses with sagebrush habitats and borders much of the INEL. Much farmland is planted with alfalfa, but fields of wheat, potatoes, and irrigated pasture are also planted (Gates 1983). These areas are used extensively by a number of passerine species, as well as by four species of game birds: mourning doves, pheasants, gray partridge, and sage grouse. About 37% of the INEL is grazed by cattle and sheep.

Aquatic habitat on the INEL consists of evaporation and percolation ponds known as sinks or playas, which are located at the termination of the Big Lost River. Plains cottonwood is the primary riparian species that is sparsely distributed along the river flood plain. Four of the sinks or playas that exist in the area have not contained water since at least 1986. Two of these areas contained water in 1967, 1970 to 1975, and 1982 to 1986. A third area was flooded in 1969, 1971, and 1983, while the fourth has been dry for at least the last 20 years. When flooded, littoral plants in these areas have included thistle, speedwell, wild lettuce, cheatgrass, wild barley, and willow. Sedges, cattails, and rushes are common macrophytes. Small man-made ponds approximately (0.5 to 4 acres) occur at several INEL facilities and receive some use by waterfowl (Halford and Markham 1983).

Common plant species occurring at the INEL are in Table 2-12. All plant species identified have been compiled in a computer data system (Floyd and Anderson 1983) and additional plant summaries are available for the site (Shumar 1983 and Floyd and Anderson 1983).

No plants on the Federal list of endangered or threatened species have been observed on the INEL (Cholewa and Henderson 1983). *Astragalus ceramicus* var. *apus* and *A. purshii* var. *ophiogenes*, were previously under review for threatened or endangered status. They were dropped from the Federal Review List because they were more abundant than previously believed (Federal Register 1983). It was once thought that this species occurred at the INEL. However, further study revealed these plants had an unusual color morphology as compared to *A. purshii* var. *glareosus*<sup>b</sup>. Thus, *A. purshii* var. *ophiogenes* has not been positively identified at the INEL.

Four species, currently listed on the State Watch List, occur at the INEL including *Corypantha missouriensis*, *Gymnosteris nudicatilis*, *Oxthea dendriodea*, and *Lesquerella kingii* (Chowela and Henderson 1983; and Idaho Rare Plant Meeting, March 25, 1989). Plants on the Idaho State Watch

---

b. Private communication with D. Henderson, University of Idaho Herbarium, Moscow, Idaho, June 30, 1989.

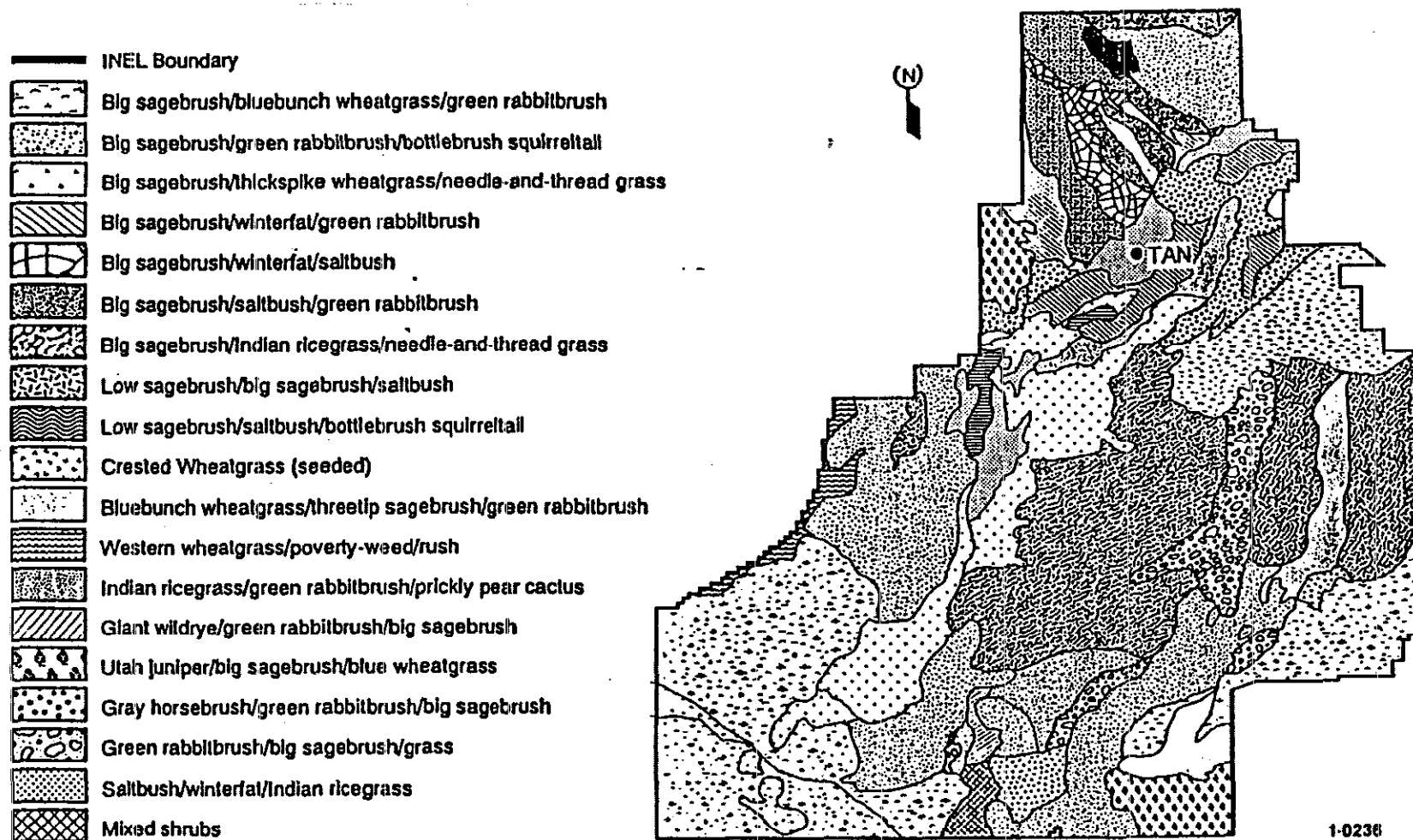


Figure 2-41. Vegetation distribution at the INEL.

List are considered rare and of special interest in Idaho, but their populations are not in jeopardy as they may be common elsewhere (Chowela and Henderson 1983). *C. missouriensis* was found on a sample site in the northwest corner of the INEL at the head of a small side canyon in the southern Lemhi Range. No immediate threats to this population were identified at the INEL (Chowela and Henderson 1983). Four distinct populations of *G. nudicatulis* were found in the southwest corner. Three were on a gravelly substrate and one was on sandy-silt on the side of a volcanic cone (Cholewa and Henderson 1983). All locations were inside the no-grazing boundary at the INEL. Potential threats to these include loss of habitat due to gravel extractions. Most populations were found on flood plain gravels with one occurring next to an active gravel pit (Chowela and Henderson 1983). *O. dendroidea* was found at eight locations in shady areas, primarily in the south-central portion of the INEL site. No apparent threats to these populations were identified (Cholewa and Henderson 1983). In addition, *L. kingii* was observed at three locations in the southeast section. No apparent threats to these populations have been identified (Cholewa and Henderson 1983). Additional information on these species is presented by Bowman et al. (1984) and Cholewa and Henderson (1983).

**2.2.7.2 Fauna.** A diverse insect population consisting of at least 150 families and 14 orders occupies the INEL rangeland ecosystems (Stafford and Barr 1983). Insects are essential components of complex food chains. They are involved in decomposition of plant and animal material, pollination, aeration, and soil turnover (Halford 1981, Stafford and Barr 1983, and Stafford 1984). One amphibian and nine reptilian species occur, the more common species are listed in Table 2-12.

At one time or another during a typical year, 159 bird species are found on the INEL, and 14 additional species have been listed as possible occurrences (Arthur et al., in press). Twenty-nine species of game birds have been recorded on the INEL, which provides important wintering and breeding habitat for this species (Connelly 1982 and Connelly and Ball 1983). The pheasant, gray partridge, chukar, blue grouse, and mourning doves are uncommon; only one observation of a blue grouse has been reported on the INEL. Additional game species at the INEL are listed in Table 2-12.

Sixty-nine species of passerines have been recorded on the INEL (Arthur et al., in press). The most common species include the horned lark, black-billed magpie, American robin, sage thrasher, Brewer's sparrow, sage sparrow, and western meadowlark (Table 2-12). These species occur throughout the INEL. The sage sparrow, Brewer's sparrow, and the sage thrasher are the most common nongame bird species breeding on the INEL (Peterson and Best 1983).

The INEL is an important nesting and wintering area for 22 species of raptors. American rough-legged hawks, American kestrels, prairie falcons, and golden eagles are the most abundant raptors observed on the INEL during the nonbreeding season. During the winter of 1981-82, most observations of raptors at the INEL included American rough-legged hawks (555 observations) and golden eagles (208 observations) (Craig et al. 1983). The most abundant breeding raptors on the site are American kestrels and long-eared owls (Craig 1979). Most raptor nests are restricted in distribution and are located in deciduous trees along the Big Lost River and in Juniper stands near Kyle Canyon in the northwest portion on the INEL or near twin Buttes to the southeast. Additional raptors occurring at the site are indicated in Table 2-12.

Eighteen of the 37 mammal species at the INEL are rodents (Arthur et al., in press). The Townsend's ground squirrel, least chipmunk, Great Basin pocket mouse, Ord's kangaroo rat, western harvest mouse, deer mouse, bushy-tailed wood rat, and the montane vole are the most common small

animals on the INEL. These animals are also relatively common throughout sage brush regions of the Intermountain West. Additional mammals occurring at the INEL are indicated in Table 2-12.

Five species of bats occur in the lava-tube caves on and adjacent to the INEL (Table 2-12). The small-footed myotis and Townsend's big-eared bat hibernate on the Site while the remaining bat species are considered migratory (Markham 1987).

Four species of leporids occur on the INEL: black-tailed jack rabbits, white-tailed jack rabbits, Nuttall cottontails, and pygmy rabbits (Table 2-12). All but the white-tailed jack rabbits are considered abundant. In addition, six species of carnivores occur on the INEL. Of these, the coyote, long-tailed weasel, and the badger are considered common (Arthur et al., in press). The bobcat ranges throughout the INEL but is generally uncommon. The mountain lion is considered rare. The spotted skunk is generally uncommon, but can be found in basalt outcrops.

The INEL supports resident populations of mule deer and pronghorn. Mule deer are considered uncommon and are generally concentrated in the southern and central portion of the INEL. They occur in greater numbers on the buttes and mountains surrounding the INEL. Pronghorn are found throughout the INEL and are generally considered abundant (Arthur et al., in press). Most pronghorn in southeastern Idaho are migratory (Hoskinson and Tester 1980). During winter months, 4,500 to 6,000 pronghorn, or about 30% of Idaho's total population, may reside on the INEL. In addition, elk (*Cervus elaphus*) may be expanding their range into the INEL, as indicated by the recent increase in elk sightings (Markham 1987).

The bald eagle and the American peregrine falcon are the only species observed on the INEL that are classified as Federally-endangered. A total of 65 observations of bald eagles were made at the INEL during the winter of 1981-1982 and 17 eagles were observed roosting in Howe, just west of the INEL (Craig et al. 1983). Bald eagle counts were conducted once each year during mid-winter surveys are as follows: 4 (1983), 3 (1984), 2 (1985), 5 (1986), and 1 (1987) (Markham 1987). No nest sites have been reported in the area. The peregrine falcon has been observed infrequently on the northern portion of the INEL (Arthur et al., in press). The population status, roosting requirements, and dispersal of this species is currently being studied at the INEL and results of these studies will be presented in future publications (Markham 1987).

Several species of wildlife observed on the INEL are of special concern to the Idaho Department of Fish and Game (Gleisner 1983) and the Bureau of Land Management. These species include the ferruginous hawk, merlin, osprey, burrowing owl, white-faced ibis, long-billed curlew, and bobcat. However, only the ferruginous hawk, burrowing owl, long-billed curlew, and bobcat occur regularly on the Site.

The INEL lies within the Pacific and Central Flyways used by a variety of migratory songbirds, waterfowl, and raptors. Most ducks use the INEL man-made ponds and flooded playas as resting areas during migration, and therefore, may act as important vectors in transporting contaminants accumulated across aquatic trophic levels (Halford and Markham 1983). In addition, each of the raptor species in the area (Table 2-12) is likely to migrate or undergo seasonal movements across the INEL. Consequently, raptors could also act as a significant pathway for transport of radionuclides or other contaminants across terrestrial trophic levels and may be important in dispersing contaminants out of the INEL.

**2.2.7.3 Important Wildlife Habitats.** Important habitats are those that are necessary for maintaining a viable wildlife population, or which have a limited distribution on the INEL and could thus be eradicated by perturbation (e.g., a fire). Because many wildlife species on the INEL are sagebrush obligates, either directly or indirectly, all sagebrush habitats within the INEL are considered important. However, the northern end of the INEL contains interspersions of low sagebrush and big sagebrush habitats (McBride et al. 1978 and Connelly 1982) that provide critical winter and spring range for sage grouse (McBride et al. 1978) and pronghorn (Hoskinson and Tester 1980).

Juniper communities on and adjacent to the INEL are important to nesting raptors (Craig 1979) and several species of songbirds. The Big Lost River sinks provide wetlands in an area where this habitat type is generally lacking. When water is present, the sinks are used by a large number of waterfowl and shorebird species (Arthur et al., in press). The relatively limited areas of these habitats and their importance to wildlife suggest that they should also be considered important. In addition, the limited and dispersed plains cottonwoods provide essential nesting locations for numerous raptors at the INEL.

**2.2.7.4 Microbiology.** The microbial populations within the soils and effluent ponds of the INEL have not been investigated or characterized, although one study conducted by Colwell (1988) addressed the surface and subsurface microbiology at the RWMC. Microscopic counts of subsurface bacteria were lower than similar counts performed on RWMC surface soils. Analyses of biologically relevant gases in the unsaturated subsurface near the RWMC indicated an environment capable of sustaining aerobic activities of many microbes. While denitrifying and methanotrophic bacteria are apparently absent from the 230-ft interbed sediments, both groups exist in the RWMC surface soils. Methanotrophic bacteria have been known to degrade low molecular weight halocarbons (Bouer and McCarty 1983).